SHEAR STRENGTH OF REINFORCED CONCRETE T-BEAMS

JANUARY, 1967

NO. 4

Joint Highway Research Project

by

K.E. WEHR

PURDUE UNIVERSITY
LAFAYETTE INDIANA

Final Report

SHEAR STRENGTH OF REINFORCED CONCRETE T-BEAMS

To: G. A. Leonards, Director
Joint Highway Research Project

January 30, 1967

File: 7-4-11

From: H. L. Michael, Associate Director
Joint Highway Research Project

Project: C-36-56K

The attached Final Report "Shear Strength of Reinforced Concrete T-Beams" has been authored by Mr. K. E. Wehr, Graduate Assistant on our staff, under the guidance of Professors M. J. Gutzwiller and R. H. Lee. Mr. Wehr also used the report as his thesis for the MSCE degree.

The report contains the results of an experimental study of the ultimate load behavior of reinforced concrete T-Beams which failed in shear. The major finding was that as the shear span-to-depth ratio increased, the average shear stress at failure decreased.

The report is presented to the Board as information and for the record.

Respectfully submitted,

Harold L. Michael

Harold L. Michael
Associate Director

HLM:jgs

Attachment

Copy: F. L. Ashbaucher
J. R. Cooper
J. W. Delleur
W. L. Dolch
W. H. Goetz
W. L. Grecco
G. K. Hallock
F. S. Hill
J. F. McLaughlin
F. B. Mendenhall
R. D. Miles
J. C. Oppenlander
W. P. Privette
M. B. Scott
F. W. Stubbs
K. B. Woods
E. J. Yoder

[illegible]

[illegible] Corporation
[illegible] Building
[illegible], [illegible]

[illegible]

[illegible]

[

Final Report

SHEAR STRENGTH OF REINFORCED CONCRETE T-BEAMS

by

K. E. Wehr
Graduate Assistant

Joint Highway Research Project

File No: 7-4-11

Project No: C-36-56K

Purdue University

Lafayette, Indiana

February 1, 1967

Digitized by the Internet Archive
in 2011 with funding from
LYRASIS members and Sloan Foundation; Indiana Department of Transportation

http://www.archive.org/details/shearstrengthofr00wehr

SHEAR STRENGTH OF REINFORCED CONCRETE T-BEAMS

A Thesis

Submitted to the Faculty

of

Purdue University

by

Kenneth E. Wehr

In Partial Fulfillment of the

Requirements for the Degree

of

Master of Science in Civil Engineering

January 1967

ACKNOWLEDGMENTS

Acknowledgment is made to the members of the board of the Joint Highway Research Project and to Professor G. A. Leonards, Director, for providing funds for the project.

Special thanks are given to Professors Martin J. Gutzwiller and Robert H. Lee, major professors, for their patient guidance and advice.

The author also wishes to express his appreciation to Mr. G. W. Foster and Mr. W. B. Telfer, laboratory technicians, and to the several graduate students for their generous assistance in the laboratory.

TABLE OF CONTENTS

	Page
LIST OF TABLES	v
LIST OF FIGURES	vii
LIST OF SYMBOLS	x
ABSTRACT	xiii
INTRODUCTION	1
Development of Design Procedures	6
Review of the Literature	12
PURPOSE OF STUDY	16
TEST SPECIMENS AND PROCEDURES	17
Materials	21
Concrete Mix	21
Aggregates	21
Reinforcing Steel	22
Fabrication and Curing	24
Instrumentation and Testing Procedures	25
TEST RESULTS	30
Series SS	38
Beam SS-1 (36" flange)	38
Beam SS-2 (30" flange)	39
Beam SS-3 (24" flange)	40
Beam SS-4 (no flange)	41
Series II T	50
Beam II T - 1 (No Stirrups)	50
Beam II T - 2 (Stirrups at 6")	51
Beam II T - 3 (Stirrups at 3-1/2")	52
Series III T	65
Beam III T - 1 (No Stirrups)	65
Beam III T - 2 (Stirrups at 8")	65
Beam III T - 3 (Stirrups at 5.5")	66
Beam III T - 4 (Stirrups at 4")	67

TABLE OF CONTENTS (CONTINUED)

	Page
Series IV T	80
Beam IV T - 1 (No Stirrups)	80
Beam IV T - 2 (Stirrups at 12")	81
Beam IV T - 3 (Stirrups at 8")	81
DISCUSSION OF TEST RESULTS	93
Modes of Failure	93
Factors Affecting Beam Behavior	94
Shear Span to Depth Ratio	94
Percentage of Web Reinforcement	95
ANALYSIS OF TEST DATA	96
Nominal Shearing Stress at Diagonal Cracking	96
Nominal Shearing Stress at Ultimate Load	96
Moment at Shear-Compression Failure	100
Ultimate Strength in Flexure	107
Comparison of Shear Strength of Rectangular Section and T-Section	108
SUMMARY AND CONCLUSIONS	112
BIBLIOGRAPHY	115
APPENDIX A - STRESS - STRAIN PROPERTIES OF THE REINFORCEMENT	117
APPENDIX B - PROCEDURES FOR APPLICATION AND WATERPROOFING OF THE SR-4 STRAIN GAGES	121
APPENDIX C - SAMPLE CALCULATIONS	125
APPENDIX D - LOAD - STRAIN DATA	128

LIST OF TABLES

Table		Page
1.	Properties of Test Specimens	18
2.	Properties of Longitudinal Reinforcement Steel	23
3.	Properties of Soft Web Reinforcement (Series SS, II T, III T)	23
4.	Properties of Soft Web Reinforcement (Series IV T)	24
5.	Summary of Test Results	31
6.	Comparison of Test Strengths with ACI and ASCE Committee Recommendations	97
7.	Comparison of Test Strengths with AASHO "Standard Specifications for Highway Bridges	99
8.	Moment at Shear-Compression Failure (Test vs. Calculated from Equations of Reference 15)	104
9.	Moment at Shear Compression Failure (Test vs. Calculated from Equations of Reference 14)	105
10.	Comparison of T-Beams and Rectangular Beams	110

Appendix
Table

D.1.	Steel and Concrete Strains - Beam SS-1	128
D.2.	Steel and Concrete Strains - Beam SS-2	129
D.3.	Steel and Concrete Strains - Beam SS-3	130
D.4.	Steel and Concrete Strains - Beam SS-4	131
D.5.	Steel and Concrete Strains - Beam IIT-1	132
D.6.	Steel and Concrete Strains - Beam IIT-2	133

LIST OF TABLES (CONTINUED)

Table		Page
D.7.	Steel and Concrete Strains - Beam II T-3 . . .	134
D.8.	Steel and Concrete Strains - Beam IIIT-1 . . .	135
D.9.	Steel and Concrete Strains - Beam IIIT-2 . . .	136
D.10.	Steel and Concrete Strains - Beam IIIT-3 . . .	137
D.11.	Steel and Concrete Strains - Beam IIIT-4 . . .	138
D.12.	Steel and Concrete Strains - Beam IVT-1 . . .	139
D.13.	Steel and Concrete Strains - Beam IVT-2 . . .	140
D.14.	Steel and Concrete Strains - Beam IVT-3 . . .	141

LIST OF FIGURES

Figure		Page
1.	Redistribution of Internal Stresses	4
2.	Shear Stresses	7
3.	Basis for Truss Analogy	10
4.	Cross-Section of Test Specimens	19
5.	Detail of Specimens	20
6.	Forms Prior to Placing Concrete	26
7.	Test Set-up	27
8.	Details of Test Set-up	28
9.	Beams After Test - Series SS	32
10.	Beams After Test - Series II T	33
11.	Beams After Test - Series III T	34
12.	Beams After Test - Series III T (cont'd)	35
13.	Beams After Test - Series IV T	36
14.	Top of Flange After Test - Series IV T	37
15.	Load vs. Steel Strain - Series SS	42
16.	Load vs. Deflection - Series SS	42
17.	Strain Distribution - Series SS	43
18.	Strain Distribution - Series SS	44
19.	Pictorial Representation of Specimen on Crack Pattern Sheet	45
20.	Beam SS-1	46
21.	Beam SS-2	47

LIST OF FIGURES (CONTINUED)

Figure		Page
22.	Beam SS-3	48
23.	Beam SS-4	49
24.	Load vs. Steel Strain - Series II T	54
25.	Load vs. Steel Strain - Series II T	55
26.	Load vs. Concrete Strain - Series II T	56
27.	Load vs. Concrete Strain - Series II T(cont'd).	57
28.	Load vs. Stirrup Strain - Series II T	58
29.	Strain Distribution - Beam II T-1	59
30.	Strain Distribution - Beam II T-2	60
31.	Strain Distribution - Beam II T-3	61
32.	Beam II T-1	62
33.	Beam II T-2	63
34.	Beam II T-3	64
35.	Load vs. Steel Strain - Series III T	68
36.	Load vs. Steel Strain - Series III T(cont'd) .	69
37.	Load vs. Deflection - Series III T	70
38.	Load vs. Concrete Strain - Series III T	71
39.	Load vs. Concrete Strain - Series III T(cont'd).	72
40.	Load vs. Stirrup Strain - Series III T	73
41.	Strain Distribution - Beam III T-3	74
42.	Strain Distribution - Beam III T-4	75
43.	Beam III T-1	76
44.	Beam III T-2	77
45.	Beam III T-3	78
46.	Beam III T-4	79

LIST OF FIGURES (CONTINUED)

Figure Page

47. Load vs. Steel Strain - Series IV T 83

48. Load vs. Deflection - Series IV T 84

49. Load vs. Concrete Strain - Series IV T 85

50. Load vs. Stirrup Strain - Series IV T 86

51. Strain Distribution - Beam IV T-1 87

52. Strain Distribution - Beam IV T-2 88

53. Strain Distribution - Beam IV T-3 89

54. Beam IV T-1 90

55. Beam IV T-2 91

56. Beam IV T-3 92

57. Criterion for Shear-Moment Capacity 102

58. Load vs. Stirrup Strain - Series II 111

Appendix
Figure

59. Typical Stress-Strain Properties - Longitudinal Steel 118

60. Typical Stress-Strain Properties - Stirrup Steel 119

61. Typical Stress-Strain Properties - Soft Stirrup Steel 120

62. Typical Waterproofed Gage 124

LIST OF SYMBOLS

A_s	nominal area of tension steel
A'_s	nominal area of compression steel
A_v	cross-sectional area of one stirrup
a	length of critical shear span (distance from section of maximum moment to point of inflection)
b	width of beam section
C	total internal compression force in concrete
d	effective depth (measured to centroid of tension steel)
d'	distance from compression face to centroid of compression steel
jd	internal moment arm, straight-line theory
E_s	modulus of elasticity of steel
E_c	secant modulus of concrete
f'_c	concrete compressive strength, 6" x 12" standard cylinder
f'_t	split-tension strength, 6" x 12" standard cylinder
f_v	stress in stirrup
f_{vy}	yield strength of stirrup steel
f_s	stress in longitudinal tension steel
f'_s	stress in longitudinal compression steel
f_{su}	stress in tension steel at failure of beam

LIST OF SYMBOLS (continued)

f_y	yield strength of longitudinal steel
M_s	ultimate shear-compression moment
M_u	ultimate flexural moment
M_1	maximum negative moment
M_2	maximum positive moment
n	E_s/E_c modular ratio
p	A_s/bd percentage longitudinal tension steel
P	total load
P_1, P_2	load on the overhang and load between supports, respectively
P_c	total load at formation of diagonal tension crack
P_u	total load at failure
r	A_v/bs - web reinforcement ratio
s	horizontal spacing of stirrups
T	total force in tension steel
V	total shear at any section
V_a	shear in critical shear span
V_c	shear assigned to concrete (working stress design)
V'	shear assigned to stirrups (working stress design)
v	nominal shearing stress = v/bjd or v/bd as defined in text
v_c	portion of total shearing stress assigned to concrete or average shear at diagonal cracking
v_s	portion of total shearing stress assigned to stirrups

LIST OF SYMBOLS (continued)

v_a	allowable nominal shearing stress (v/bjd)
v_u	ultimate shear strength
α	inclination of stirrups with respect to longitudinal axis
θ	inclination of compression diagonal with respect to longitudinal axis
ϵ_{cu}	strain at outermost compression fiber at failure
ϵ_{su}	strain in tension steel at failure
S.C.	shear-compression failure
D.T.	diagonal tension failure
F.T.	flexural tension failure
MII	strain in micro-inches per inch

ABSTRACT

Wehr, Kenneth E. M.S.C.E., Purdue University, January 1967. "Shear Strength of Reinforced Concrete T-Beams." Major Professors: Martin J. Gutzwiller and Robert H. Lee.

This research is an experimental study of the ultimate load behavior of reinforced concrete beams which fail in shear. Specifically, the objectives of this investigation were:

1. to observe the behavior of T-Beams with various shear span-to-depth ratios and amounts of web reinforcement and
2. to compare these beams to similar rectangular beams in an attempt to justify the standard practice of neglecting the effect of the flange on the shear strength of the beam.

Ten T-beams with a web of 6 inches by 13 inches rectangular cross-section and 3-inch thick flange of 30 inches total flange width were loaded to simulate a portion of a continuous girder subjected to concentrated loads. The beams were designed so that the critical section for failure was located between the section of zero moment and the section of maximum negative moment - commonly called the shear span.

The major variables were the shear span-to-depth ratio and the amount of vertical stirrups within the shear span. Beams with shear span-to-depth ratios of 2.86, 3.93, and 5.00 were tested.

Four additional beams were tested as simply-supported members with two concentrated loads. The major variable in these beams was the total flange width. Beams with total flange widths of 36 inches, 30 inches, 24 inches and no flange were tested.

It was found that as the shear span-to-depth ratio increased, the average shear stress at failure decreased. The comparison of T-beams to rectangular beams justified the standard practice of neglecting the effect of the flange on the shear strength of a beam.

Detailed discussion of the failure patterns and individual beam behaviors are presented along with a summary of test results.

INTRODUCTION

Over the past fifty years much research has been conducted on the behavior of reinforced concrete members. The art of predicting the behavior of members in axial compression, combined bending and axial compression, and pure bending has been develcped to the point where these predictions are quite accurate. Although as much, if not more, work has been done with members subjected to combined bending and shear stress, the predictions for the behavior of such members are often erratic.

For a simply-supported beam with two equal loads placed near the center (in other words, with a large shear span to depth ratio), the effect of shear on the ultimate strength of the beam is very small, if not negligible. The member will fail by flexure with either crushing of the concrete or initial yielding of the tension steel followed by crushing of the concrete. This condition of loading approaches the case of pure bending, in which a very close prediction of the ultimate load can be made.

As the two equal loads are moved toward the supports (or, the shear span to depth ratio is decreased), the shear begins to affect the formation of cracks and the ultimate load. The flexural cracks will begin to incline toward the

load as the load is increased. Diagonal tension cracks may also form independently from the flexural cracks and at a location closer to the support. These independent cracks form near the neutral axis and at approximately forty-five degrees to the neutral axis. Once the diagonal tension crack has formed, there are two typically observed types of behavior which may occur. One, the diagonal tension crack, once formed, spreads immediately or at a slightly higher load, crossing the entire cross-section from the tension steel to the compression face, splitting it into two separate pieces and hence failing the beam. This type of failure is referred to as a diagonal tension failure and occurs suddenly and without warning, and is most frequently observed in beams with larger shear span to depth ratios. Second, the diagonal tension crack, once formed, spreads toward and partially into the compression zone but stops before penetrating to the compression face. This type of failure is called a shear compression failure. No sudden collapse occurs, and failure load is usually significantly higher than that at which the diagonal tension crack first forms. This behavior is chiefly observed in beams with smaller span to depth ratios.

It can be concluded that qualitatively shear affects the behavior of beams through the formation of diagonal tension cracks. The formation of these cracks may cause the beam to simultaneously fail.

On the other hand, there are situations in which the beam is not capable of carrying a load large enough to cause a diagonal tension crack. Shear limits the ultimate strength of a beam if a diagonal tension crack forms before the ultimate load is reached. If this crack does not form, shear has no effect.

When a critical diagonal tension crack forms, an internal redistribution of stresses must take place. The crack cannot transfer shear stresses; therefore, the longitudinal steel must by dowel action transfer some of the shear while the uncracked concrete cross-section must resist the remainder. Until the diagonal crack forms, the stress in the longitudinal steel and in the concrete is proportional to the moment in the beam. The formation of the diagonal tension crack changes this distribution. This change is referred to as "the redistribution of internal stresses."

Figure 1(a) illustrates a beam without web reinforcement and with a diagonal tension crack. The section of the beam to the left of the crack is shown in Figure 1(b) as a free body. After the diagonal crack has formed, the concrete above the crack is assumed to resist the entire shear force. In reality the longitudinal steel transfers some of the shear by dowel action but this transfer is believed to be negligible. The remaining forces on the free body are the tensile force in the steel (T), the compression force on the concrete (C'), and the reaction (R).

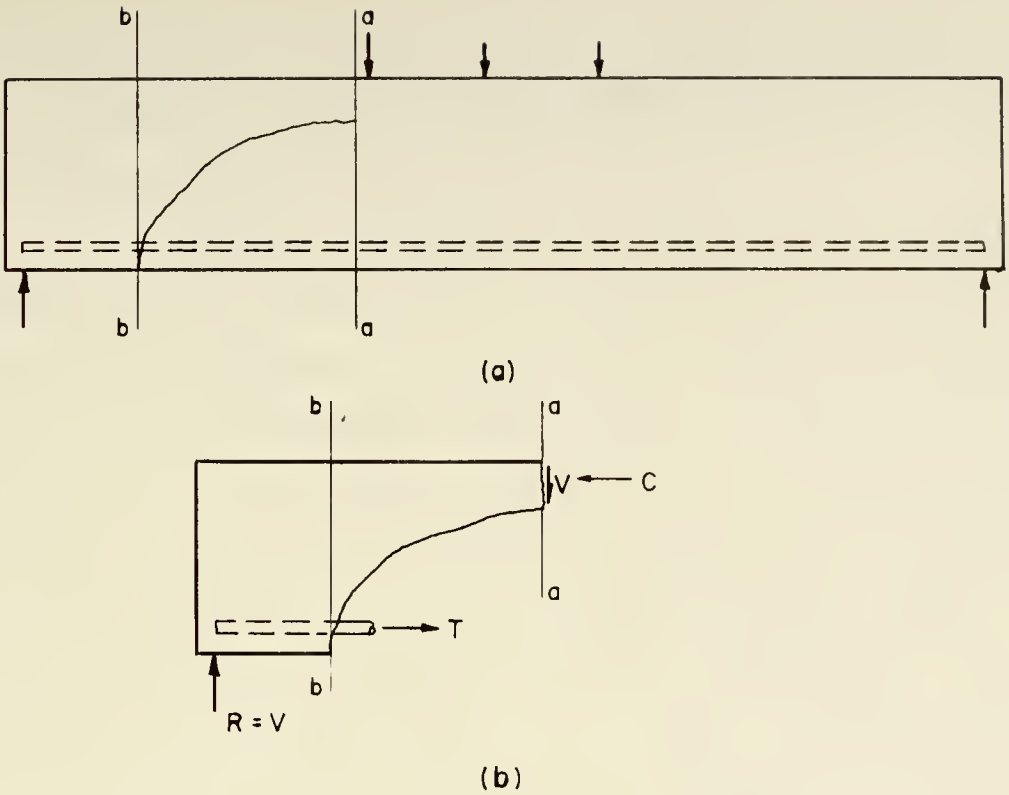

Figure 1. Redistribution of internal stresses

When the forces in Figure 1(b) are in equilibrium, it can be seen that the steel at section b-b must resist the moment at section a-a. In order for the member to adjust to this redistribution of forces, the steel section at b-b must be capable of the increase in stress due to the diagonal crack. If the beam is not able to reach a force equilibrium after this redistribution, the steel will yield and cause spontaneous collapse of the member.

The ability of a beam to reach a force equilibrium after redistribution of forces seems to depend primarily upon the stability of the compression zone, but it is also affected by the length of the shear span and the percentage

of reinforcement. In the case of a simply-supported T-beam, the compression zone has greater stability than a similar rectangular beam.

Although many specimens tested have failed in shear-compression at loads as much as 100% higher than loads causing the critical diagonal tension crack, a sufficient number have failed in diagonal tension simultaneously with formation of the diagonal tension crack to indicate that the diagonal crack load should be used as the ultimate load carrying capacity of a beam without web reinforcement. Web reinforcement has little or no effect on the beam's behavior prior to diagonal cracking. Measurements have shown no appreciable stress present in the stirrups prior to cracking. Upon cracking, only the stirrups immediately crossed by the crack receive a part of the stress originally carried by the concrete before cracking; all other stirrups are still unaffected. As the load is increased, the stirrups crossed by the crack are stressed proportional to the additional load. Besides carrying part of the load, stirrups add shear resistance in two other ways: (1) by restricting the propagation of the diagonal crack and reducing its penetration into the compression zone; and (2) the stirrups tie the longitudinal steel to the mass of the concrete beam, restricting the splitting of the concrete along the longitudinal steel. A specific case for this would be a simply-supported T-beam in which the flange splits away from the stem upon failure caused by diagonal tension cracking.

With the addition of web reinforcement, this splitting is postponed, at least until much higher loads are applied.

Beams with web reinforcement usually fail by crushing of the concrete after the stirrups yield, unless the percentage of web reinforcement is so high that the stirrups do not yield before a flexural failure occurs. The only time the beam will fail suddenly at formation of the diagonal tension crack is when the percentage of web reinforcement is so small that the reinforcement yields before equilibrium is reached.

Since stirrups become effective after formation of the diagonal tension crack and since failure is usually slow, it would seem to be safe to design web reinforcement for the member on the basis of ultimate load capacity.

Development of Design Procedures

For the case of an ideal material, the diagonal tensile stress at the neutral axis is equal to the unit shear; therefore, the unit shear stress has been used as a measure of diagonal tension. The unit shear is derived as follows. Consider a short length Δx of the beam in Figure 2(a), subjected to a constant shear V and moments M and $M + \Delta M$. Summation of moments about point A (Figure 2(b)) must equal zero, therefore

$$\Delta T \; jd = V \Delta x$$

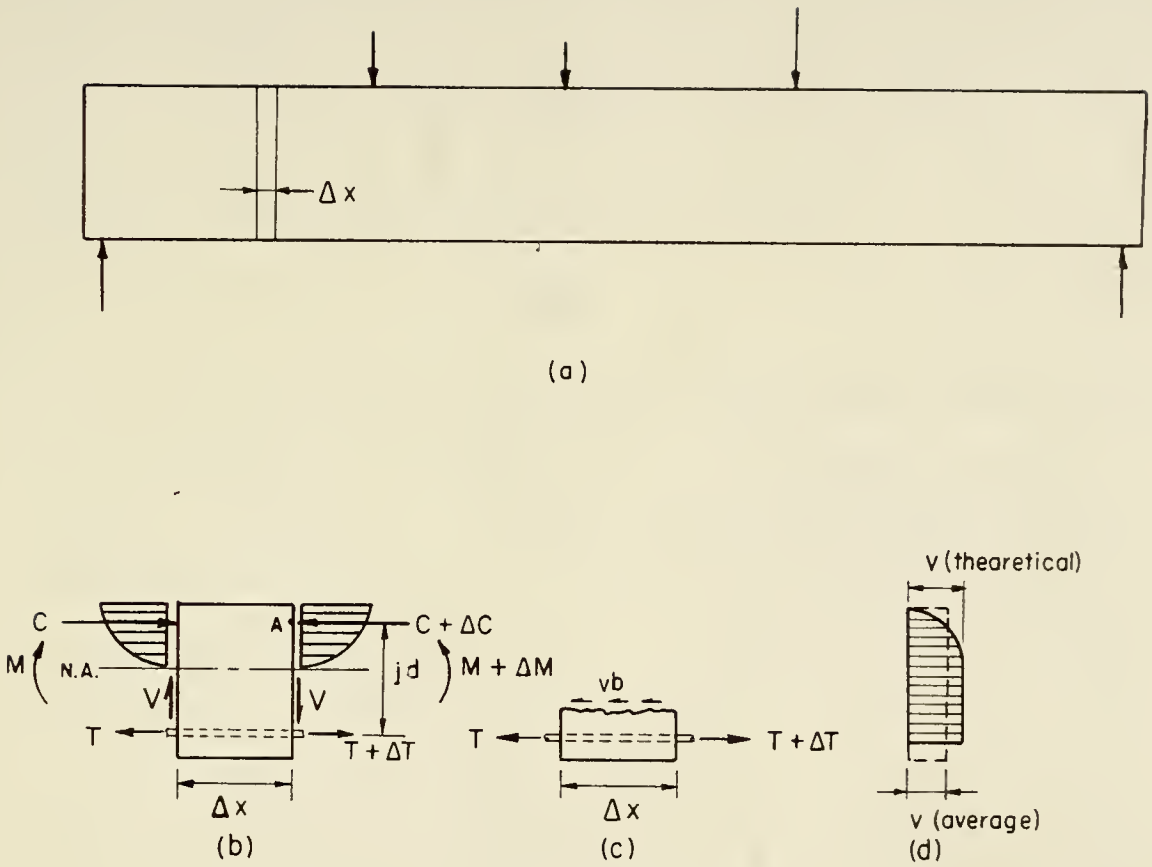

FIGURE 2. SHEAR STRESSES

or

$$\Delta T = \frac{V \Delta x}{jd}$$

Summation of horizontal forces (Figure 2(c)) must also equal zero, therefore

$$\Delta T = vb(\Delta x)$$

Equating these two values for ΔT gives:

$$v = \frac{V}{bjd} \qquad (1)$$

This is only a nominal or average shear stress, based on the assumption that the concrete carries no tensile bending stress. It ignores the complications at the moment cracks where shear concentrates above the crack. This assumes the unit shear stress distribution as parabolic in the compression zone and constant below the neutral axis (Figure 2(d)).

This equation has been adopted almost universally as a measure of diagonal tension for a basis to design for shear. An allowable value for this shear stress is then established. Until the 1963 ACI Building Code[3]* was adopted, this allowable value was established as a percentage of the compressive strength with a set upper limit. Most American standards before the adoption of the 1963 code, as well as the AASHO specifications[5] at present (1966), set this percentage at

---

*Superscripted numbers in parentheses refer to items in the Bibliography.

.03 f'_c with a maximum allowable shearing stress of 90 psi for members without web reinforcement. The 1963 ACI Code, upon recommendation made in a report by a joint ASCE-ACI committee 326[1] on shear and diagonal tension, adopted a simple average shear produced by the load causing the first diagonal tension cracking (dotted distribution in Figure 2(d)). The nominal ultimate shear stress, as a measurement of diagonal tension, is then computed using $v_u = V_u/bd$. The shear stress capacity of the concrete, v_u, is then taken as a factor of the concrete strength (f'_c), moment to shear ratio (M/Vd), and percentage of longitudinal steel (p). In the case of T-beams, the flange area is neglected, therefore the web width b' replaces b in the above formula.

Wherever the allowable concrete shearing stress is exceeded, shear reinforcement is required. Once a diagonal crack opens, the vertical stirrups act in tension to carry load from one side of the crack to the other. A common analogy (the "truss analogy") considers the stirrups acting as tension diagonals and the concrete acting as compression diagonals in the form of a truss.

Using the truss analogy, the strength of a beam with web reinforcement is derived as follows:

θ = inclination of compression diagonal

α = inclination of stirrups

s = horizontal spacing of stirrups

V = total shear

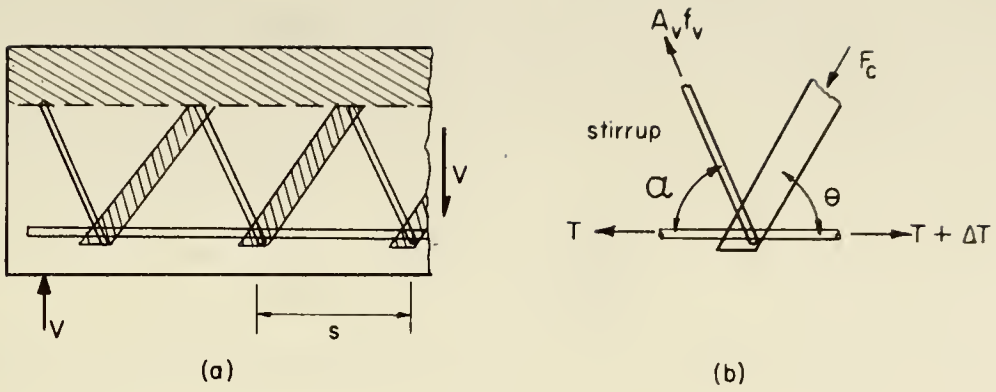

Figure 3. Basis for truss analogy

V_c = shear assumed to be carried by concrete

V_s = shear assumed to be carried by stirrups

A_v = area of a stirrup

f_v = stress in a stirrup

From equilibrium,

(1) summation of vertical forces yields

$$F_c = \frac{A_v f_v \sin\alpha}{\sin\theta}$$

and (2) summation of horizontal forces yields

$$\Delta T = A_v f_v \cos\alpha + F_c \cos\theta$$

$$= A_v f_v \cos\alpha + A_v f_v \sin\alpha \frac{\cos\theta}{\sin\theta}$$

Assuming constant shear,

$$\Delta T = \frac{\Delta M}{jd} = \frac{Vs}{jd}$$

Equating values for ΔT yields

$$A_v = \frac{Vs}{f_v\ jd\ (\cos\alpha + \frac{\sin\alpha}{\tan\theta})}$$

Making the usual assumption that $\theta = 45^o$ yields:

$$A_v = \frac{Vs}{f_v\ jd\ (\cos\alpha + \sin\alpha)} \qquad (2)$$

Since the uncracked concrete section carries a certain amount of the shear, $\underline{V}$ is replaced by $V_s = V - V_c$.

Letting

$$r = \frac{A_v}{bs\ \sin\alpha} \quad \text{(stirrup ratio)}$$

$$K = (\sin\alpha + \cos\alpha)\ \sin\alpha \quad \text{(stirrup efficiency)}$$

$$v_s = \frac{V_s}{bjd}$$

then Equation 2 becomes

$$rbs\ \sin\alpha = \frac{v_s\ bjd}{f_v\ jd\ (\cos\alpha + \sin\alpha)}$$

or

$$v_s = rKf_v \qquad (3)$$

For vertical stirrups ($\alpha = 90^{\circ}$), K = 1 and Equation 3 becomes

$$v_s = r f_v$$

Standard design procedure in this country is to assume the total allowable shear stress, v, equals the summation of $v_c + v_s$. The greatest error in this derivation is the assumption of the amount of shear carried by the uncracked concrete.

Review of the Literature

Several comprehensive reviews have been written within the last few years on the shear strength of reinforced concrete beams. An excellent review of work in this area up to 1951 was written by Hognestad [11]. Hognestad's review was brought up to date by the Joint ACI-ASCE Committee 326[1] in 1962 and by William Harvey's thesis[10] for his MSCE degree in 1964. It would seem unnecessary to undertake such a review again at this time. Therefore, only points which pertain directly to the shear strength of T-beams will be presented here.

In a study of previous investigations. Laupa, Siess, and Newmark[13] derived the following equation for the moment at which a simply-supported reinforced concrete beam without web reinforcement and under one load or two symmetrical concentrated loads fails in shear.

$$\frac{M_s}{bd^2 f'_c} = (k + np') \left(0.57 - \frac{4.5\ f'_c}{10^5}\right) \qquad (4)$$

Shear-Compression Moment

This equation was then applied to simply-supported T-beams with a slight modification made by a shape factor

$$F_t = \frac{I_t + I_{cr}}{I_r + I_{cr}},$$

where I_r refers to the moment of inertia of the uncracked rectangular section with the same width as the flange of the T-section, and I_t refers to the uncracked T-section. I_{cr} refers to the "straight line" cracked transformed section since both have very nearly the same moment of inertia.

The compressive area A_c of the T-section, as determined by the conventional "straight line" theory, is substituted for $\underline{bkd}$ and Equation 4 may then be rewritten as

$$\frac{M_s}{A_c\ d\ f'_c\ F_t} = 0.57 - \frac{4.5\ f'_c}{10^5} \qquad (5)$$

Laupa, Siess and Newmark found that Equation 5 gave reasonable agreement with test results, except for beams with large d/t (structural depth to flange depth) and g/b, (flange width to web width) ratios. It is known that in such beams part of the flange at some distance from the web does not resist its full share of the bending moment. This phenomenon is discussed in some detail for an elastic medium

by Timoshenko[17]. This reduction in effective width can be counteracted by use of transverse reinforcement in the flange, thus expanding the application of Equation 5.

The above-mentioned study also concluded that the shear strength of a simply-supported T-beam with web reinforcement can be determined by the same expression as that for rectangular beams

$$\frac{P_{sw}}{P_s} = 1 - \frac{2rf_{yw}}{10^3}$$

where P_s is from Equation 5, P_{sw} is the shear strength of a beam with stirrups, and r is from the following equation:

$$f = \frac{A_v}{b's \sin\alpha}$$

In another study conducted by Al-Alusi[4] it was observed that the presence of neither mesh reinforcement in the compression flange nor compression reinforcement affected the ultimate or cracking strength of T-beams. Al-Alusi also observed that there were no local compression failures in either the regular or the inverted simply-supported T-beam. The inverted T-beam was tested in such a way that the flange was in a state of tension rather than the usual compression. He found that the ratio of ultimate shear stress to cracking shear stress (v_u/v_{cr}), decreased with an increase in the a/d ratio from 2.0 to 4.0, but then remained constant for a/d ratios from 4.0 to 8.0. The quantity a is defined as the shear span, which is the distance between the section of zero

moment and the section of maximum moment.

The only T-beams, to the investigator's knowledge, that were tested as restrained beams were included in research by Elstner, Moody, Viest, and Hognestad[7]. It was found that the cracking, as well as the ultimate load, was much higher for the T-beam than for the rectangular beam. At equal loads, the strains measured in the stirrups were approximately equal in the rectangular and the T-beam. The rectangular beam failed in shear before the stirrups yielded but the T-beam's stirrups were well into the yield zone before shear-compression failure occurred.

PURPOSE OF STUDY

The object of this study was to observe the behavior of T-beams with various shear span-to-depth ratios and amounts of web reinforcement. These observations were to be compared to tests on similar rectangular beams, in an attempt to justify the standard practice of neglecting the effect of the flange on the shear strength of the beams.

Observations were to be made also on the effect of varying the width of the flange on the shear strength.

TEST SPECIMENS AND PROCEDURES

The first series of four beams were simply-supported beams with two concentrated loads applied at the third points. All the other beams were supported at two points with an overhang on one end. A load (P_1) was applied to the cantilever portion and a second load (P_2) was applied to the beam between the supports. These two loads were delivered to the beam by a steel I-section through knife edges. The desired ratio of P_1 to P_2 was obtained by positioning the load applied to the I-section. The loads, the shear and moment variation, and the details of the specimens can be seen in Figure 4.

The web of all specimens was a 6" by 13" rectangular section. For the SS series the total flange width varied from 6" to 36", while in all subsequent series the total flange width remained at 30". The flange thickness for all specimens was 3". The main variables were a/d ratio and the amount of web reinforcement within the critical shear span "a".

To restrict failure to the shear span "a", an excesssive amount of web reinforcement was placed in the other shear spans.

f_{vy} psi)	Concrete Comp. Strength	Split Tension (psi)	E (psi)
–	4020	431	4.17×10^6
–	4560	474	3.62×10^6
–	4290	475	4.32×10^6
–	3510	410	4.19×10^6
–	3950	428	3.80×10^6
.2	4010	544	3.75×10^6
.5	3890	386	3.60×10^6
	3740	392	3.64×10^6
.8	4370	416	3.79×10^6
.2	4150	388	3.50×10^6
.7	3720	426	3.49×10^6
	4470	437	3.84×10^6
.3	4680	499	3.94×10^6
.1	3900	388	3.56×10^6

Table 1. Properties of Test Specimens.

Beam No.	Flange Width	a	d	d'	a/d	Longitudinal Reinforcement Top	Longitudinal Reinforcement Bottom	Web Reinforcement Size and Spacing	r (av/bs)	rf_{vy} (psi)	Concrete Comp. Strength	Split Tension (psi)	E (psi)
SS-I	36"	44"	11"	-	4.0	-	2-#6	-	-	-	4020	431	4.17×10^6
SS-II	30"	44	11	-	"	-	"	-	-	-	4560	474	3.62×10^6
SS-III	24"	44	11	-	"	-	"	-	-	-	4290	475	4.32×10^6
SS-IV	6"	44	11	-	"	-	"	-	-	-	3510	410	4.19×10^6
II T-1	30"	32	11.2	2.25	2.86	2-#6	2-#5	-	-	-	3950	428	3.80×10^6
II T-2	"	32	"	"	"	"	"	#4 Wire @ 6"	.00211	77.2	4010	544	3.75×10^6
II T-3	"	32	"	"	"	"	"	#4 Wire @ 3-1/2"	.00362	132.5	3890	386	3.60×10^6
III T-1	"	44	"	"	3.93	"	"	-	-	-	3740	392	3.64×10^6
III T-2	"	44	"	"	"	"	"	#4 Wire @ 8"	.00158	57.8	4370	416	3.79×10^6
III T-3	"	44	"	"	"	"	"	#4 Wire @ 5-1/2"	.00230	84.2	4150	388	3.50×10^6
III T-4	"	44	"	"	"	"	"	#4 Wire @ 4"	.00316	115.7	3720	426	3.49×10^6
IV T-1	"	56	"	"	5.00	"	"	-	-	-	4470	437	3.84×10^6
IV T-2	"	56	"	"	"	"	"	#4 Wire @ 12" (new)	.00105	21.3	4680	499	3.94×10^6
IV T-3	"	56	"	"	"	"	"	#4 Wire @ 8" (new)	.00158	32.1	3900	388	3.56×10^6

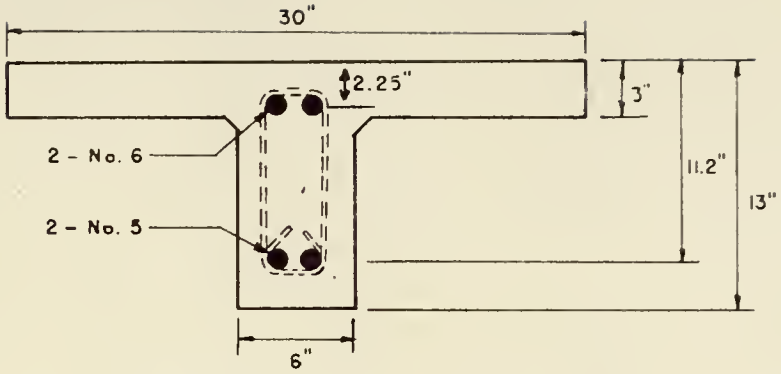

SERIES IIT, IIIT, & IVT

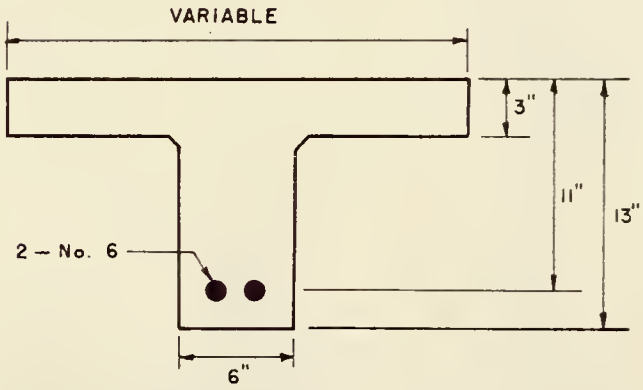

SERIES SS

FIGURE 4. CROSS - SECTION OF TEST SPECIMENS

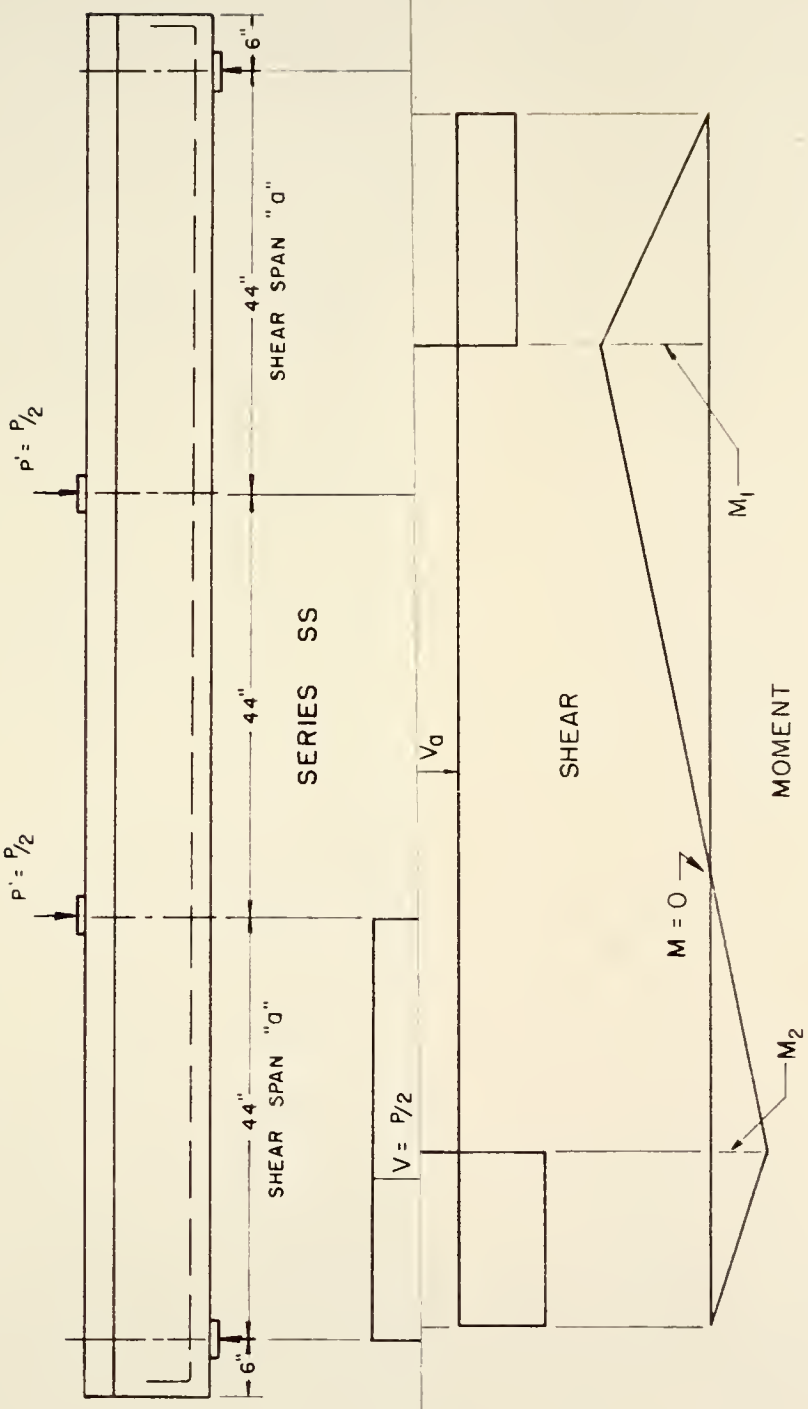

FIGURE 5. DETAIL OF SPECIMENS

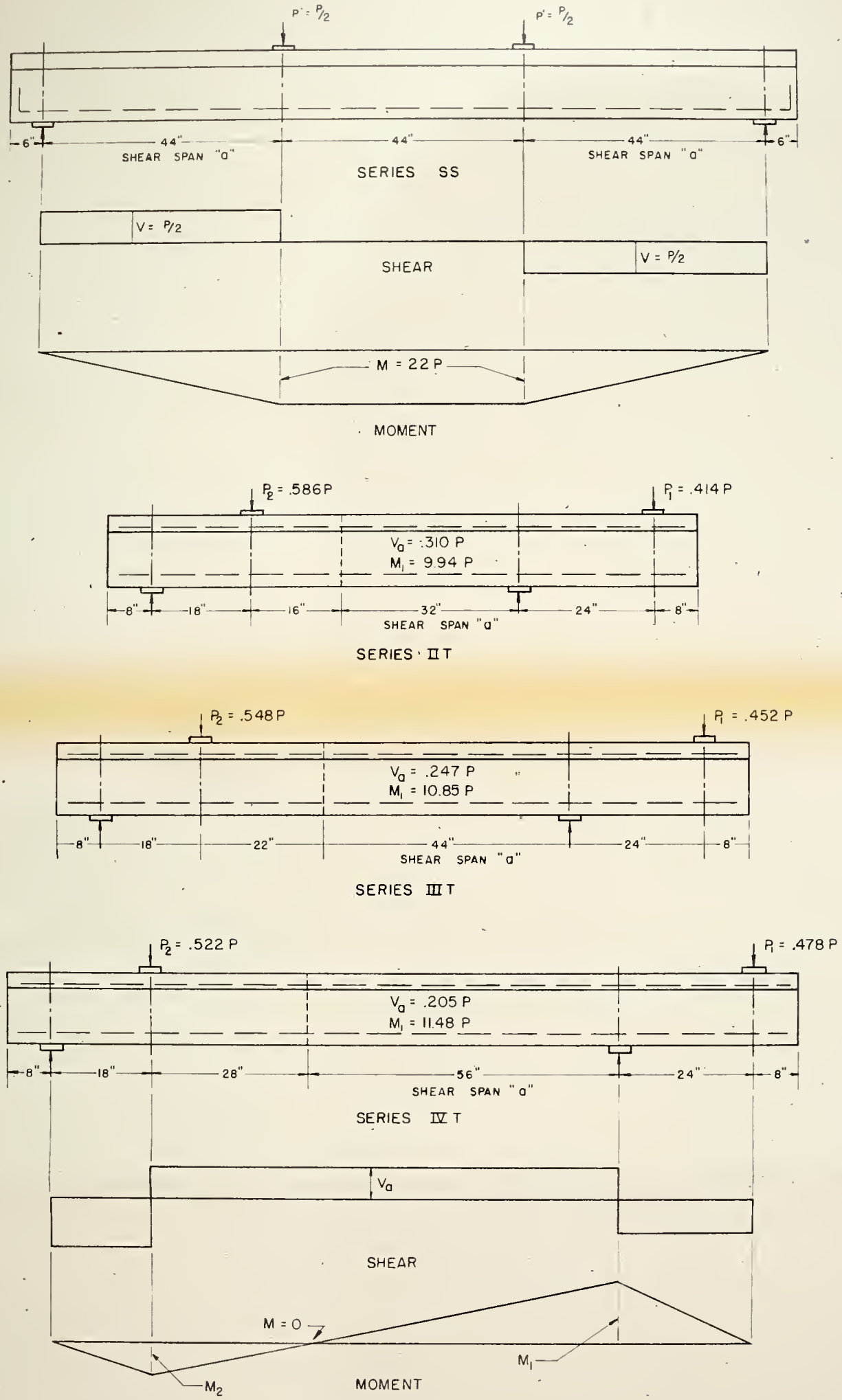

FIGURE 5. DETAIL OF SPECIMENS

The longitudinal steel in the SS series consisted of two No. 6 bars in the bottom of the web. The remaining series were reinforced with two No. 6 bars in the top and two No. 5 bars in the bottom of the web.

Materials

Concrete Mix

All concrete was made with Type I Portland cement. The concrete strength was intended to be maintained at 4000 psi, but varied from approximately 3500 to 4500 psi at seven days. The proportions of this mix by saturated-surface-dry weight were 1:2.06:3.51 (cement to fine aggregate to coarse aggregate) with a water-cement ratio (w/c) of .506 by weight and a cement factor of 6.12 sacks/yd^3.

Aggregates

The aggregates used were purchased from Western Indiana Aggregates Corporation, Lafayette. The coarse aggregate was a natural gravel of 1½ inches maximum size. In the laboratory it was separated into two sizes to minimize segregation during handling and all aggregate larger than one inch was discarded. By Fuller's Maximum Density Curve, 48 percent of No.4 to 1/2 inch was combined with 52 percent of 1/2 inch to 1 inch, by weight. Average properties of the fine and coarse aggregate were as shown below.

	Sp. Gr.*	Absorption*	Fineness Modulus
Fine	2.64	1.57%	2.76
Coarse	2.69	1.26%	--- 1" max. size

* Based on saturated-surface-dry weight.

Gradation of Fine Aggregate

Sieve Size	Percent Retained
No. 4	1.1
8	10.1
16	32.0
30	51.0
50	87.2
100	94.5

Reinforcing Steel

The longitudinal reinforcing was a high strength steel with the average properties shown in Table 2. The No. 5 and 6 deformed bars were rolled from the same heat. The properties shown are for coupons selected at random. A representative stress-strain curve is shown in Figure 59, Appendix A. The deformations met the requirements of ASTM-A305.

The No. 2 plain bar used for stirrups in the overhang and the 18" interior span were of hard grade steel with an average yield point of 50,000 psi.

Table 2. Properties of Longitudinal Reinforcement Steel.

Yield Stress	73.7 ksi
Ultimate Strength	117.0 ksi
Modulus of Elasticity	29.6×10^6 psi
Elongation in 8"	14.8%

The No. 4 wire used for stirrups in the critical shear span "a" was a very soft wire (diameter = .220 inch). This wire was obtained from Continental Steel Corporation, Kokomo, Indiana. Several coupons were randomly selected to determine the stress-strain properties shown in Table 3. A representative stress-strain curve is shown in Figure 60, Appendix A.

Table 3. Properties of Soft Web Reinforcement (Series SS, II T, III T).

Yield Stress	36.6 ksi
Ultimate Strength	52.9 ksi
Modulus of Elasticity	30.0×10^6 psi

Another type of soft web reinforcement was used for Series IV T. The properties of this steel are shown in Table 4 and a representative stress-strain curve is given in Figure 61, Appendix A.

Table 4. Properties of Soft Web Reinforcement (Series IV T).

Yield Stress	20.3 ksi
Ultimate Strength	43.1 ksi
Modulus of Elasticity	27.6×10^6 psi

Fabrication and Curing

All specimens were cast in 3/4 inch plywood forms coated with a polyester resin to prevent the wood from becoming rough due to repeated wetting and drying. The forms are shown partially assembled in Figure 6. The flanges were supported to prevent the form from tipping during casting of the specimens. Tie rods were placed through the stem of the specimen and below the bottom of the specimen to hold the forms together during casting.

The reinforcement was wired into a rigid cage, with the stirrups wrapped around the longitudinal steel. A minimum of 1.4 inches clear between the longitudinal bars and 1.5 inches concrete cover was maintained by wiring the longitudinal bars to the stirrups. The cage was supported in the forms by placing a steel bar across the stem and resting on the bottom of the flange portion of the forms. Lateral position was maintained by using wood blocks which were removed as the concrete was placed.

The concrete was mixed in a tilting drum mixer in batches of approximately three cubic feet. Control (6" by 12") cylinders were made from each batch. All materials were

weighed out before beginning to mix thus minimizing the time required in casting the specimen.

The last series (IV T) was mixed using a stationary rotating drum mixer with eleven cubic feet maximum capacity. This permitted more uniformity throughout the specimen.

Forms were left on as long as possible to facilitate curing the specimen. The top of the flange was covered with moist burlap until the sixth day, when both the forms and burlap were removed to set up the specimen for testing.

Instrumentation and Testing Procedures

An Amsler Pendulum Dynamometer with automatic load maintainer was used to actuate remote hydraulic jacks. A view of the test setup and details of the setup are shown in Figures 7 and 8 respectively.

Steel strains were measured using foil type SR - 4 electric strain gages. Strain gage readings were taken with a Budd digital read-out strain indicator. Strain in the longitudinal steel was measured at the point of maximum moment. Strains were also measured on those stirrups located within the critical shear span. The actual location of each of these gages is indicated on the crack pattern sheets. All strain gages were applied and waterproofed as described in Appendix B.

Compressive strains were measured in the concrete at points described on the crack pattern sheets. To provide for Whittemore gage points, steel plugs were placed in the

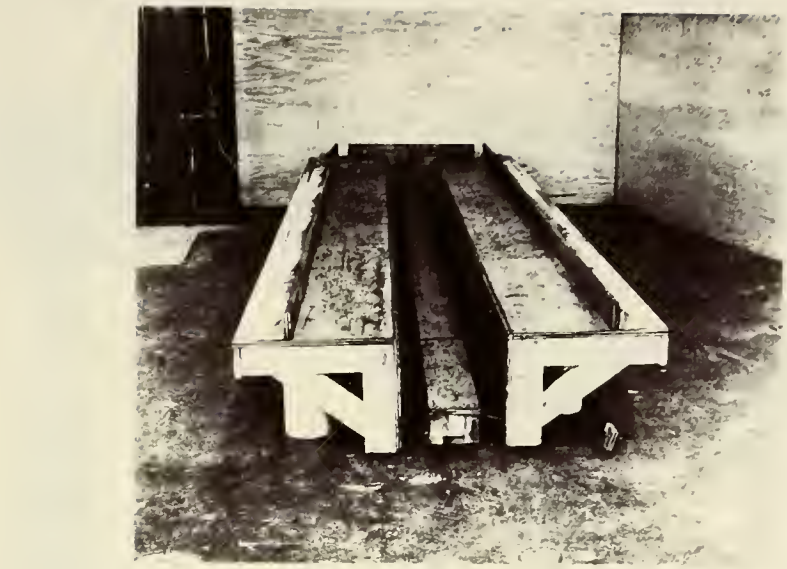

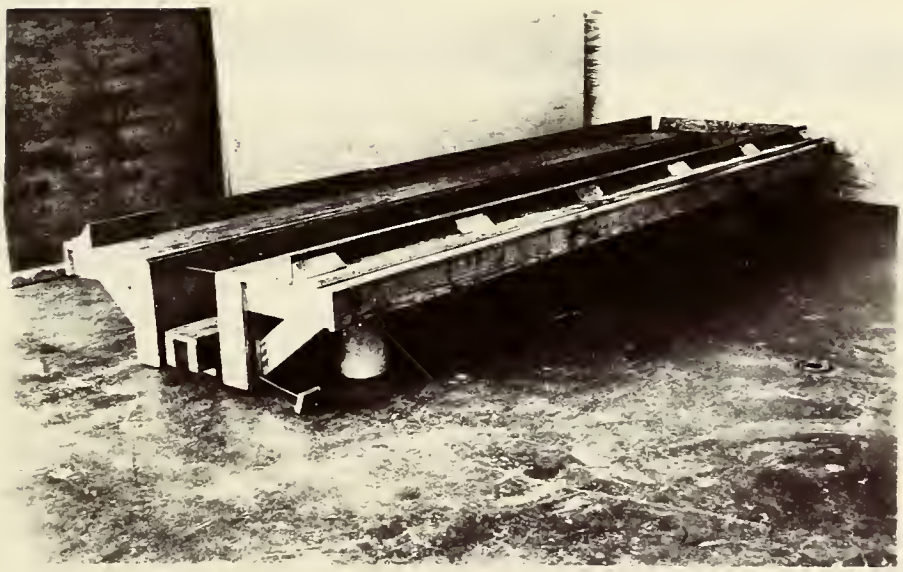

FIGURE 6. FORMS PRIOR TO PLACING CONCRETE

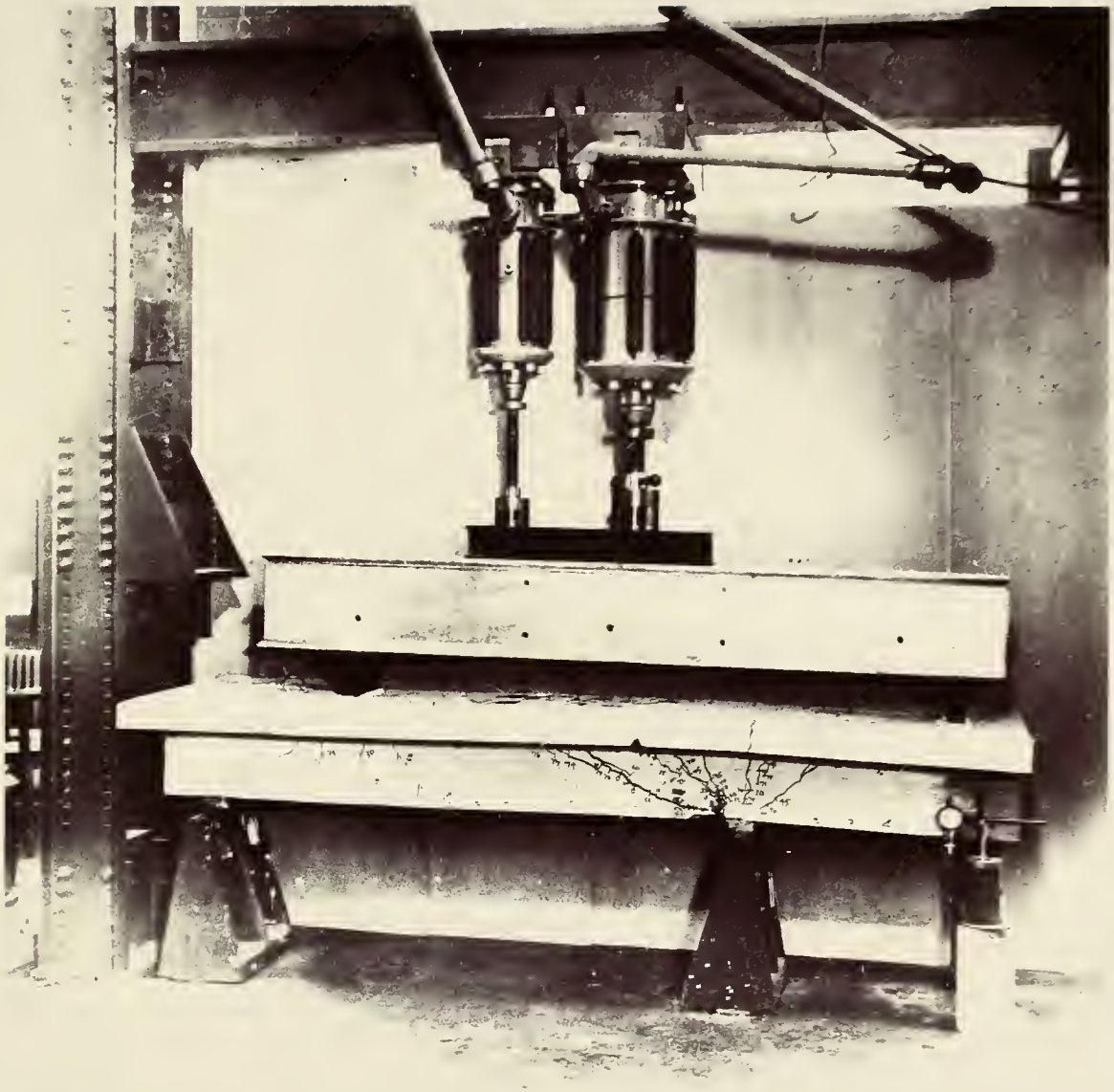

FIGURE 7. TEST SET-UP

SERIES	U	V
IIT	42.2"	29.8"
IIIT	49.2"	40.8"
IVT	56.4"	51.6"

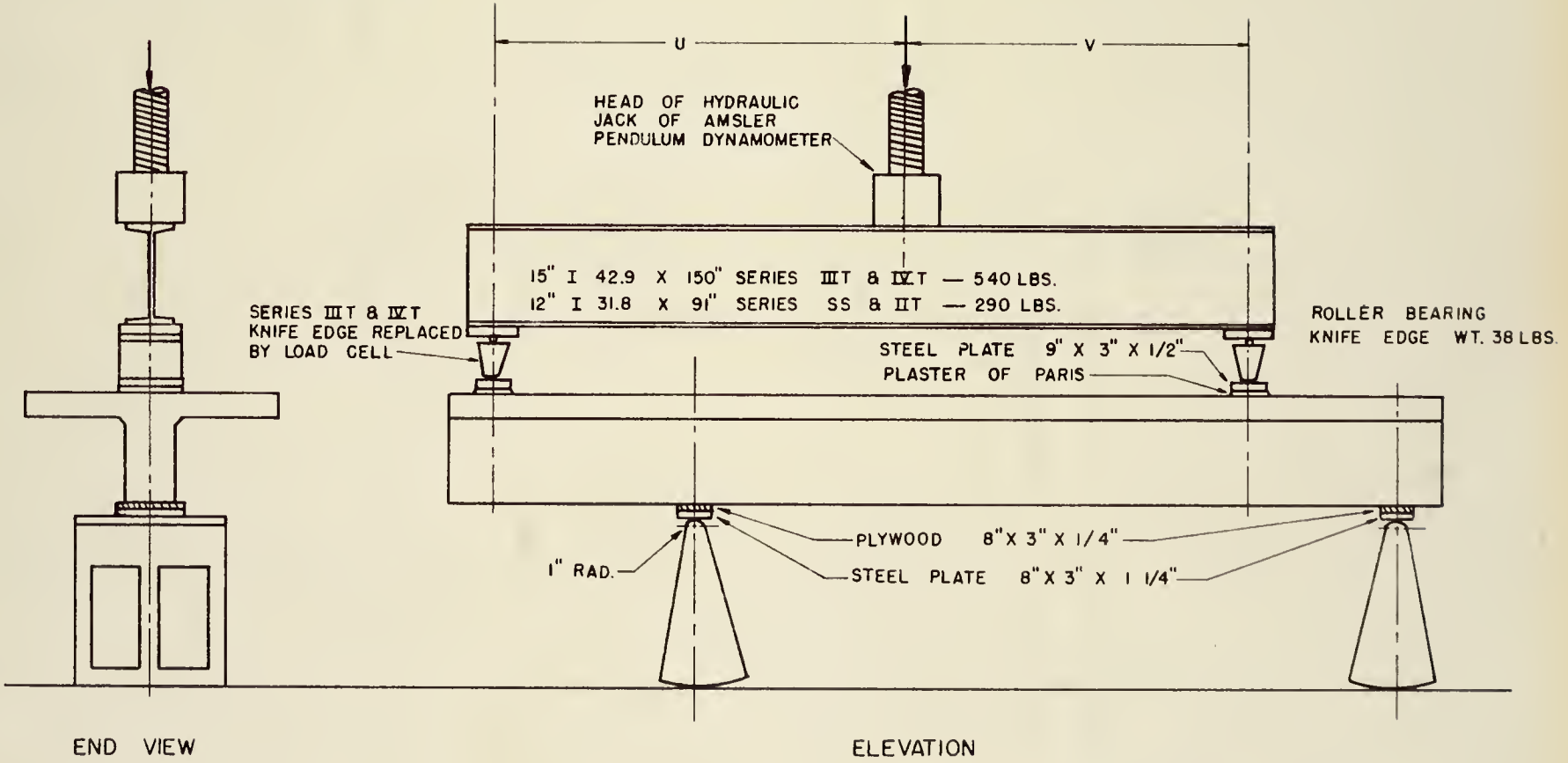
U
V
HEAD OF HYDRAULIC JACK OF AMSLER PENDULUM DYNAMOMETER
15" I 42.9 X 150" SERIES IIIT & IVT — 540 LBS.
12" I 31.8 X 91" SERIES SS & IIT — 290 LBS.
SERIES IIIT & IVT KNIFE EDGE REPLACED BY LOAD CELL
ROLLER BEARING KNIFE EDGE WT. 38 LBS.
STEEL PLATE 9" X 3" X 1/2"
PLASTER OF PARIS
PLYWOOD 8"X 3" X 1/4"
1" RAD.
STEEL PLATE 8"X 3" X 1 1/4"
END VIEW
ELEVATION
Scale: 1"= 20"

FIGURE 8. DETAILS OF TEST SET-UP

forms with five inch gage lengths before the specimen was cast, so that they would be embedded in the concrete. The displacements were measured to the nearest .0001 inch.

Vertical deflections were measured at the quarter points for the simple-span series and under the load, P_1 for the cantilever portion of the restrained series using Federal dial gages with accuracy to the nearest .001 inch. These deflection dials were mounted on solid supports with the movable stem of the gage compressed and resting on an aluminum tee which was mounted on the bottom of the beam. When the beam deflected, the stem of the gage moved down or out; thus, upon failure of the beam the aluminum tee would move away from the gage without any possibility of harming the gage.

The sides of each beam were painted white and gridded so that the crack pattern could be traced and later recorded on crack pattern sheets. After each increase in load, the crack penetration was traced and the load marked on the beam.

The beam was loaded in increments of one to five kips, with decreasing increments used as the load approached the ultimate load.

Some of the concrete control cylinders were tested in compression with the remainder being tested in split-tension. Two of the compression cylinders were used to determine the modulus of elasticity of the concrete, with the aid of a ten-inch extensometer attached to the cylinders.

TEST RESULTS

The pertinent test results are given in tabular form in Table 5. Pictures of the beams after testing are presented in Figures 9 thru 14. Graphical representations of strains and deflections are presented in this section and tabular values can be found in Appendix D. Each beam has been drawn to scale, showing the crack pattern and the locations of Whittemore and SR-4 gages. A brief discussion of each beam is presented in an attempt to correlate the strains and deflections with the observations made during the test. The loads reported are total applied loads, not including the weight of the loading set-up, which can be obtained from Figure 7. Note: Figure 19 is a pictorial explanation of the way in which the specimens are presented on the crack pattern sheets.

The critical diagonal tension crack in beams without web reinforcement was easily determined. However, for beams with web reinforcement the effects of the diagonal tension crack were less noticeable and a definite diagonal cracking load was difficult to determine. For this reason the diagonal cracking load is herein defined as the load at which the critical diagonal crack was observed to cross the neutral axis, using the cracked-section theory. The depth

Table 5. Summary of Test Results.

Beam Designation	Diagonal Cracking Load P_c# (kips)	Ultimate Load P_c# (kips)	Shearing Stress At Diagonal Cracking v_c## (psi)	Ultimate Shear Stress v_c## (psi)	Mode of Failure###	Remarks
SS-1	20	20.0	151.7	151.7	D.T.	
SS-2	22.9	22.9	173.1	173.1	D.T.	
SS-3	20	20.0	151.7	151.7	D.T.	
SS-4	20	21.9	151.7	166.0	D.T.	
II T-1	49	49.0	226.0	226.0	D.T.	
II T-2	38	68.0	175.7	314.0	S.C.	
II T-3	66	77.0	305.5	355.0	S.C.-F.T.	Tension Steel Yielding at P = 64^k
III T-1	35	49.0	128.7	180.0	S.C.	
III T-2	40	51.3	147.2	188.0	D.T.	
III T-3	35	53.0	128.7	195.0	S.C.-F.T.	Tension Steel Yielding at P=49^k
III T-4	30	57.9	110.2	213.0	S.C.-F.T.	Tension Steel Yielding at P=50^k
IV T-1	42	48.0	128.0	146.0	S.C.	
IV T-2	54	61.3	164.2	187.0	S.C.	
IV T-3	48	59.2	146.3	181.0	S.C.-F.T.	Tension Steel Yielding at P=57^k

Total applied load. (Does not include dead weight of specimen and loading apparatus.)
Average shearing stress v = v/bd, in critical shear span.
D.T. - Diagonal Tension; S.C. - Shear Compression; F.T. Flexural Tension.

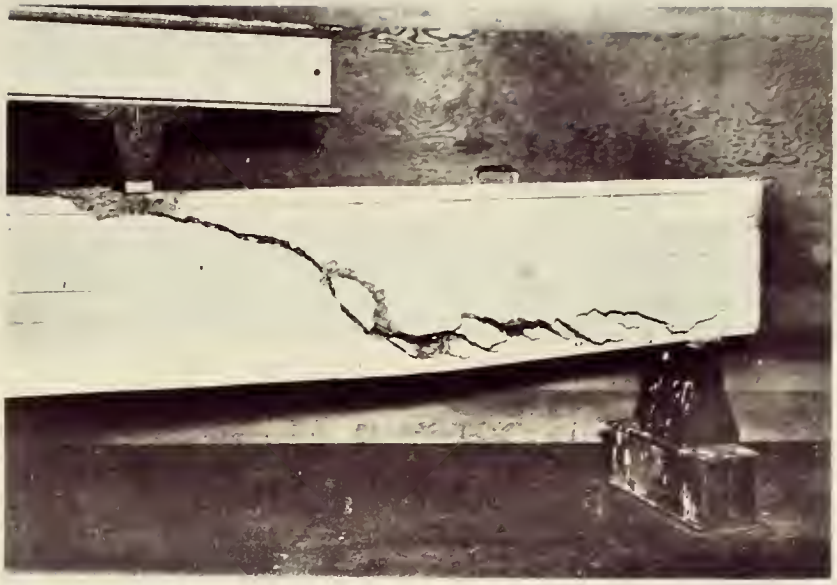

BEAM SS - 4

TYPICAL BEAM OF SERIES SS
(BEAM SS-1)

FIGURE 3. BEAMS AFTER TEST -- SERIES S

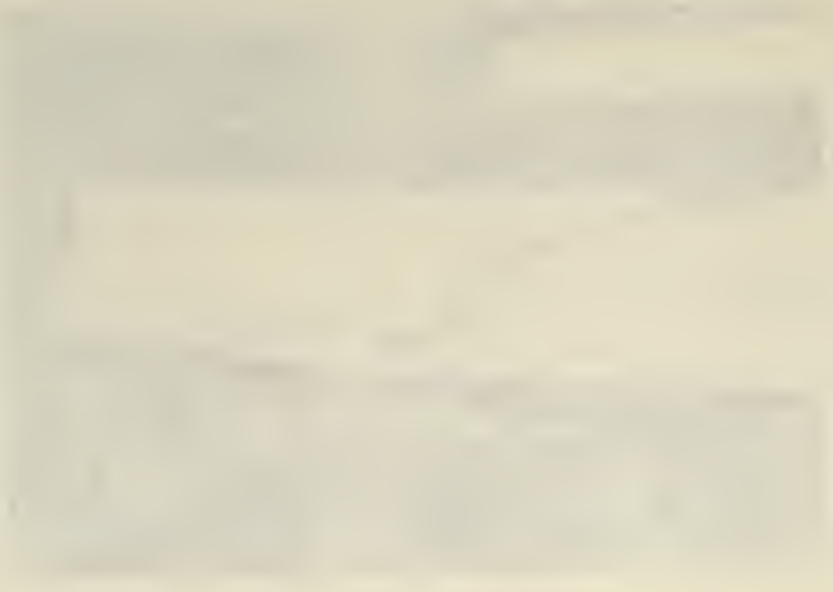

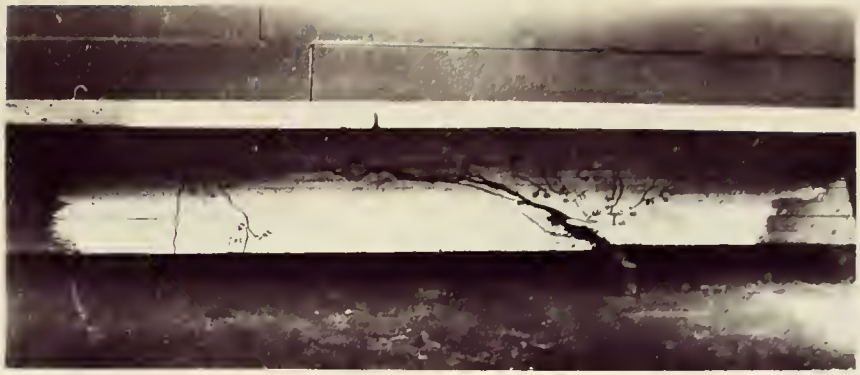

BEAM IIT—1

BEAM IIT-2

BEAM IIT-3

FIGURE 10. BEAMS AFTER TEST — SERIES IIT

BEAM IIIT-1

BEAM IIIT-2

FIGURE 11. BEAMS AFTER TEST – SERIES IIIT

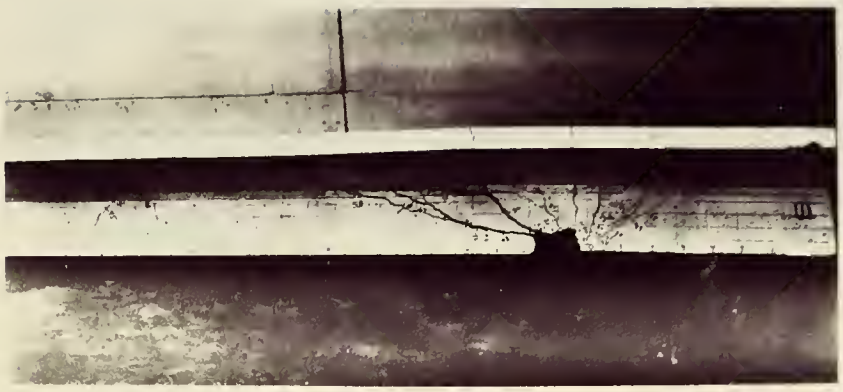

BEAM IIIT - 3

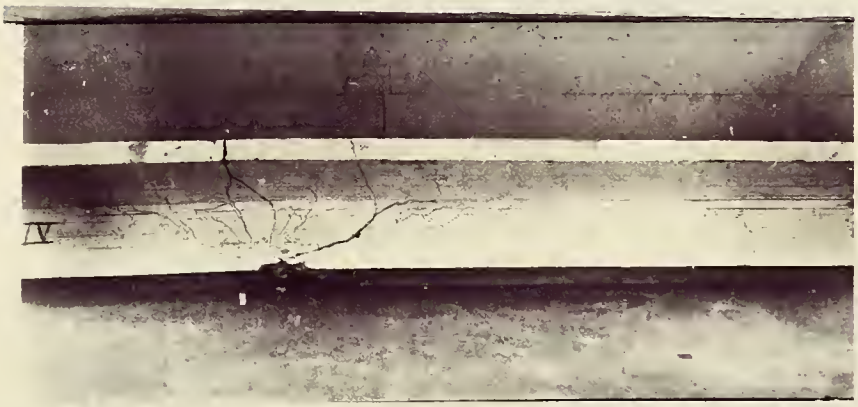

BEAM IIIT - 4

FIGURE 12. BEAMS AFTER TEST — SERIES IIIT (cont'd)

BEAM IVT-1

BEAM IVT - 2

BEAM IVT - 3

FIGURE 13. BEAMS AFTER TEST — SERIES IVT

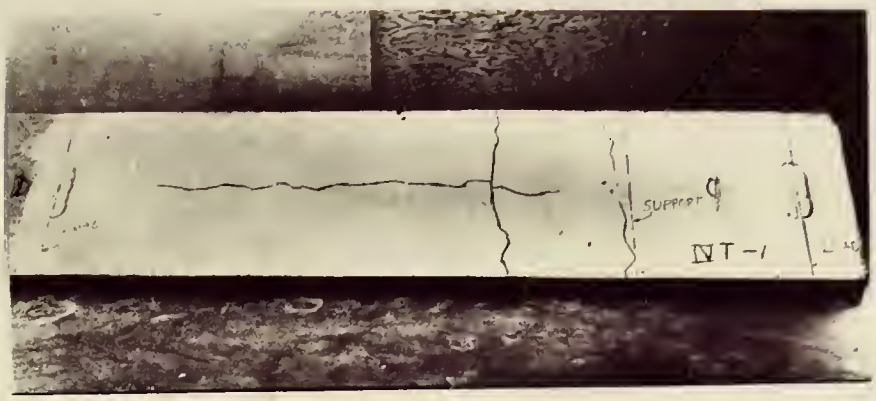

BEAM IVT-1

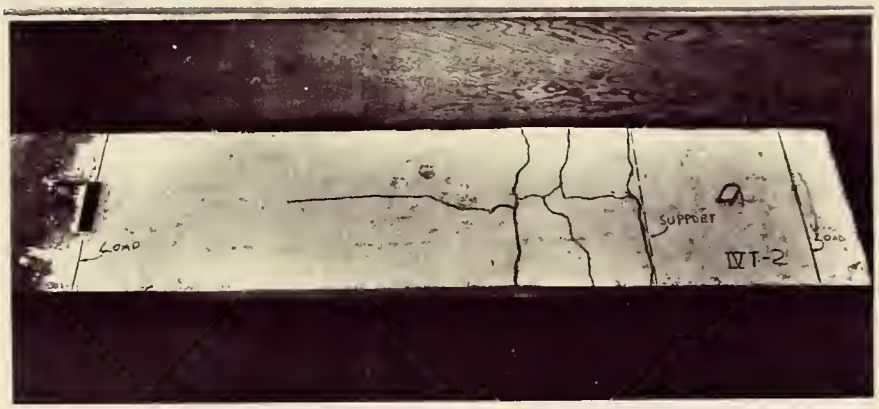

BEAM IVT-2

BEAM IVT-3

FIGURE 14. TOP OF FLANGE AFTER TEST — SERIES IVT

of cracked-section neutral axis for the restrained beams was 3.66" and for the simply supported series varied from 1.88 to 2.27 inches.

Series SS

This series was tested to determine the effect of different flange widths on the behavior of a simply supported T-beam. The beams were 12'-0" long with the flange varying from no flange to 36" total flange width. Equal concentrated loads were placed at the third points of these beams. These beams had a shear span-to-depth ratio (a/d) of 4.00. Whittemore gage points were embedded in the top and bottom of the flange to determine any variation in the strain across the flange. These gage points are located at the centerline of span, and are described on the crack pattern sheets. Two 10" gage lengths were used at each gage location and the readings were averaged. This procedure was used due to the low strain levels which were encountered. These low strains were anticipated because the calculated ultimate load on the beam to cause a shear failure was approximately half of the necessary load to cause a flexural failure.

Beam SS-1 (36" flange)

At a load of 10-11^{k} the flexural cracks began to incline toward the loading points. With increasing load, these cracks continued to progress toward the load points but did not enter the flange, even though the bottom of the flange was in tension (Figure 17). (Note: The values on the

ordinate axis are reference values; not an ordinate from the abscissa axis. Notice the point of zero strain indicated on each plot in the center section of each graph.) At load of 19^{k} the critical diagonal crack was noticeable on the east side but appeared on the west side as a slight inclination of a flexural crack. This crack opened slightly more upon increasing the load to 21^{k}, but when the load reached 21.3^{k} the beam suddenly failed in a diagonal tension mode. The crack extended thru the flange and also split the concrete along the longitudinal steel back to the support. This splitting continued along the portion of the longitudinal steel which was bent up at the end. The constant slope of the steel strain and deflection plots (Figures 15 and 16) indicates that the beam did not show any signs of a failure by flexure.

Beam SS-2 (30" flange)

The flexural cracks began to incline toward the loads at $10\text{-}11^{k}$, as was the case with Beam SS-1. The first appearance of the critical crack was at 20^{k} and, with an increase in load to 22^{k}, the crack progressed a small distance as can be seen in the crack pattern of the west side (see Figure 19). Then with a small increase in load (to 22.9^{k}), the beam failed as this crack extended through the flange to the loading point and back to the support, splitting the concrete away from the reinforcing steel. The flange also cracked at the point where the diagonal crack in the stem reached the bottom of the flange, and then the portion of

the flange between the two cracks buckled as the beam failed.

Here, as in Beam SS-1, the steel strains and deflections were still quite linear (see Figures 15 and 16), thus indicating that the beam had not shown any signs of a flexural failure.

Beam SS-3 (24" flange)

The flexural cracks started to show the effect of shear at approximately 12^k by inclining toward the loading points. A diagonal crack appeared near the mid-height of the web on the west side of the south end at a load of 16^k. With an increase in load to 18^k, this crack progressed a small distance in both directions. On the east side no diagonal crack could be found; only an inclination of the flexural crack was apparent. At a load of 20^k, a new diagonal crack appeared at the south end of the west side and opened up wide but the beam continued to carry the load. Again, the east side showed only a small diagonal crack near the flange. The beam continued to carry the load until all readings were taken and then suddenly failed in a diagonal tension mode. Here again, another crack formed in the flange upon failure and then a portion of the flange buckled (see Figure 22). The concrete split back along the steel as it did in the two previous beams. In the two previous beams (SS-1 and SS-2) no distinct variation in the strain across the flange could be observed. However, the

concrete strain for Beam SS-3 showed a slight decrease near the edge of the flange (see Figure 18). The stresses or strains are so low (455 MII max.) that this could very well have been a variation in the readings alone.

Beam SS-4 (No flange)

The flexural cracks began to incline toward the loading point at a load of approximately 6-8^{k}. At a load of 20^{k} the critical diagonal crack, an extension of a flexural crack, began to open up by small amounts at each load increase. The ultimate load was 21^{k}, and the beam held this load long enough for all readings to be taken and then suddenly failed.

From the crack pattern sheet, Figure 23, it can be seen that the cracking pattern of this beam was similar to that of the three previous beams. The flexural cracks came within 3 to 4 inches of the top and then stopped until failure. In the case of SS-4, the neutral axis was 4.00 inches down from the top (by straight line theory). The neutral axis depth of the three previous beams ranged between 2.27 and 1.88 inches, but the flange prevented the full penetration of the flexural cracks in these beams.

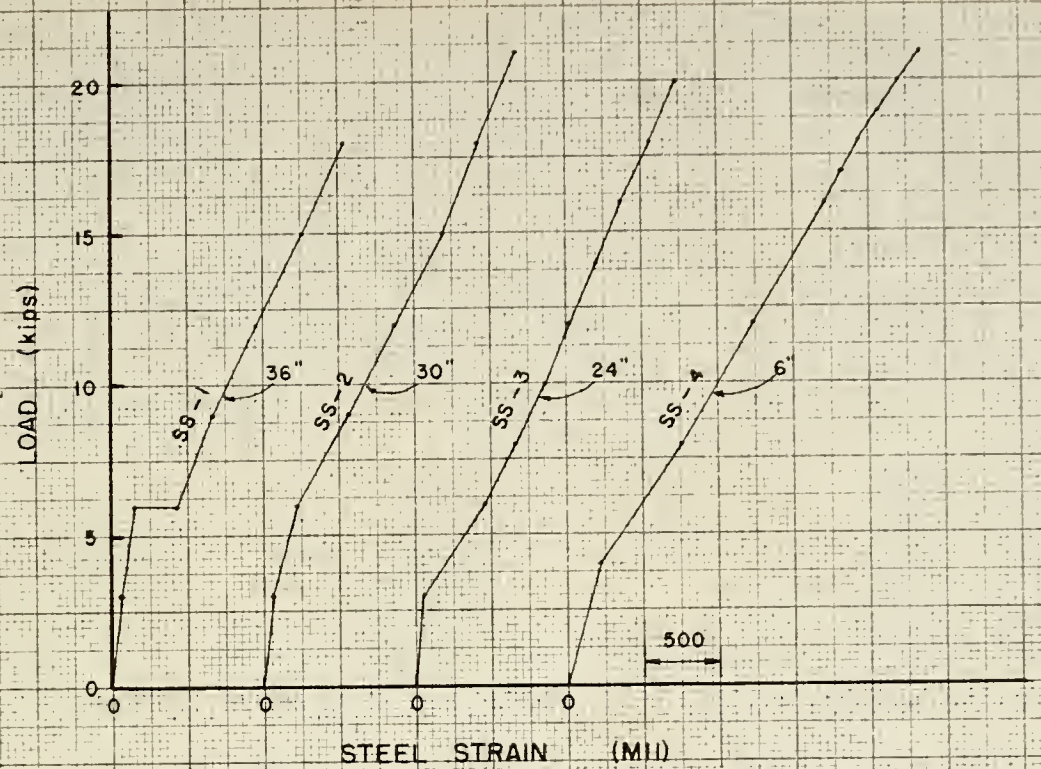

FIGURE 15. LOAD vs. STEEL STRAIN — SERIES SS

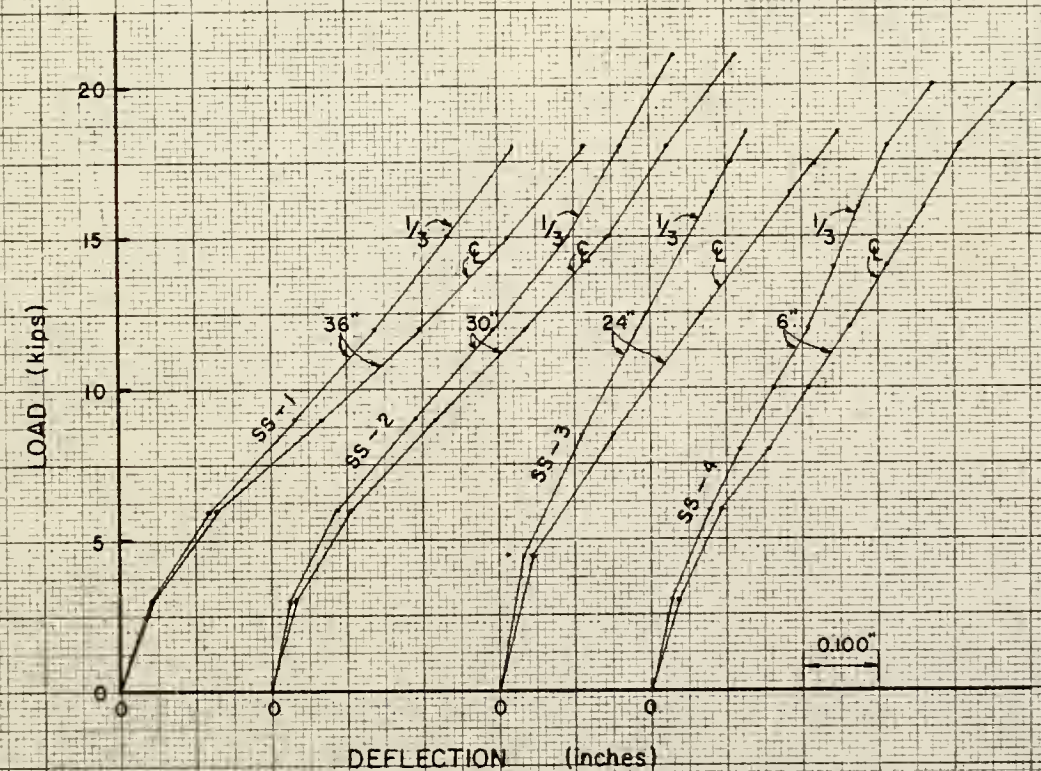

FIGURE 16. LOAD vs. DEFLECTION — SERIES SS

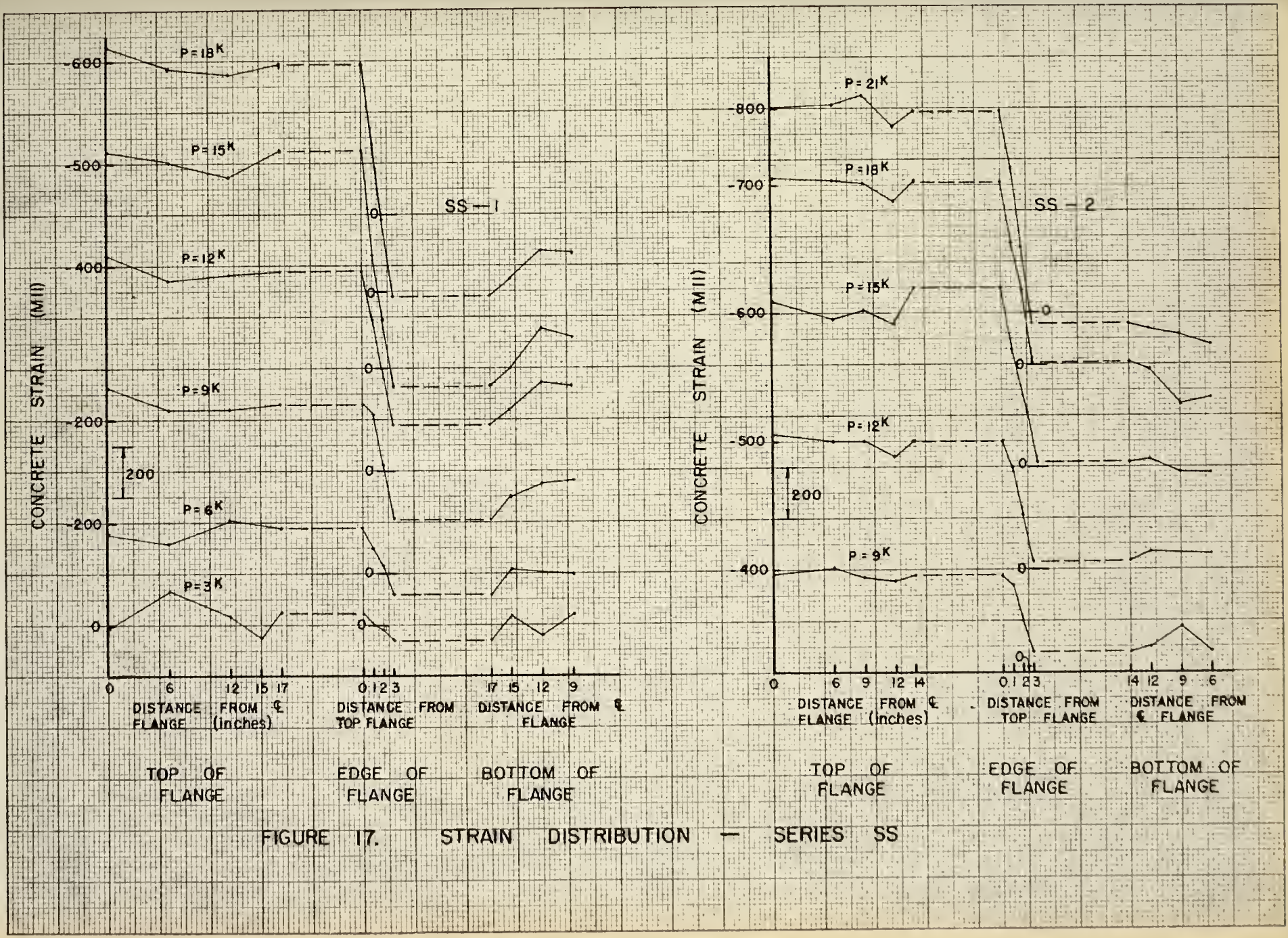

FIGURE 17. STRAIN DISTRIBUTION — SERIES SS

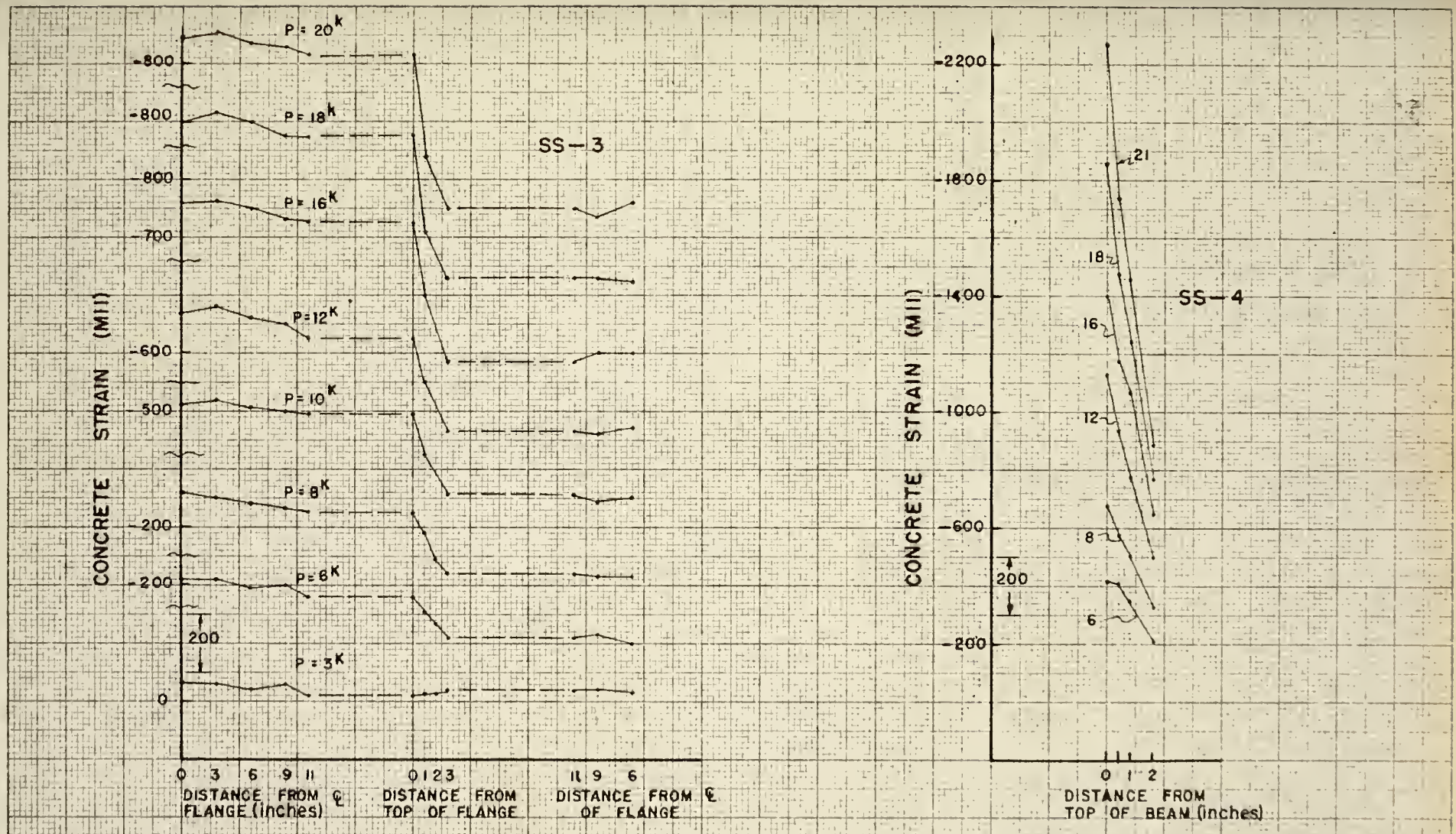

FIGURE 18. STRAIN DISTRIBUTION — SERIES SS

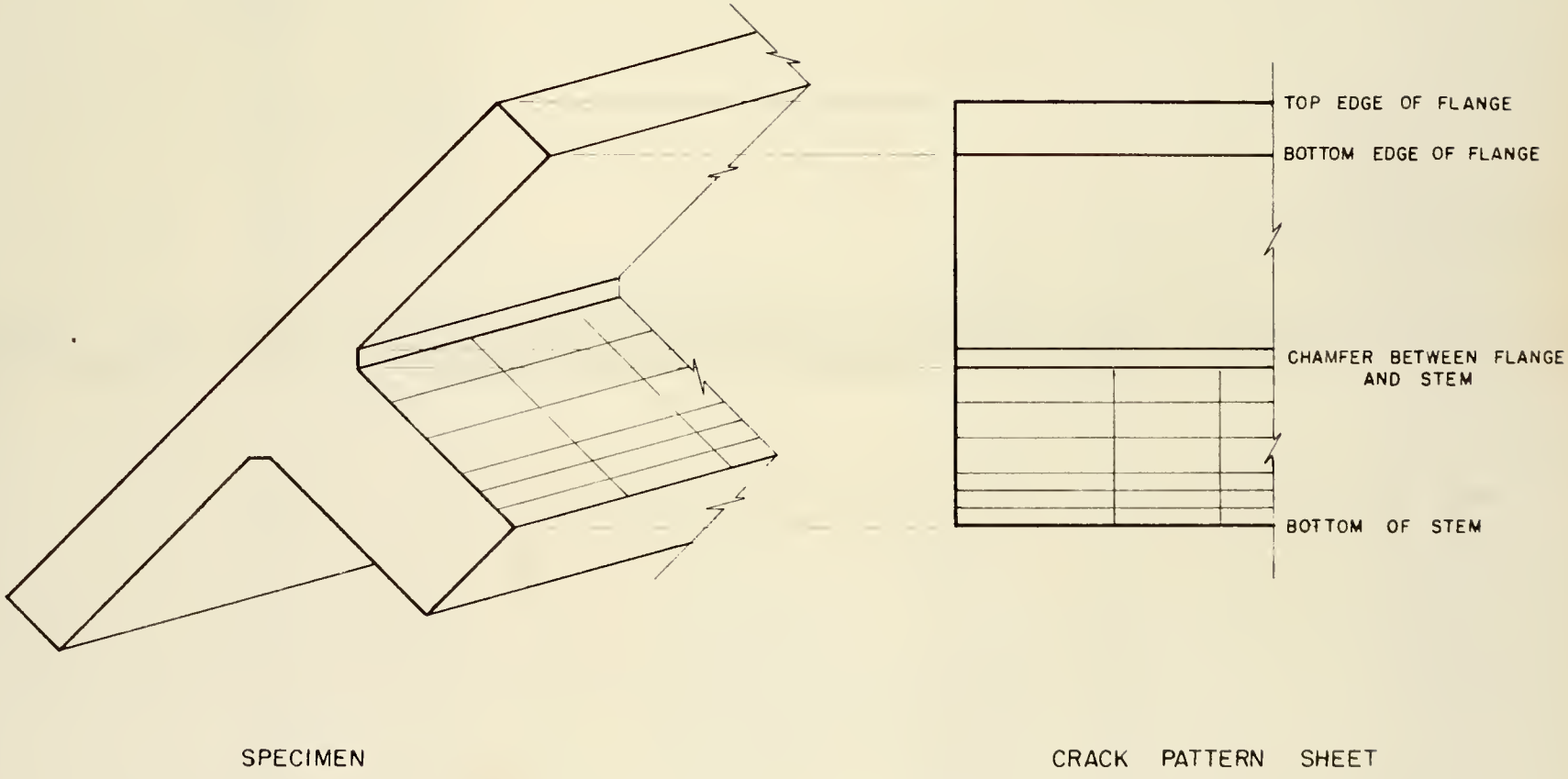

FIGURE 19. PICTORIAL REPRESENTATION OF SPECIMEN ON CRACK PATTERN SHEET

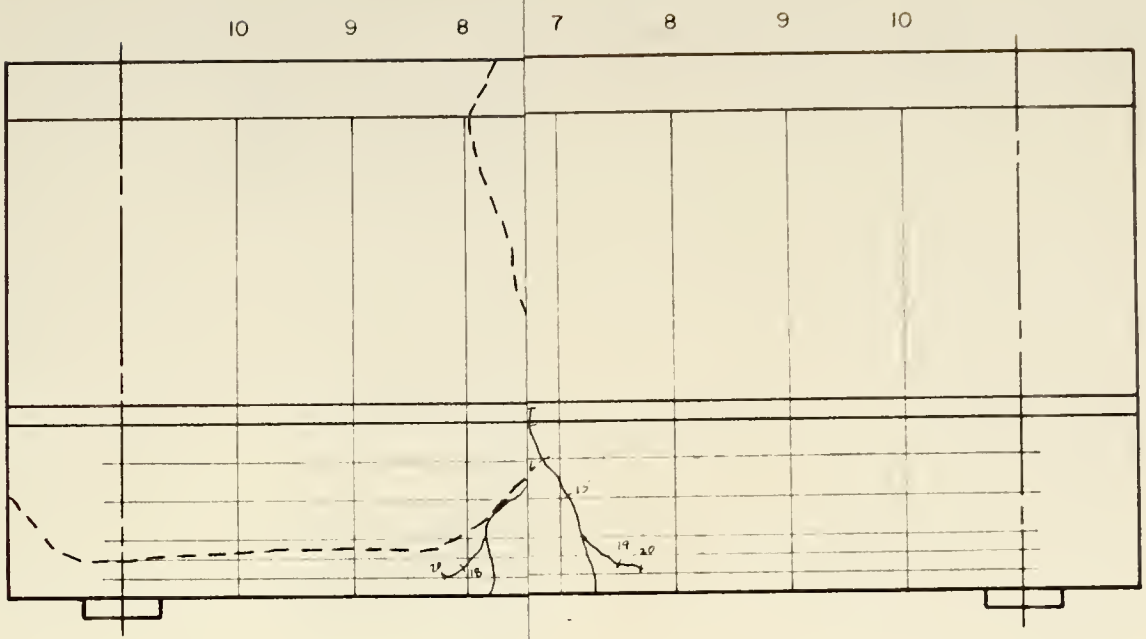

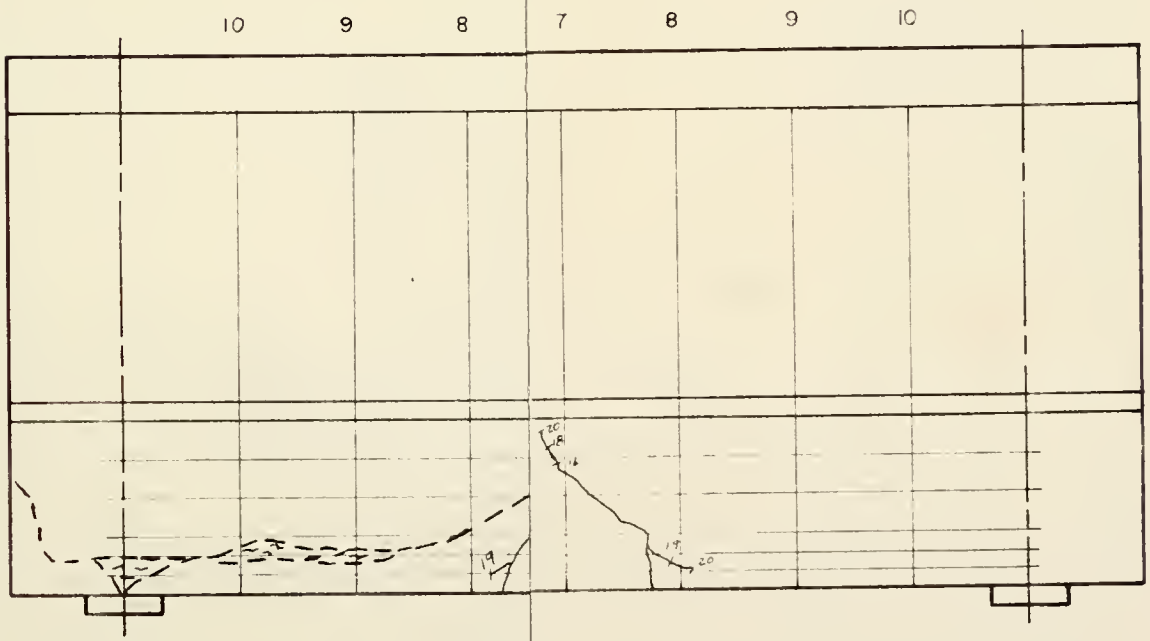

SR – 4 Gage
No. 6

Whittemore
Top
Edge
Botto

BEAM SS – I

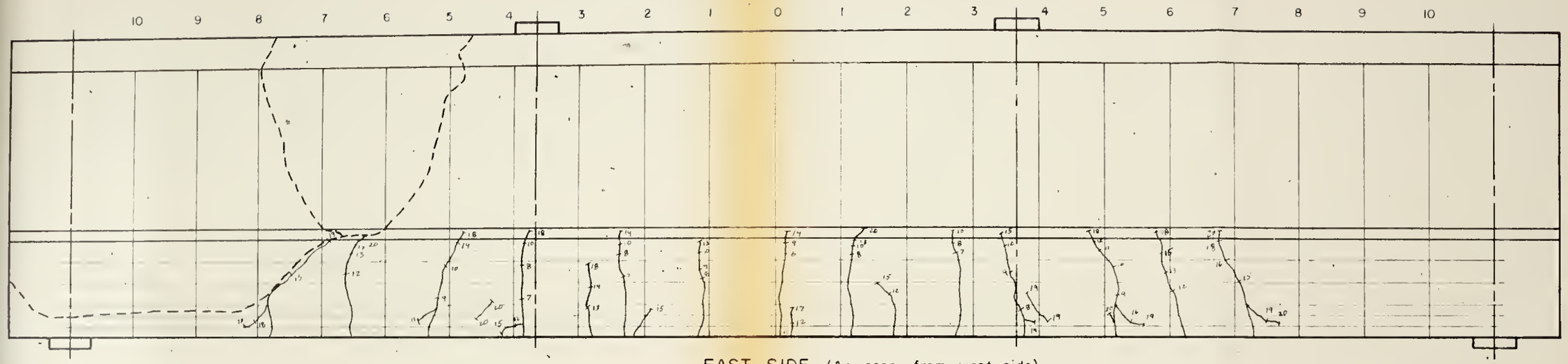

EAST SIDE (As seen from west side)

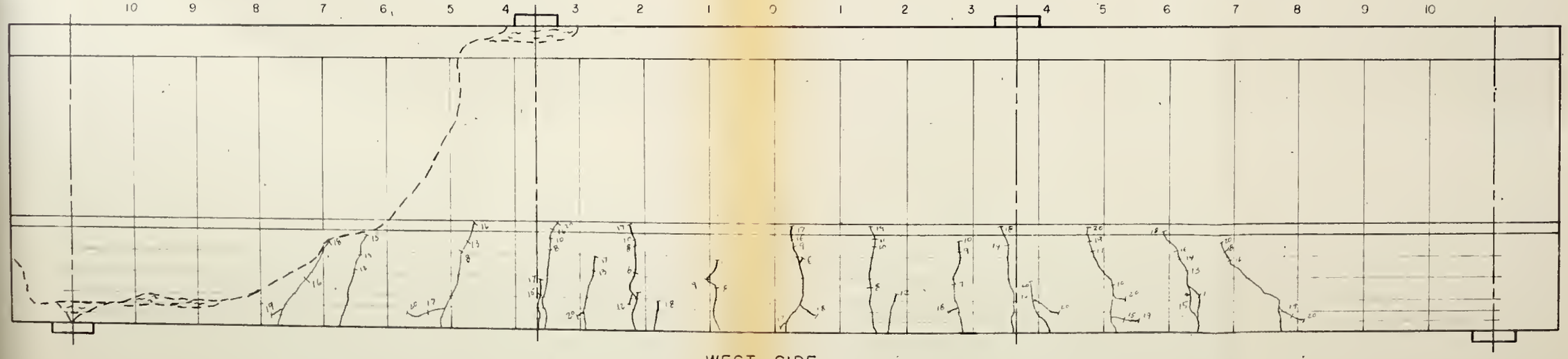

WEST SIDE

SR – 4 Gage Locations:
No. 6 Bar — At centerline of beam (W & E)

Whittemore Gage Locations:
Top of beam — 0", 6", 12", 15", 17" from centerline of beam
Edge of flange — 1", 2" down from top of flange
Bottom of flange — 6", 12", 15", 17" from centerline of beam

FIGURE 20. BEAM SS – 1

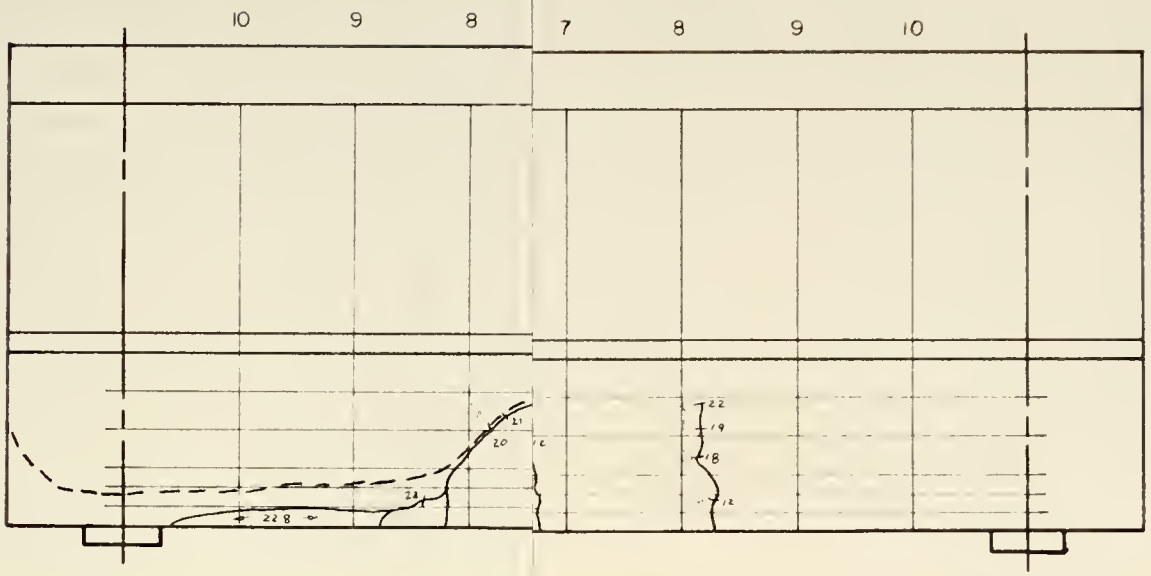

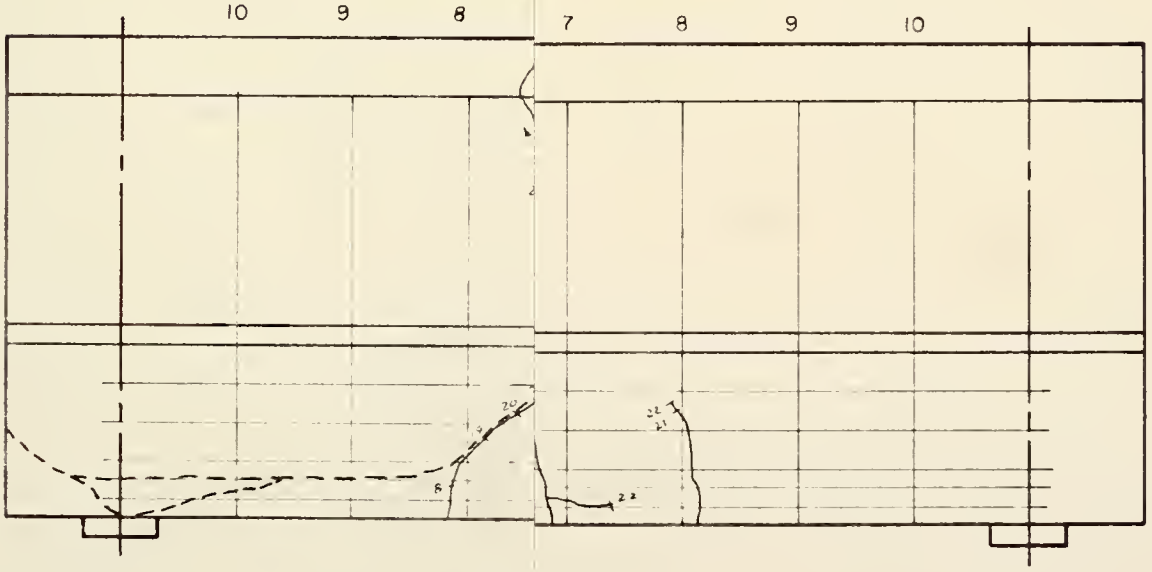

SR – 4 Gage
No. 6
Whittemore G
Top o
Edge
Botto

BEAM SS – 2

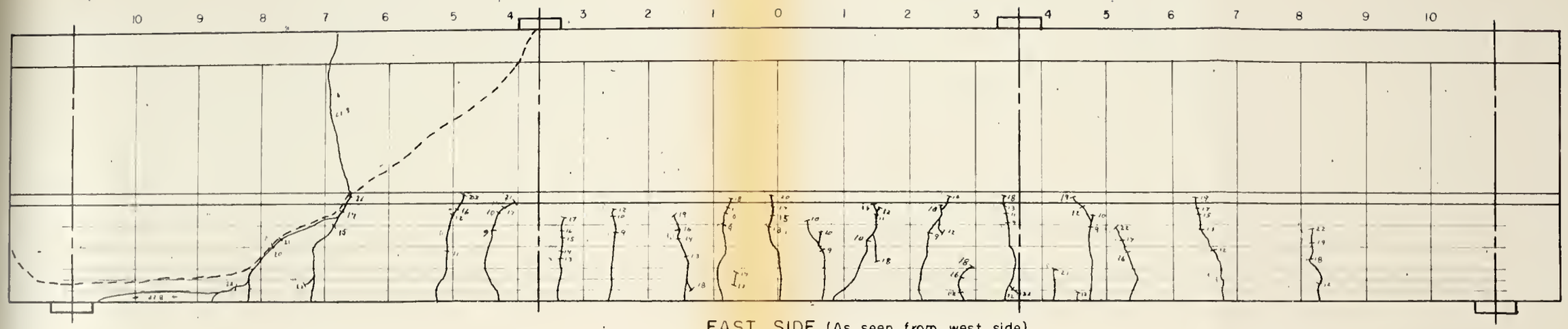

EAST SIDE (As seen from west side)

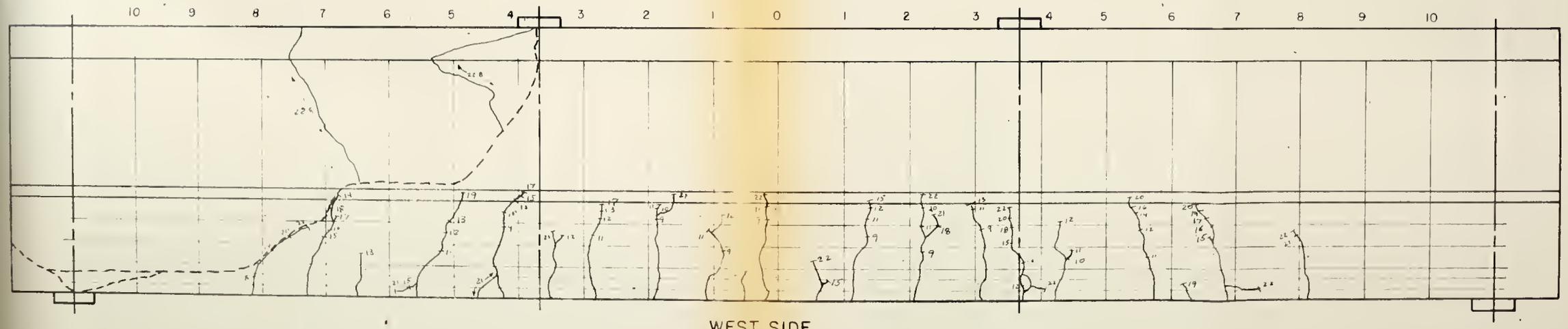

WEST SIDE

SR – 4 Gage Locations:

No. 6 Bar – At centerline of beam (E & W)

Whittemore Gage Locations:

Top of flange – 0,6",9",12",14" from centerline of beam
Edge of " – 1", 2" down from top of flange
Bottom of flange – 6",9",12",14" from centerline of beam

FIGURE 21. BEAM SS – 2

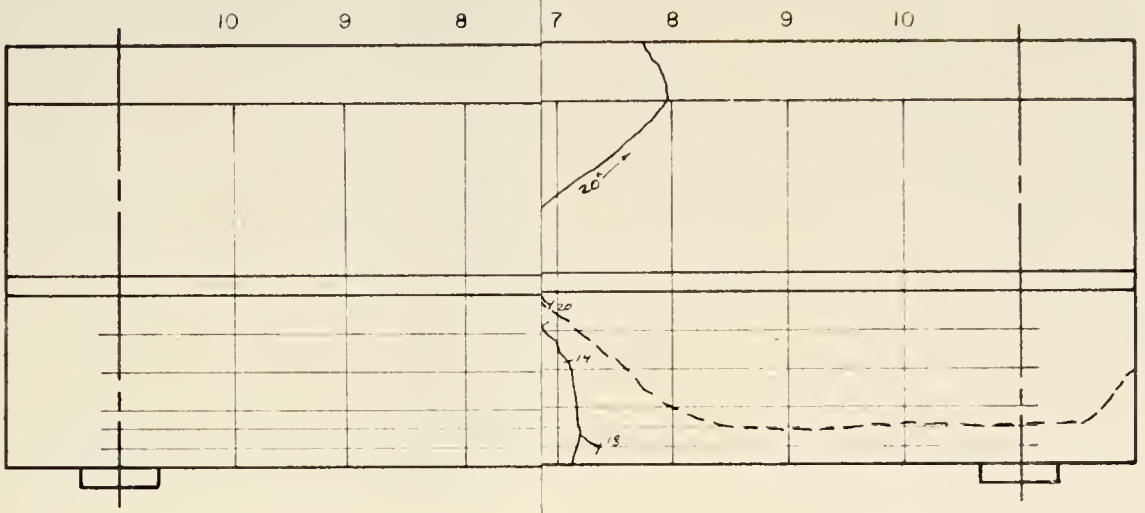

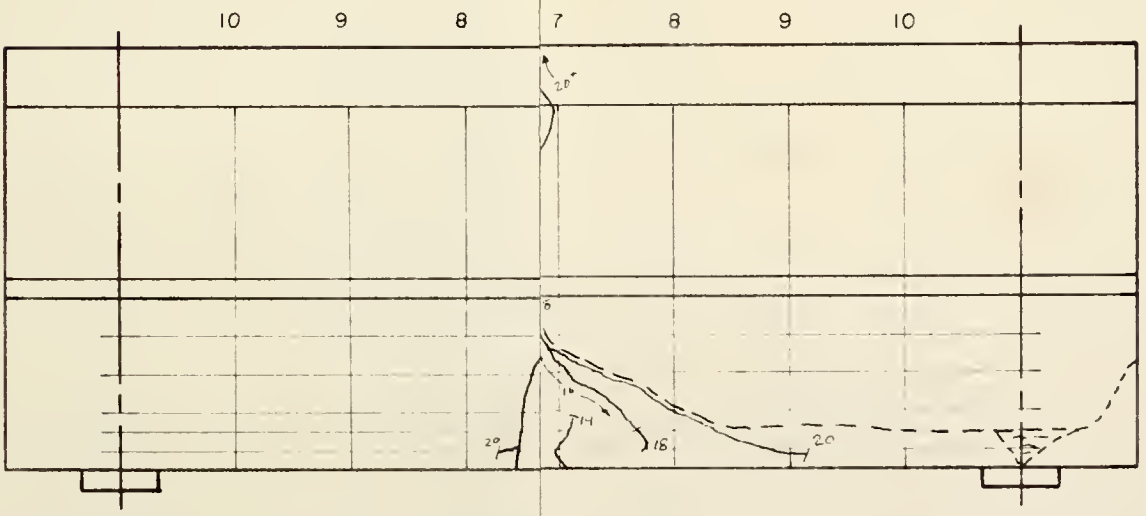

SR-4 Gage L
No. 6 E

Whittemore Gag
Top of b
Edge of
Bottom o

BEAM SS-3

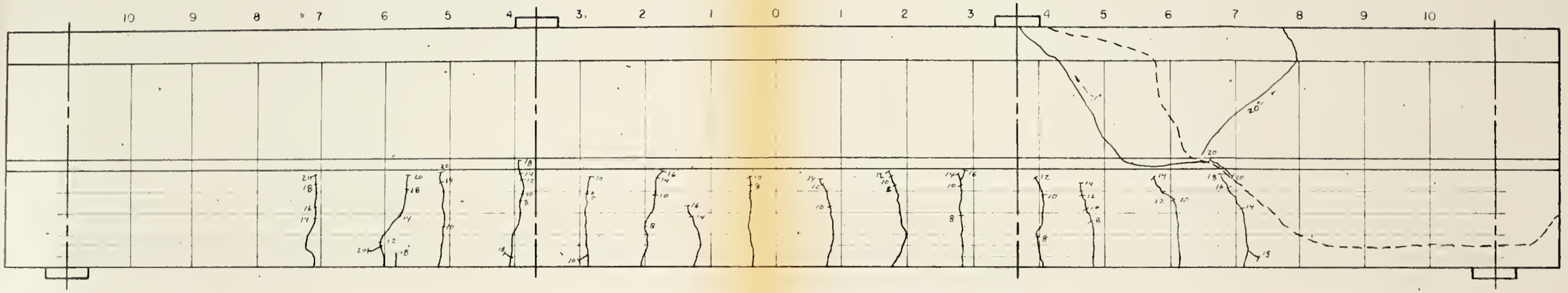

EAST SIDE - (As seen from west side)

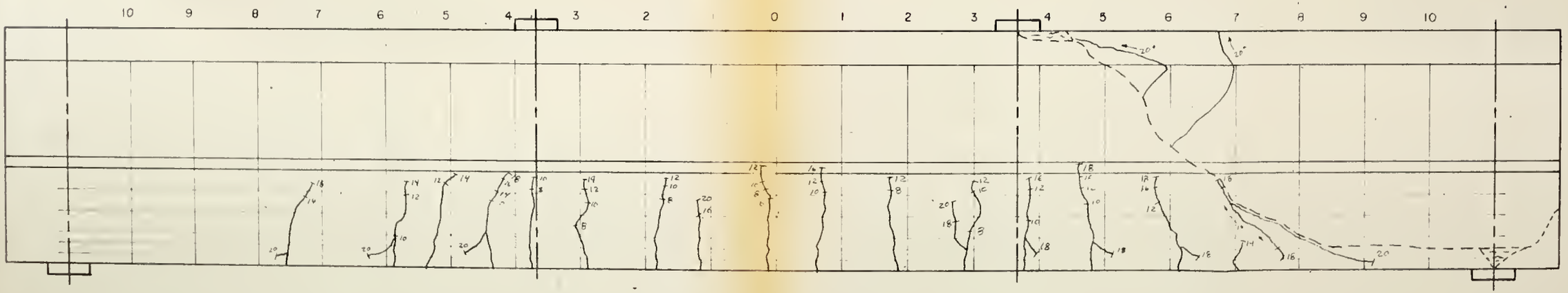

WEST SIDE

SR-4 Gage Locations:
No 6 Bar — At centerline of beam (W)

Whittemore Gage Locations:
Top of beam — 0", 3", 6", 9", & 11" from centerline of beam
Edge of flange — 1" & 2" down from top of flange
Bottom of " — 6", 9", & 11" " centerline of beam

FIGURE 22. BEAM SS-3

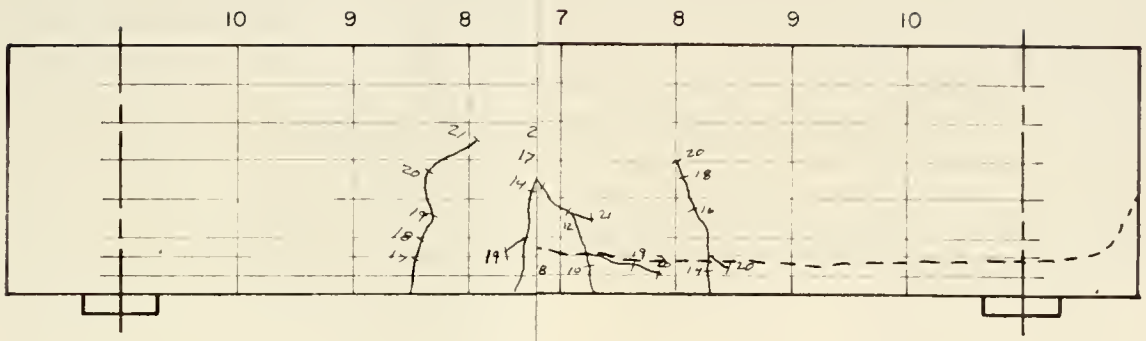

SR - 4 Gage
No. 6

Whittemore Gc
Top of
0.5", 1"

BEAM SS - 4

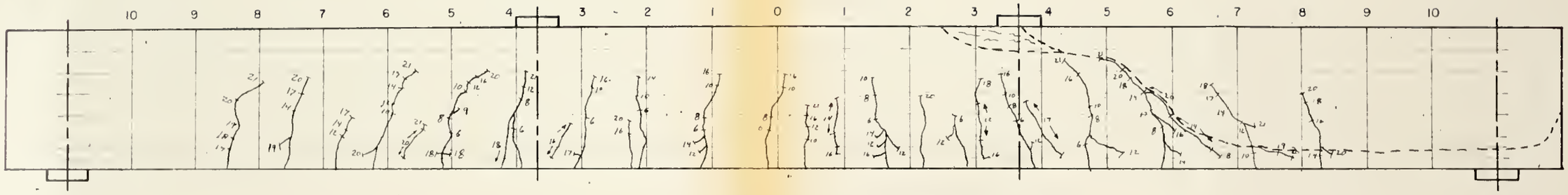

EAST SIDE (As seen from west side)

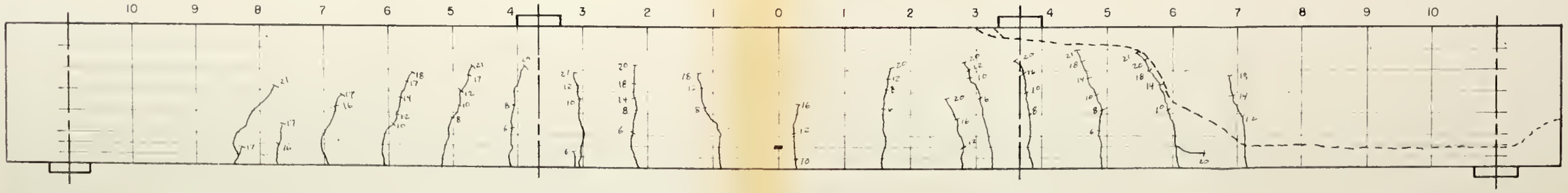

WEST SIDE

SR - 4 Gage Locations:

No. 6 Bar — At centerline of beam (W)

Whittemore Gage Locations:

Top of beam — 0" & 2" from centerline of beam

0.5", 1", 2" down from top of beam (W)

FIGURE 23. BEAM SS - 4

Series II T

The beams in this series all had one restrained end with the ratio of restraining moment to positive moment (M_1/M_2) equal to 2.0 (see Figure 4). A constant flange width of 30 inches was maintained. The amount of web reinforcement was the intended variable for beams in this series.

Beam II T - 1 (No Stirrups)

All measured strains and the deflections of the cantilevered end were very small until the occurrence of the first tension crack through the flange at a load of 26.7^k. This crack penetrated to within about 4 inches from the bottom face. At this load there was a significant increase in the strains and in the cantilever deflection (see Figures 24, 25 and 26). The next cracks to appear were diagonal cracks beginning at the intersection of the flange and the stem. These cracks occurred at a load of 35^k. Also, at 35^k, a longitudinal crack formed along the chamfer between the stem and flange, directly over the support on the west side. With subsequent increase in load, new diagonal cracks appeared farther from the support and extended straight toward the support as well as into the flange. At a load of 43^k, a new diagonal crack developed about 18 inches from the support on the east side and at the chamfer. This crack did not appear on the west side until a load of 46^k was reached. Upon increasing the load to 49^k, this crack extended

into the compression zone to within about 3 inches from the compression face, on the west side. The entire length of this critical crack was not observed on the east side before the beam failed. All readings were recorded and cracks traced prior to the beam's sudden failure, by this diagonal crack opening wide, as can be seen in Figure 32. Upon failure, the crack extended back to within about 8 inches of the interior load point before splitting through the flange. The strain distribution (Figure 29) indicates that the neutral axis moved to within about 4 inches of the compression face at a load of approximately 40^{k}. This plot also shows that the concrete strain 1/2 inch from the bottom was greater than that at the bottom for loads greater than 40^{k}. It also indicates the stress concentration due to the presence of the diagonal crack.

Beam II T - 2 (Stirrups at 6")

The first flexural crack appeared at a load of 22^{k} and extended to within 4 inches of the support. The next cracks to form were inclined and originated at the chamfer. At a load of 48^{k}, short diagonal cracks began to form in the chamfer on the west side, and with increasing load these cracks appeared farther from the support. At 48^{k} two critical diagonal cracks had formed. One had penetrated to a point 3 inches from the compression face. The other diagonal crack was farther from the support and at a flatter slope. By 59^{k} the latter crack extended to within 2 inches of the

bottom side, but did not penetrate any farther with increased load. At a load of 61^k a loud cracking noise was heard and the load dropped off to 56^k. At this point the gages on the stirrups showed that all the monitored stirrups were yielding. The load then picked up again and increased to 68^k before the beam failed by crushing of the concrete at the support.

At a load of about 50^k the concrete strain began increasing more rapidly, as can be seen by the change in slope of the concrete strain plot in Figure 26. All of the instrumented stirrups began picking up strain prior to a load of 45^k, but stirrups (b) and (c) were not crossed by a visible crack until loads of 48^k and 52^k, respectively were reached (see Figure 33). At this time each gage showed about 800 micro-inches per inch (MII) strain in each stirrup.

Beam II T - 3 (Stirrups at 3-1/2")

The first flexural crack appeared at 30^k, with subsequent cracks showing the effect of diagonal tension by inclining toward the support. The crack development was quite similar to that of Beam II T - 2, but with the cracks beginning at slightly higher loads in the case of Beam II T - 3. The critical diagonal crack formed at a load of 60^k and progressed directly toward the support on the east side. The same crack opened on the west side at the same load but a new diagonal crack just below the first crack opened at 66^k and progressed toward the support. At 75^k the second crack extended back toward P_2, parallel to the

crack which appeared at 60^k. The longitudinal steel began yielding at a load of 64^k. By failure, the first flexural crack had opened to a width of 3/8 to 1/2 inch, indicating the ductility of this beam, which can also be seen in the deflection plot (Figure 25).

Stirrups (a) and (c) began picking up strain at a load of 40^k, while stirrup (b) did not pick up strain until a load of 50^k was reached. However, at 50^k both stirrups (a) and (b) had been crossed by a diagonal crack; stirrup (c) was not crossed by a visible crack until a load of 60^k was attained. At 60^k stirrup (c) had a strain of about 1200 MII. Stirrup (b) had reached a strain of about 1500 MII at a load of 66^k when the critical diagonal crack load was first reached, but then the strain dropped off to 1250 MII by 70^k, indicating a decrease in stress of about 7500 psi. This decrease was probably due to redistribution of stress, with an increased rate of strain being taken by stirrup (a) beginning at 64^k and continuing until failure. Maximum load obtained was 77^k, which was the maximum capacity of the jacks being used. This was considered the ultimate load, since the concrete had spalled off about 1 inch up from the bottom. Strain of nearly 6000 MII had been recorded at the bottom surface at a load of 74^k. Also, the steel was well into the yield zone at the maximum load of 77^k. The beam was still carrying the load but the cantilever was continuing to deflect without increase in load.

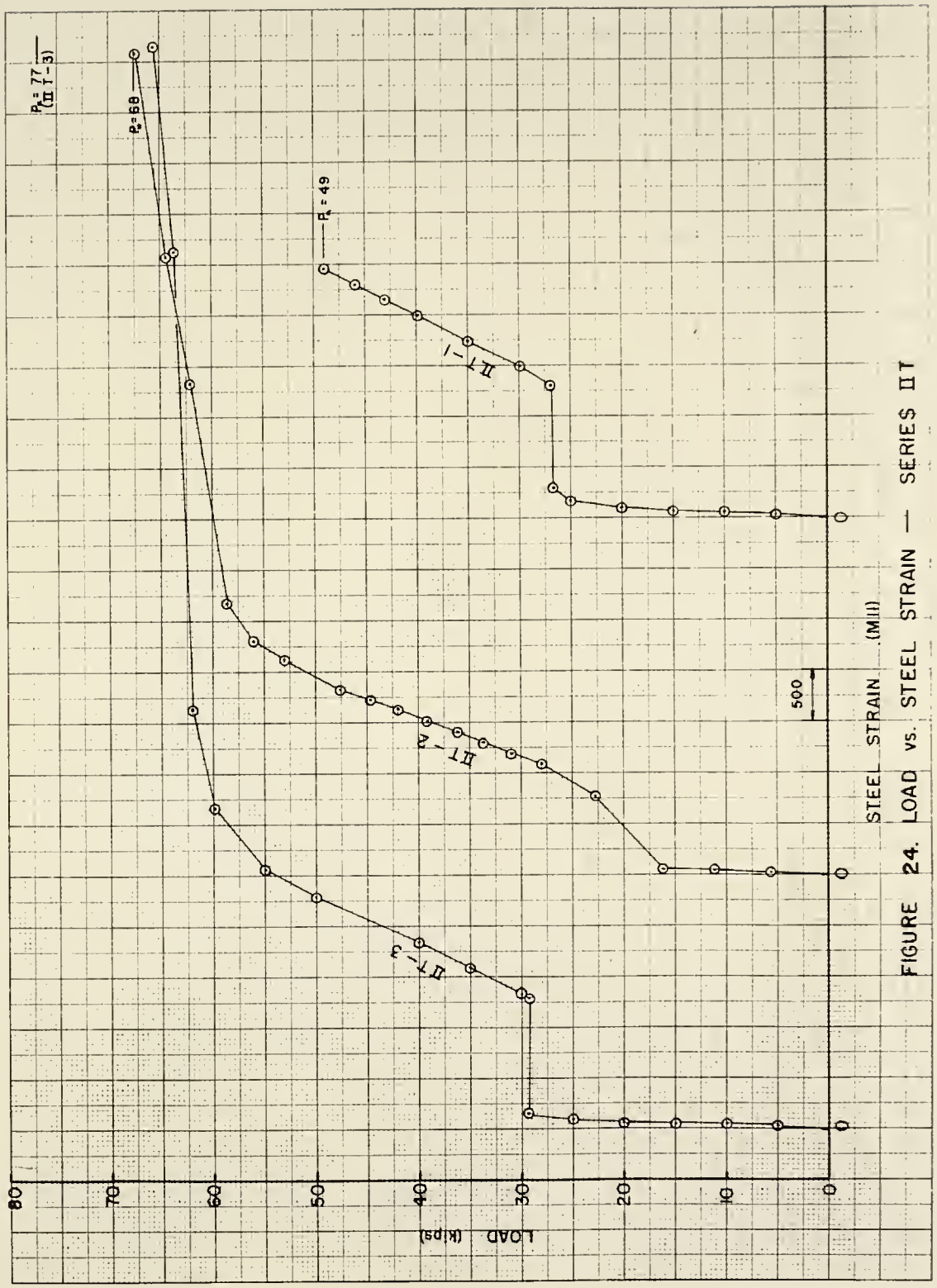

FIGURE 24. LOAD vs. STEEL STRAIN — SERIES Ω T

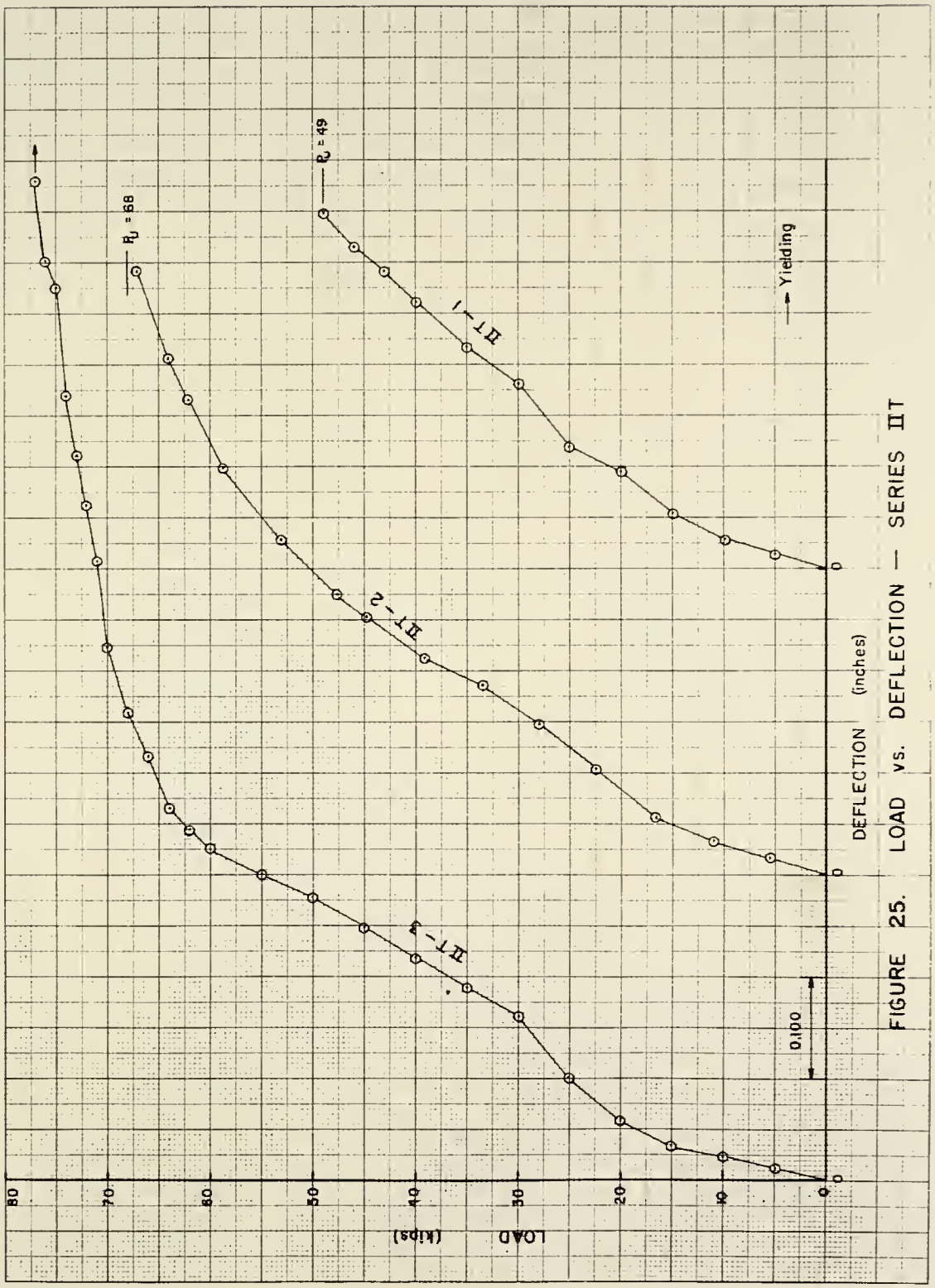

FIGURE 25. LOAD vs. DEFLECTION — SERIES IIT

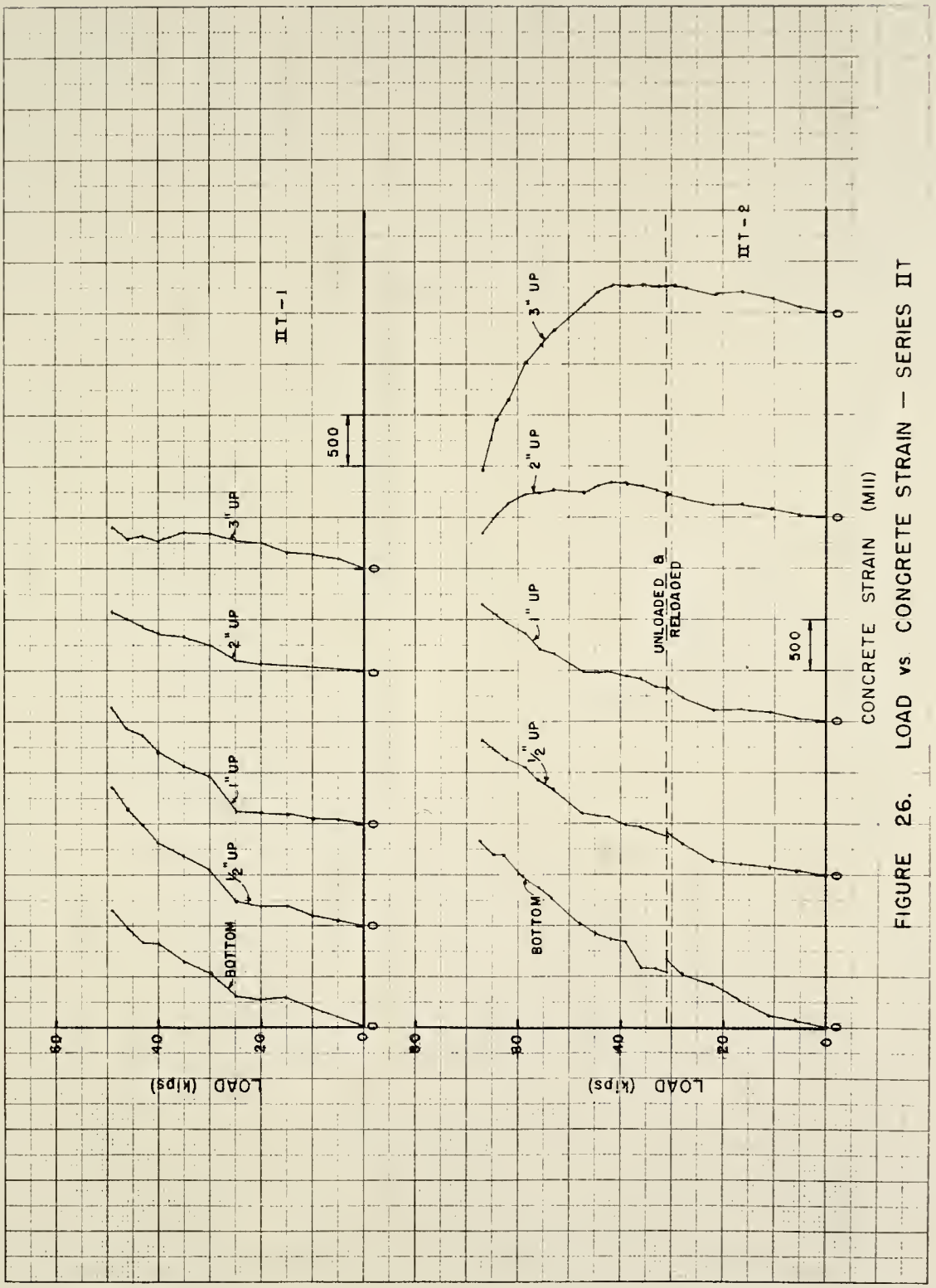

FIGURE 26. LOAD vs. CONCRETE STRAIN — SERIES IIT

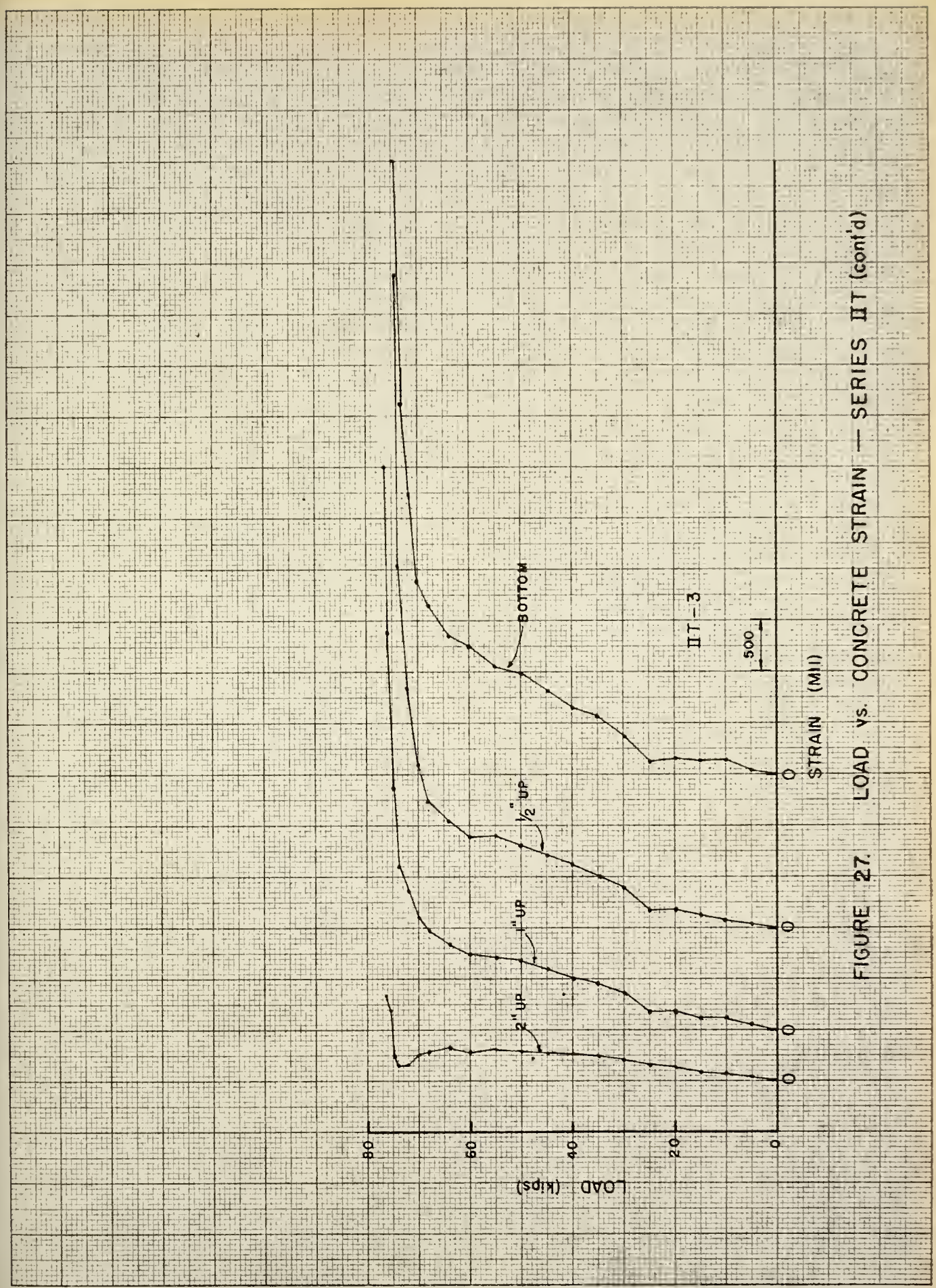

FIGURE 27. LOAD vs. CONCRETE STRAIN — SERIES IIT (cont'd)

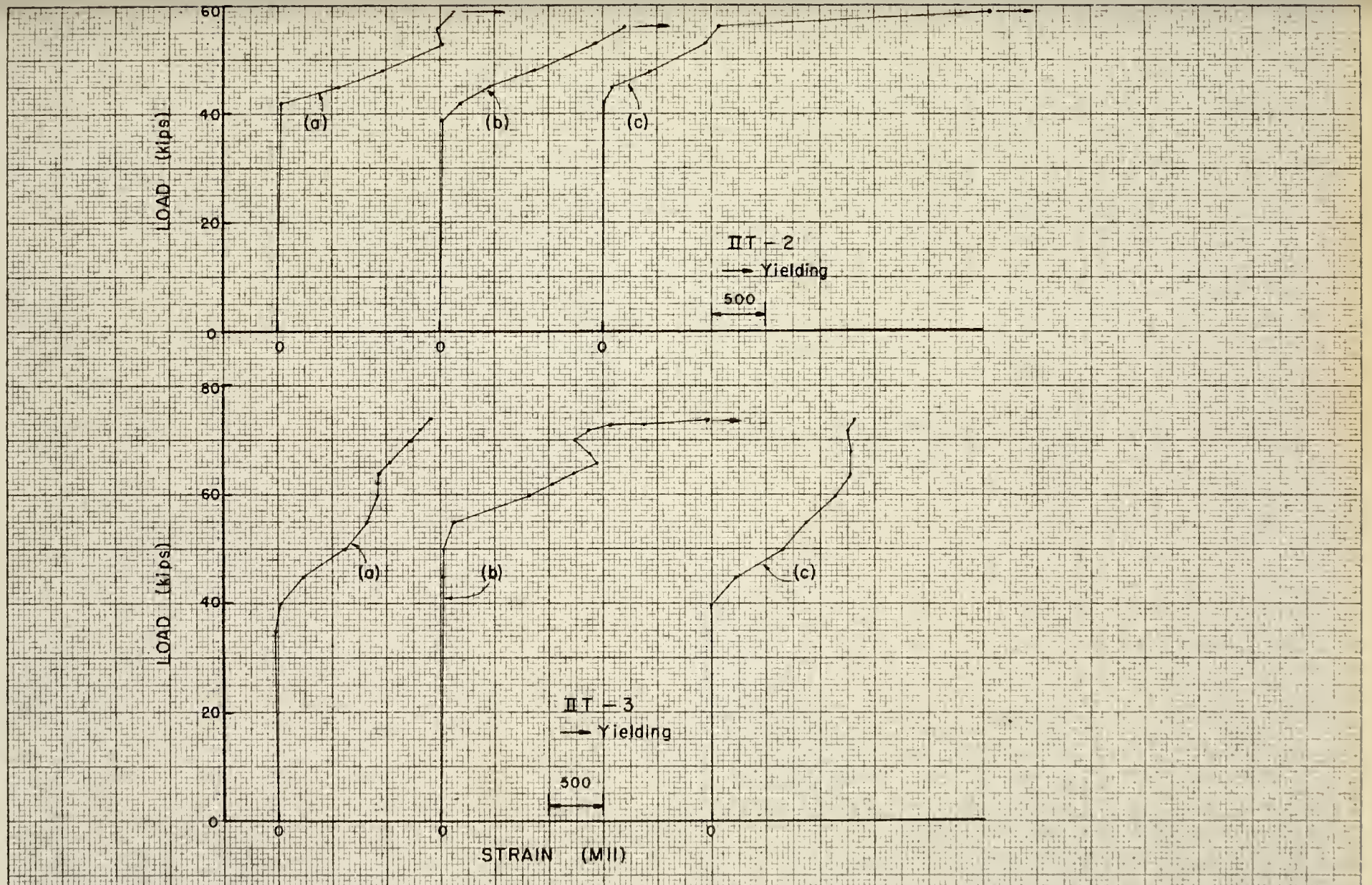

FIGURE 28. LOAD vs. STIRRUP STRAIN — SERIES IIT

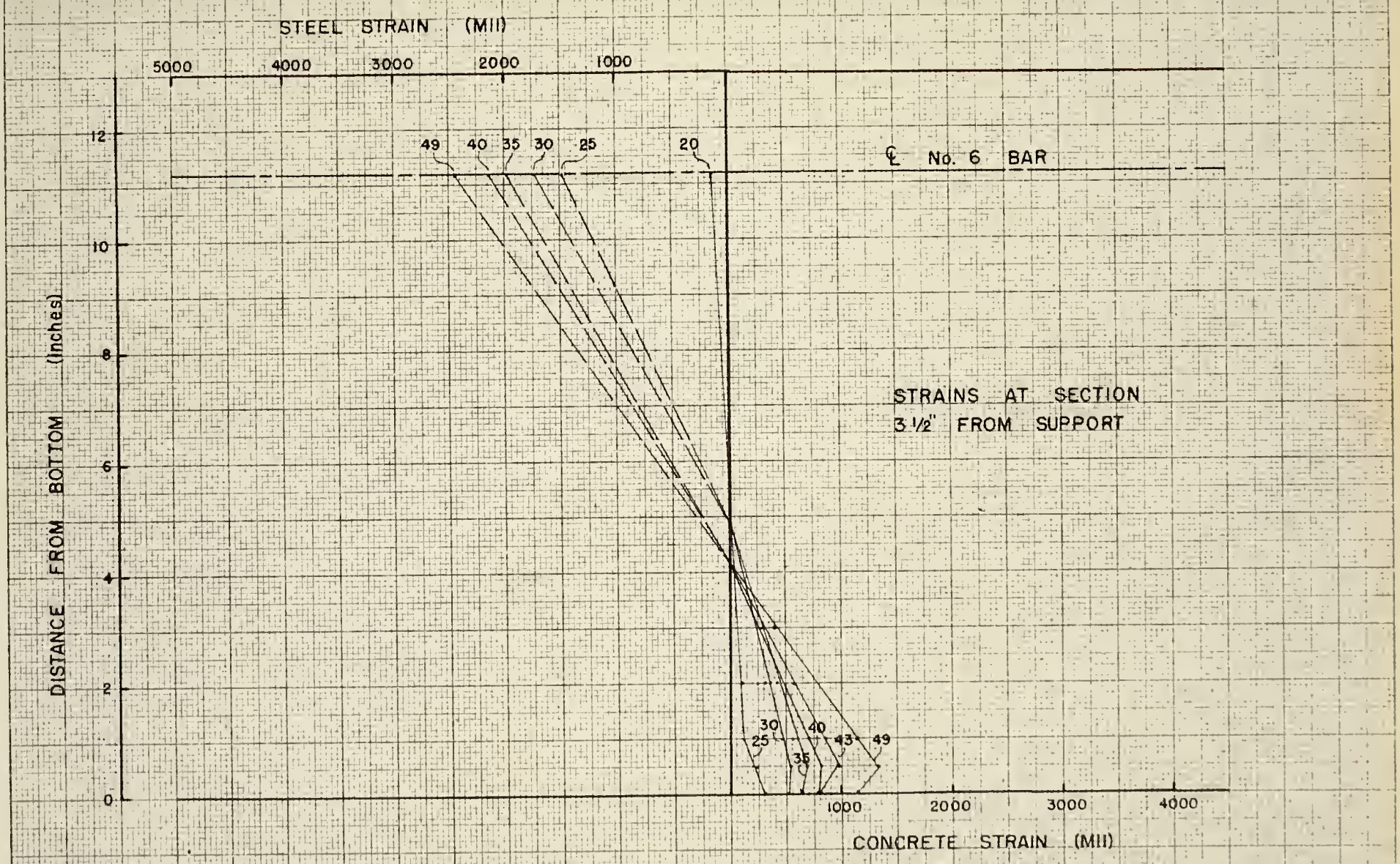

FIGURE 29. STRAIN DISTRIBUTION — BEAM IIT-1

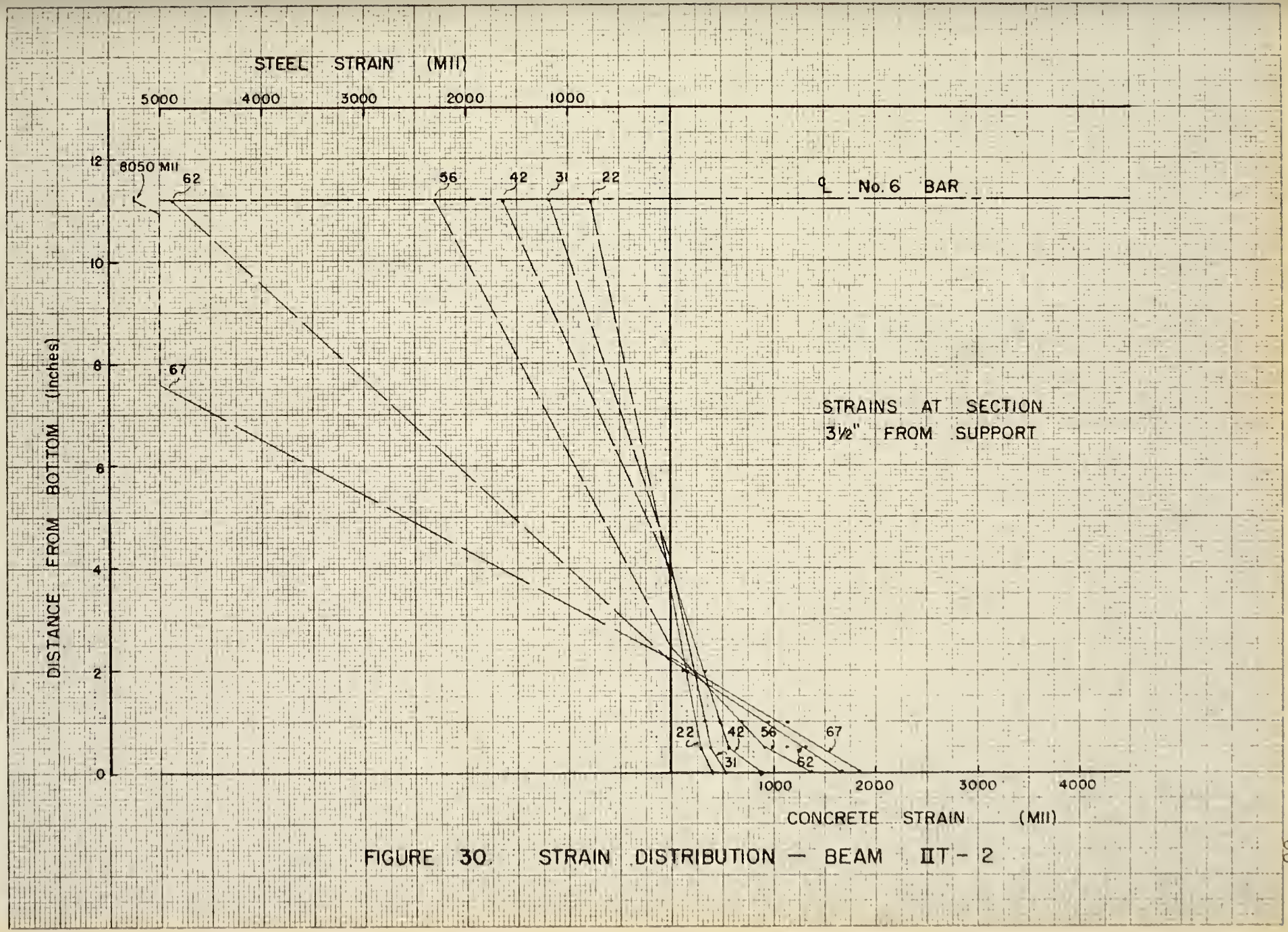

FIGURE 30. STRAIN DISTRIBUTION — BEAM IIT - 2

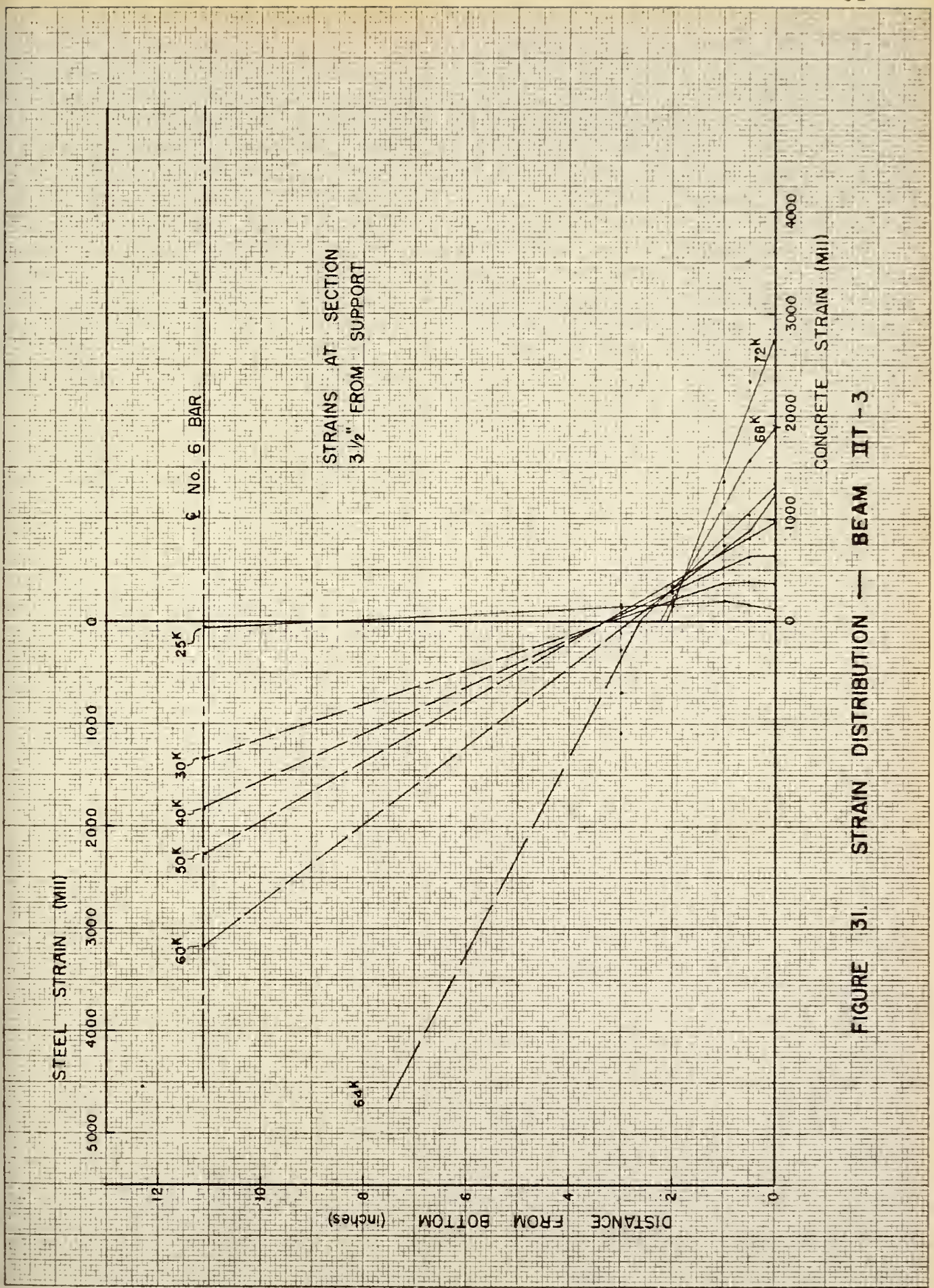

FIGURE 31. STRAIN DISTRIBUTION — BEAM IIT-3

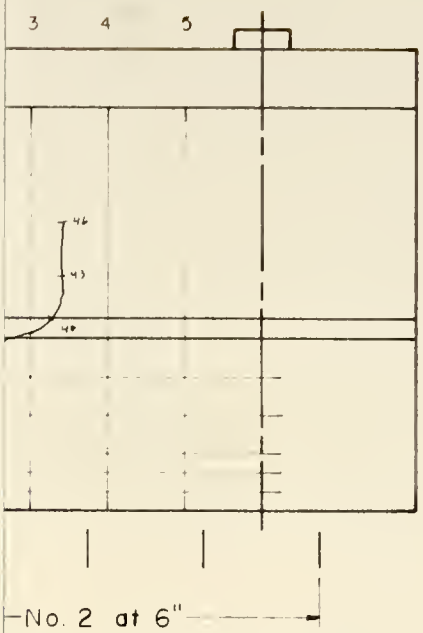

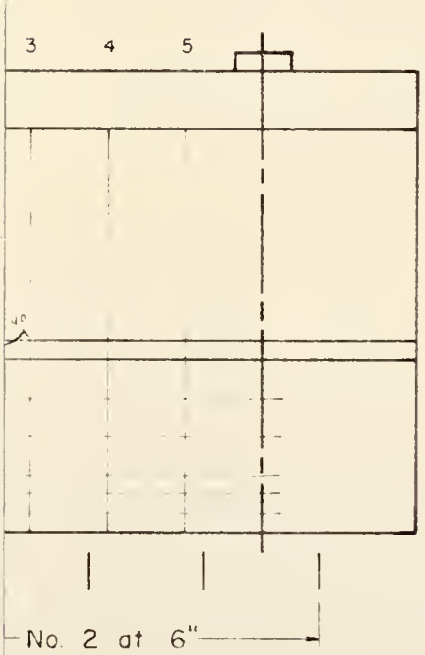

to failure

g wide at failure

in Gage Scale: 1" = 10"

BEAM IIT-1

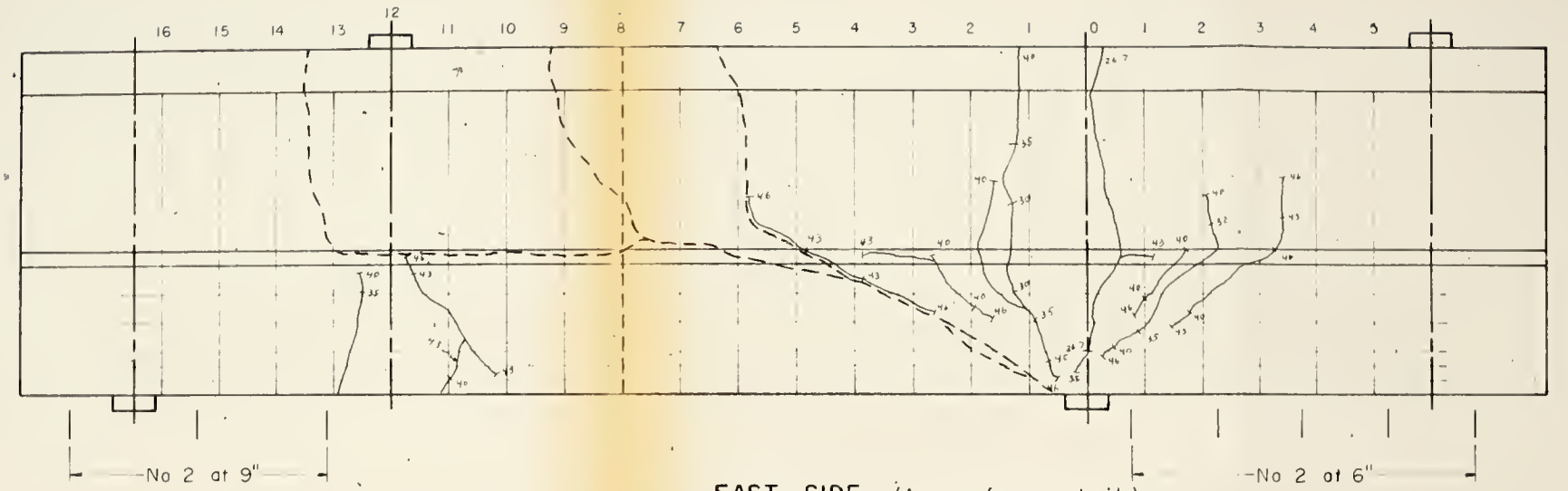

EAST SIDE (As seen from west side)

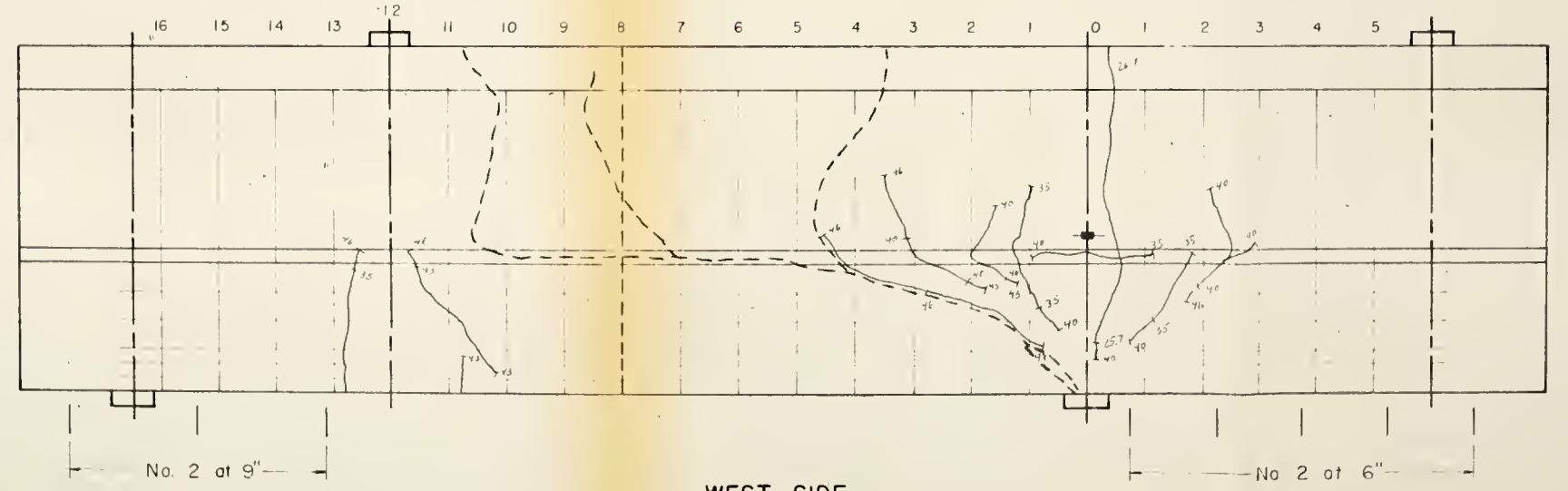

WEST SIDE

SR-4 Gage Locations:
. No 6 Bar — At support (W)

Whittemore Gage Locations:
0, 0.5", 1", 2", 3" from bottom (W)., 3.5" from support

Cracks prior to failure
Cracks opening wide at failure
SR-4 Strain Gage

Scale: 1" = 10"

FIGURE 32. BEAM IIT-1

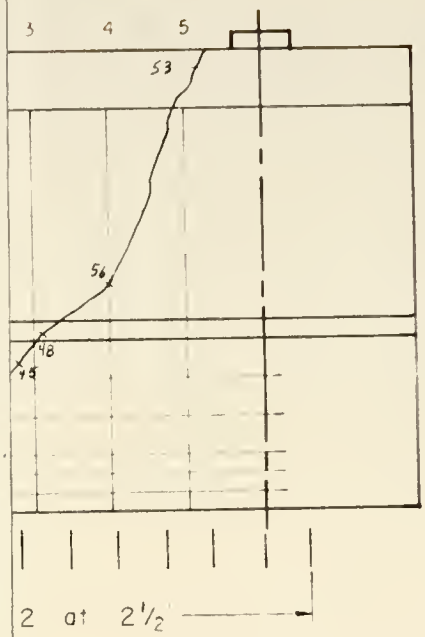

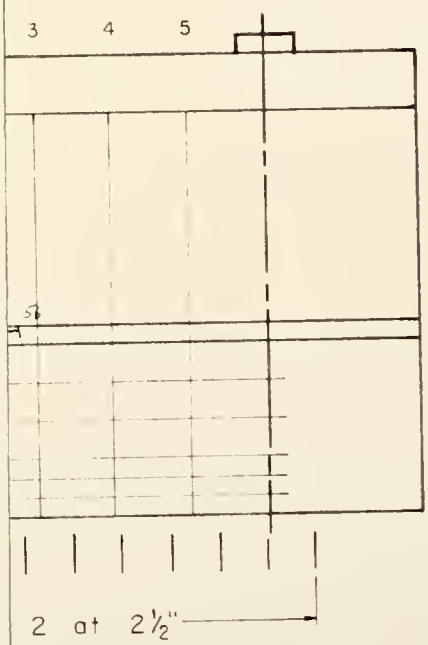

BEAM IIT-2

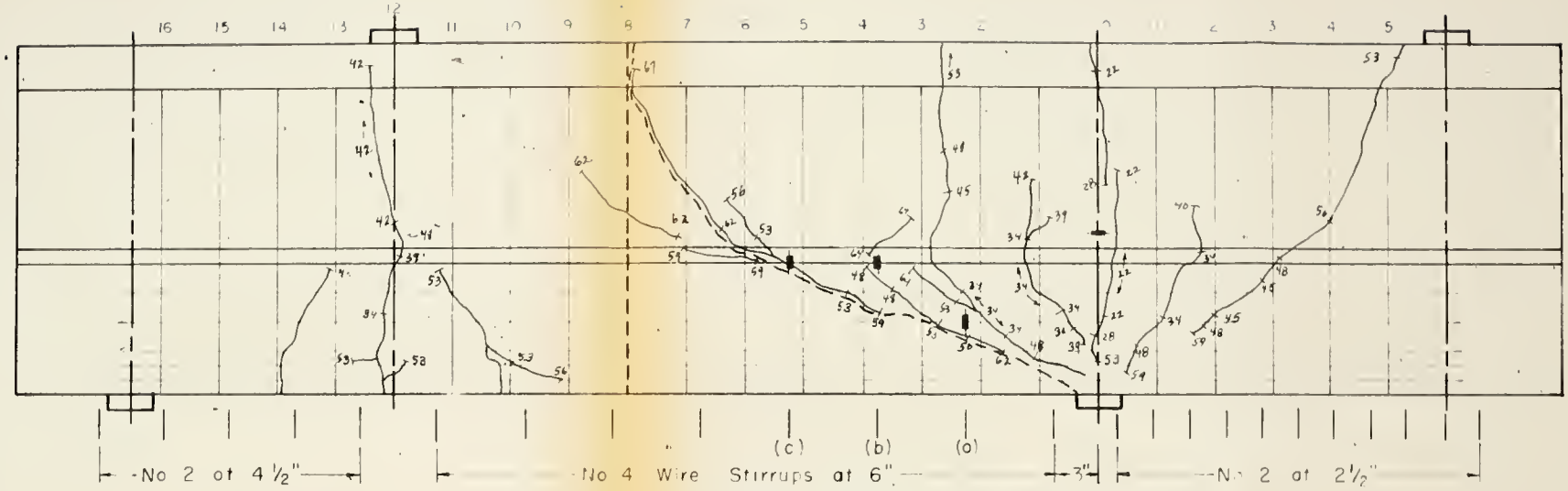

EAST SIDE (As seen from west side)

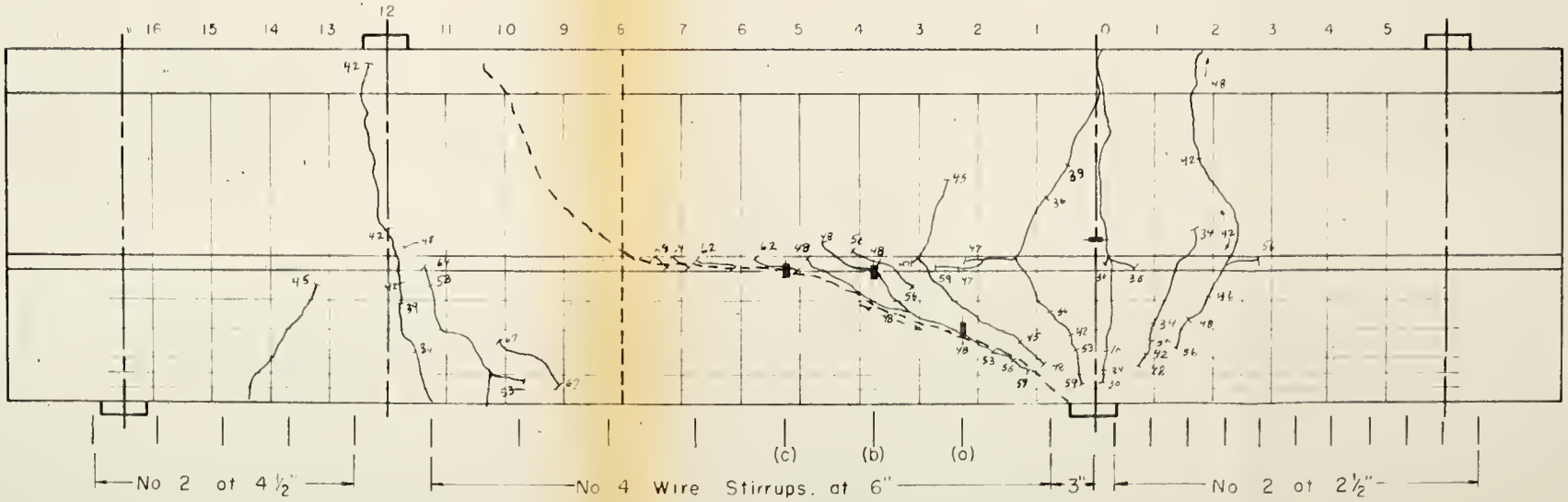

WEST SIDE

SR-4 Gage Locations.

No 6 Bar — At support (W)
Stirrup (a) — 5" from bottom (W)
" (b) — 9" " " "
" (c) — 9" " " "

Whittemore Gage Locations:
0, 0.5", 1", 2", 3", from bottom (W), 3.5" from support

FIGURE 33. BEAM IIT-2

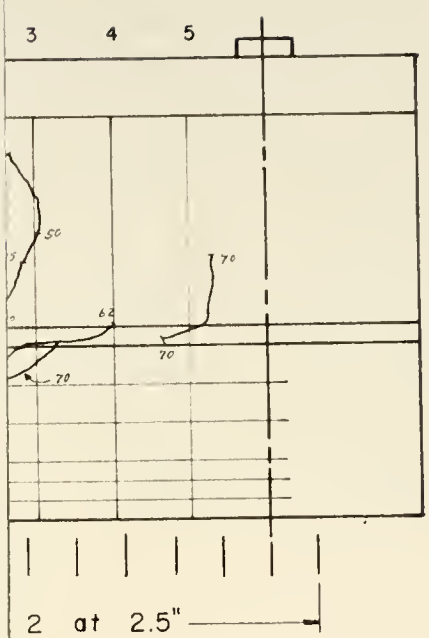

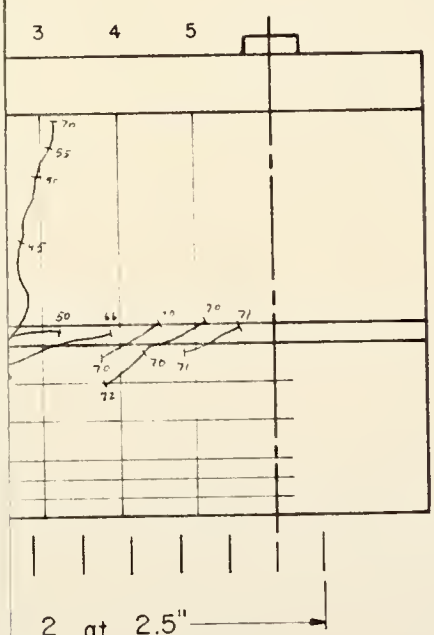

ort

BEAM IIT-3

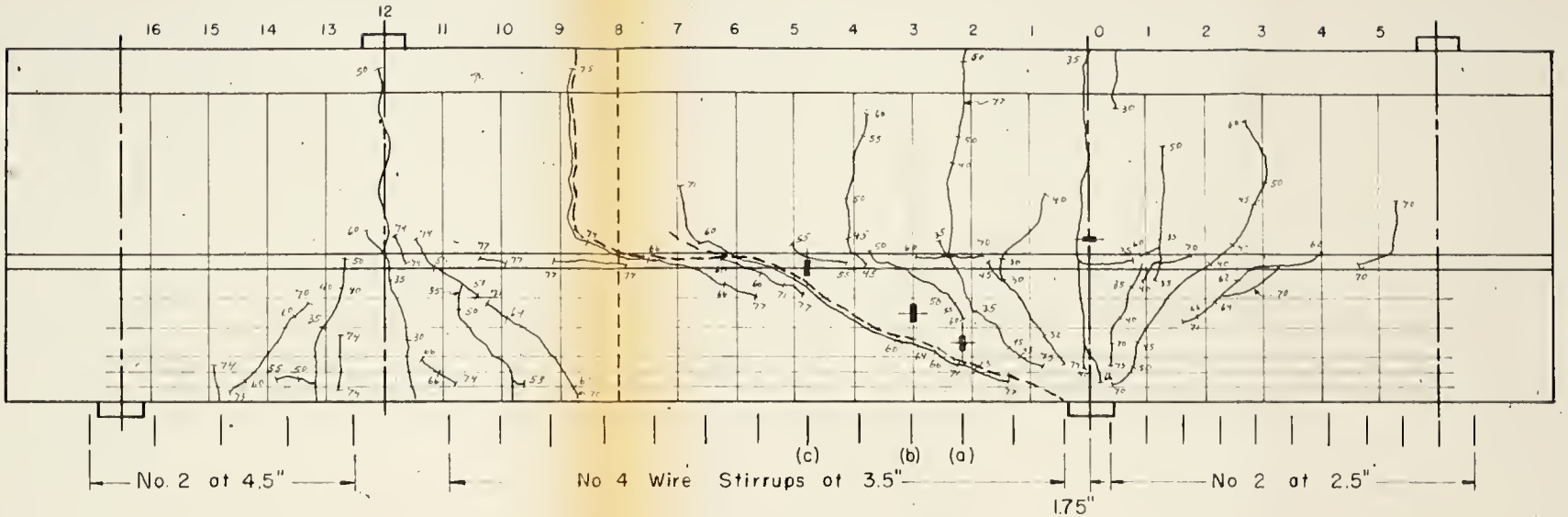

EAST SIDE (As seen from west side)

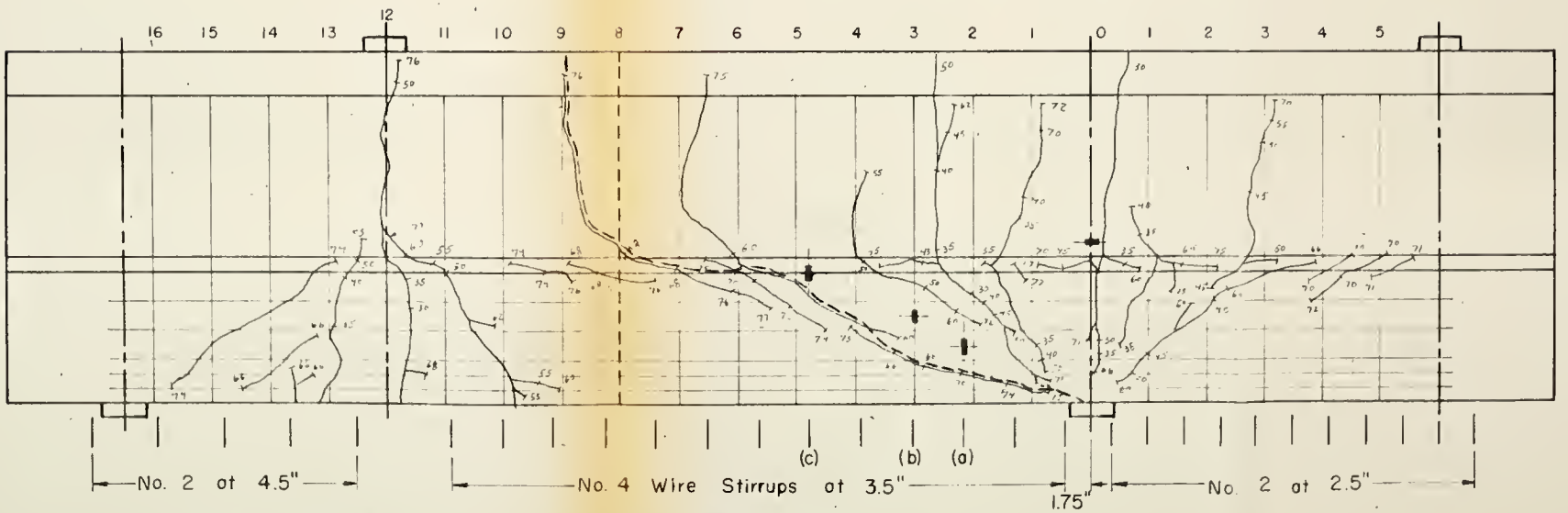

WEST SIDE

SR – 4 Gage Locations:

No. 6 Bar — At support (W)
Stirrup (a) — 4" from bottom (W)
" (b) — 6" " " "
" (c) — 9" " " "

Whittemore Gage Locations:

0, 0.5", 1", 2", 3" from bottom (W), 3.5" from support

FIGURE 34. BEAM IIT – 3

Series III T

This series had an a/d ratio of 3.93 and a shear span of 44 inches. The percentage of web reinforcement (A_v/bs) was variable, as shown in Table 5.

Beam III T - 1 (No Stirrups)

A load of 30^k was reached before the flexural cracks reached the neutral axis. At this same load, diagonal tension cracks began to form. At 40^k a distinct diagonal crack had penetrated into the compression zone. No significant change in slope of the load-deflection or steel strain curves occurred at any time prior to failure at 49^k (see Figures 35 and 37). The load dropped off to 47^k and held there for a short time. Then the beam suddenly failed as the critical diagonal crack penetrated through the compression zone to the support and slit back along the bottom of the flange.

Beam III T -2 (Stirrups at 8")

The first flexural crack formed at a load of 23.6^k and extended down to within 2-1/2 inches of the support, with a jump of 1500 MII in the longitudinal steel strain. The next cracks, as in the Series II T beams, were inclined extensions of flexural cracks but were farther from the support (see Figure 44). The first inclined crack was at the same load and in the same location as in Beam III T - 1. In Beam III T - 1 this crack subsequently became the critical diagonal crack. The critical diagonal tension crack in Beam III T - 2

formed at a load of 40^{k} and crossed the stirrup on which SR-4 gage (b) was mounted. All the gages on stirrups indicated no strain until a crack had crossed them or just prior to the crack's crossing them. Stirrup (c) began showing strain at 35^{k} and was yielding by a load of 40^{k}. This could have been due to the low web reinforcement ratio. The remaining two instrumented stirrups began yielding at 48^{k}. The beam failed by diagonal tension at a load of 51.3^{k}. The longitudinal steel had just begun to yield at failure but the stiffness of the beam had decreased only slightly (see Figure 37).

Beam III T - 3 (Stirrups at 5.5")

The crack formation was similar to Beam II T - 2, which had nearly the same web reinforcement ratio. The diagonal crack which opened on failure was in exactly the same location for both beams but appeared at a slightly higher load in Beam II T - 2 than in III T - 3.. In Beam III T - 3 a diagonal crack opened about 20 inches from the support at a load of 40^{k}. This crack penetrated into the compression zone to within 2-1/2 inches of the compression face at a very flat slope. The beam held a load of 53^{k} until all readings were taken and then failed by crushing of concrete at the head of the diagonal crack adjacent to the support. This crack, which was at the same location as the critical diagonal crack in Beam II T - 2, opened widely on failure and extended back into the web along the bottom side of the

flange about 36 inches on the west side and 24 inches on the east side before entering and extending through the flange.

Stirrup (a) began picking up strain at a load of 35^k but the nearest visible crack at this load was just approaching the stirrup. Both instrumented stirrups were yielding at a load of 51^k. A concentration of strain in the concrete at the bottom surface can be seen in Figure 41.

Beam III T - 4 (Stirrups at 4")

The crack formation was similar to that of Beam II T - 3, which had nearly the same web reinforcement ratio as this beam (see Figure 46). The critical diagonal crack was in almost exactly the same location as in Beam II T - 3, but here again there was a diagonal crack farther from the support than the critical diagonal crack. The critical diagonal crack in this beam was slighlty closer to the support than in Beam III T - 3. This beam failed by crushing of the concrete at the support after the tension steel had yielded. The steel began to yield at a load between 45^k and 50^k. Near the support the strain distribution, Figure 42, shows that 1/2 inch up from the bottom the strain was much greater than at the bottom.

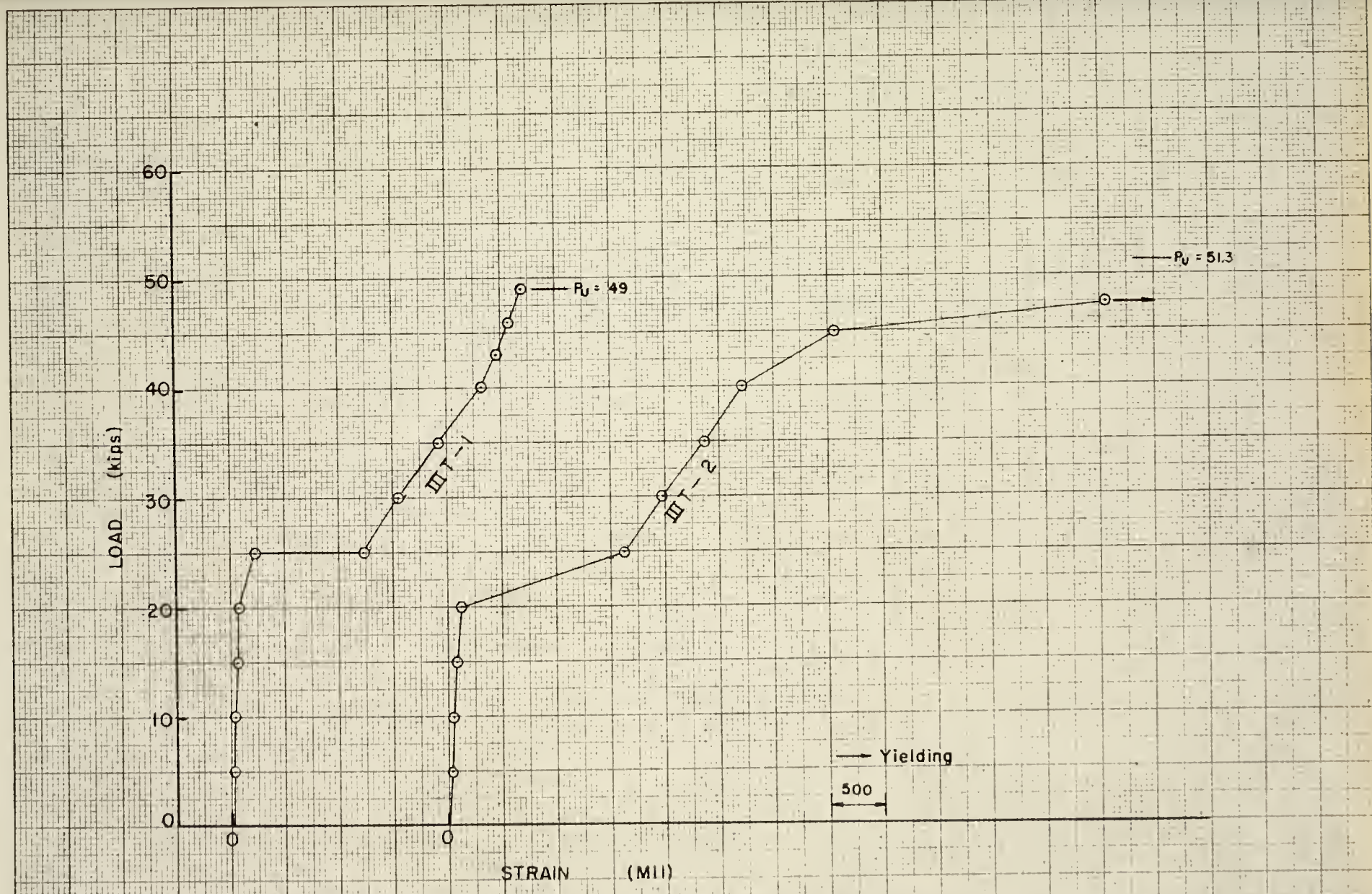

FIGURE 35. LOAD vs. STEEL STRAIN – SERIES III T

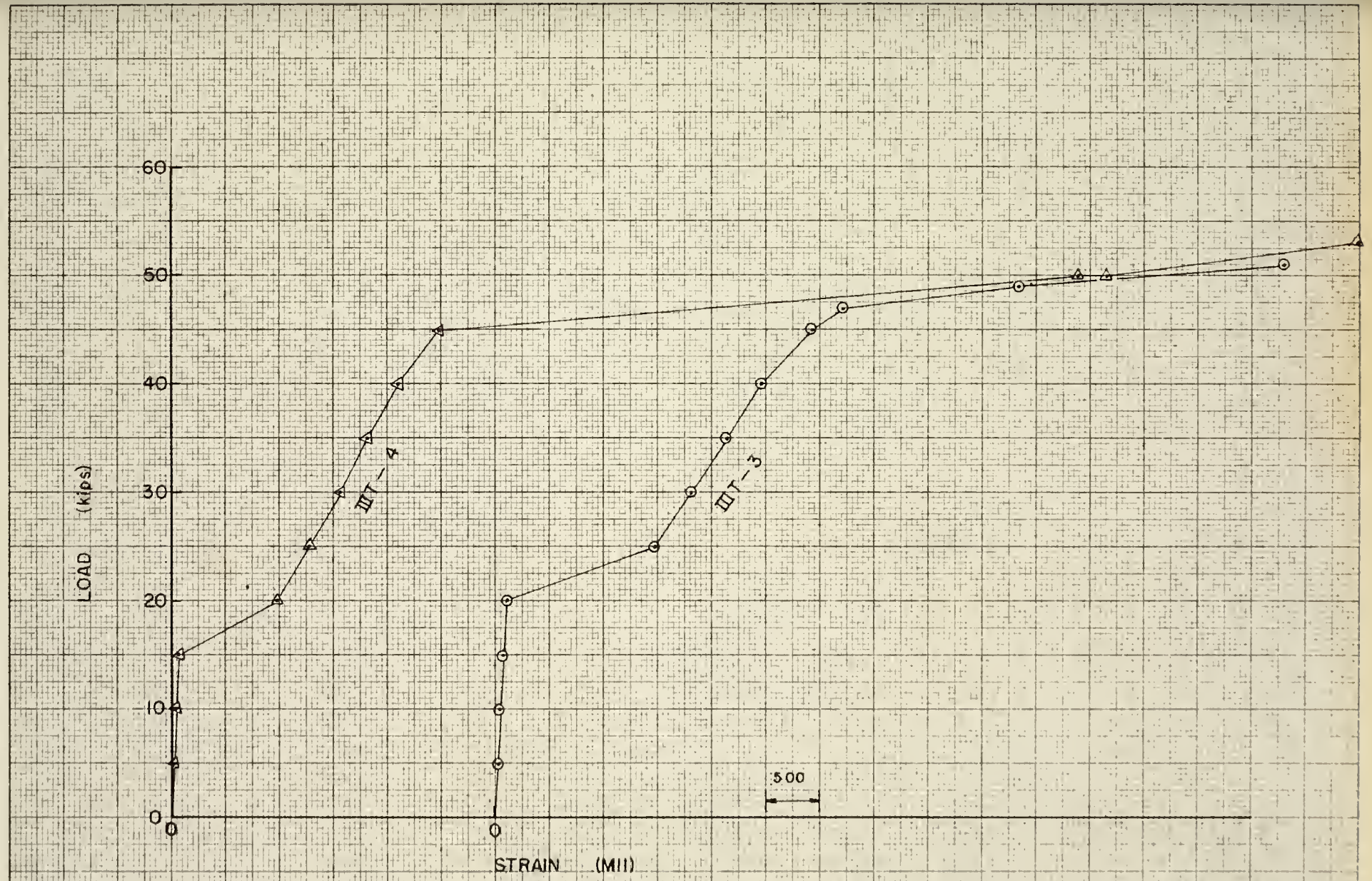

FIGURE 36. LOAD vs. STEEL STRAIN — SERIES III T (Cont'd)

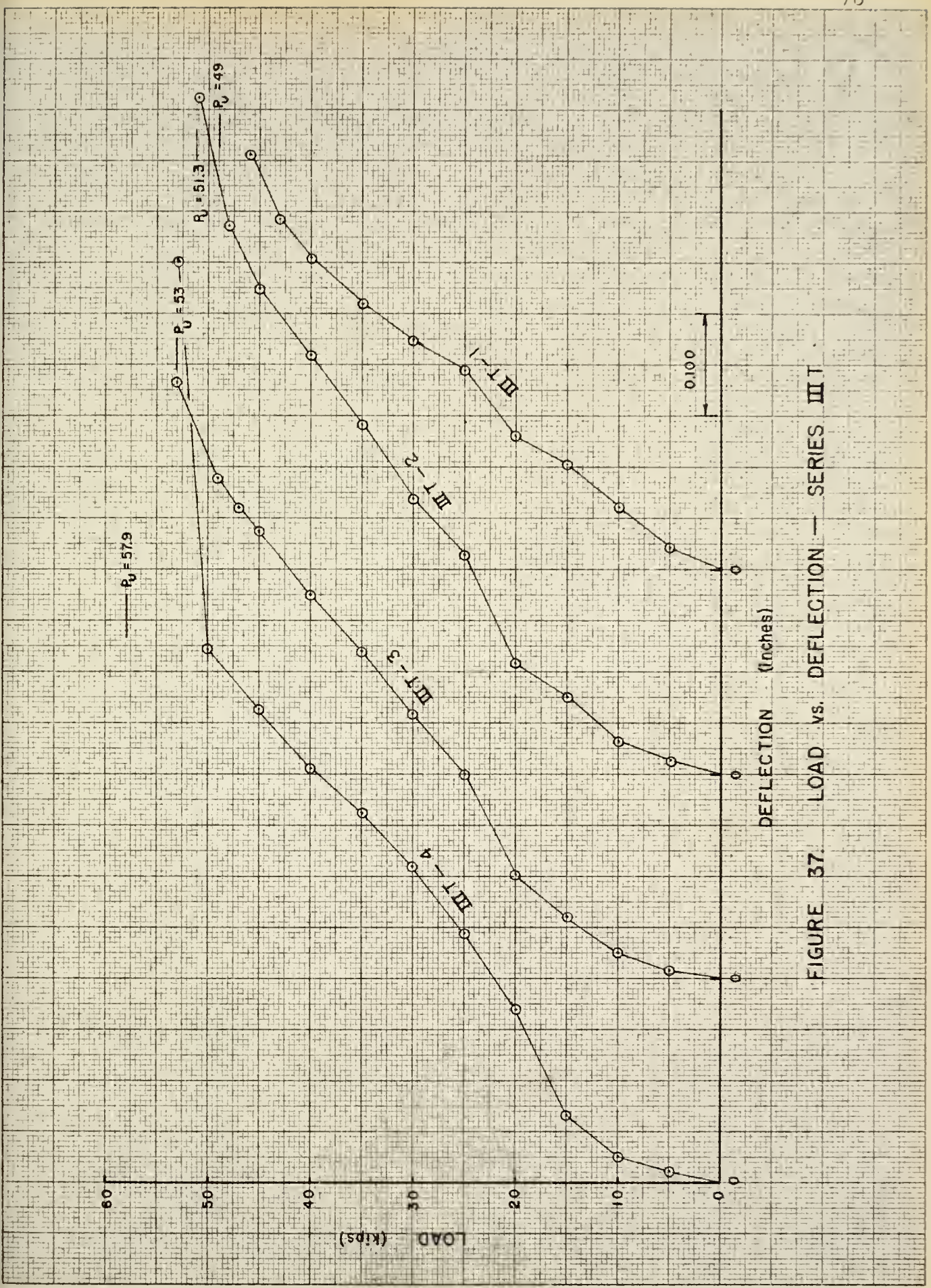

FIGURE 37. LOAD vs. DEFLECTION — SERIES III T

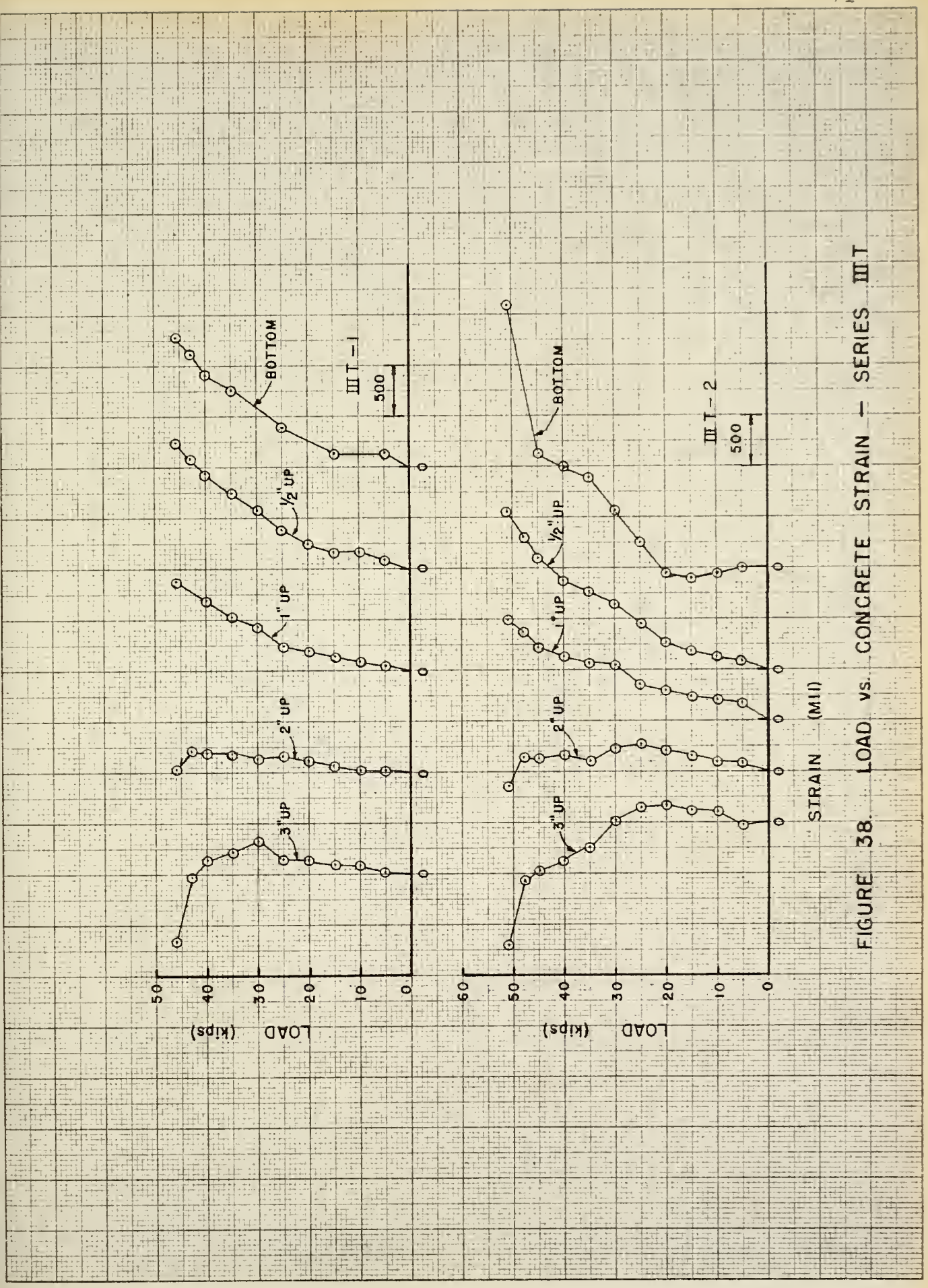

FIGURE 38. LOAD vs. CONCRETE STRAIN — SERIES III T

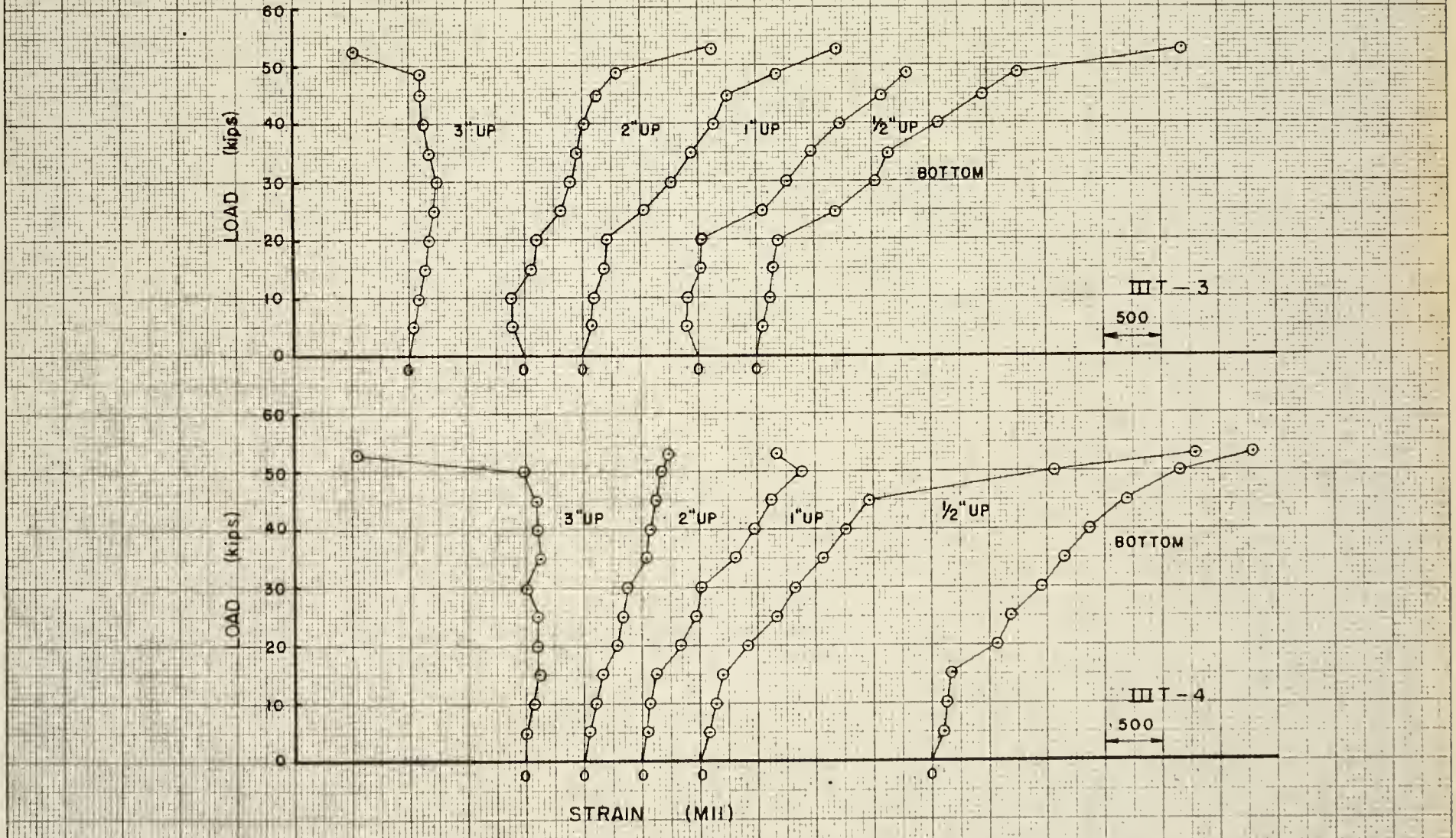

FIGURE 39. LOAD vs. CONCRETE STRAIN — SERIES III T (cont'd)

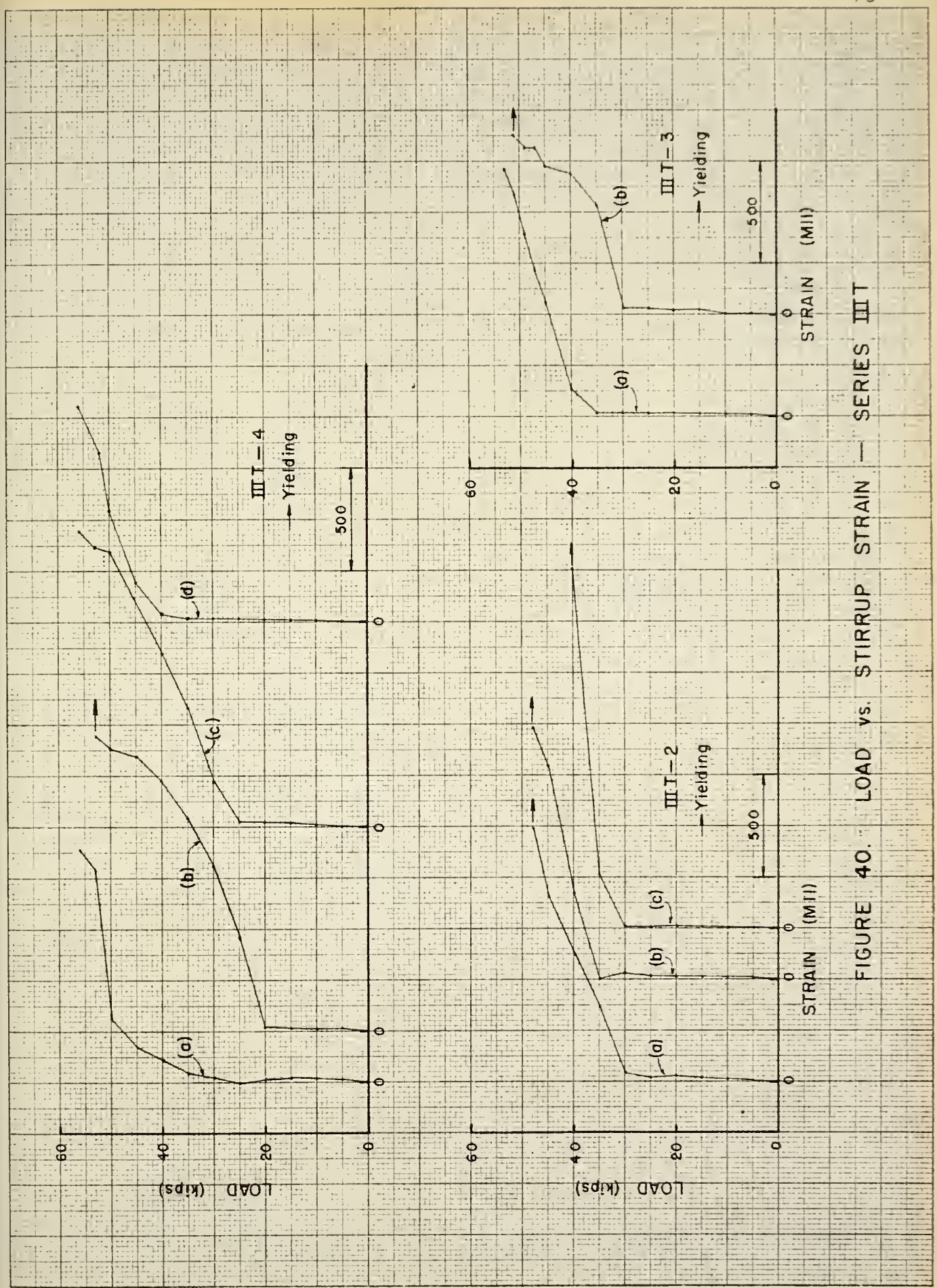

FIGURE 40. LOAD vs. STIRRUP STRAIN — SERIES III T

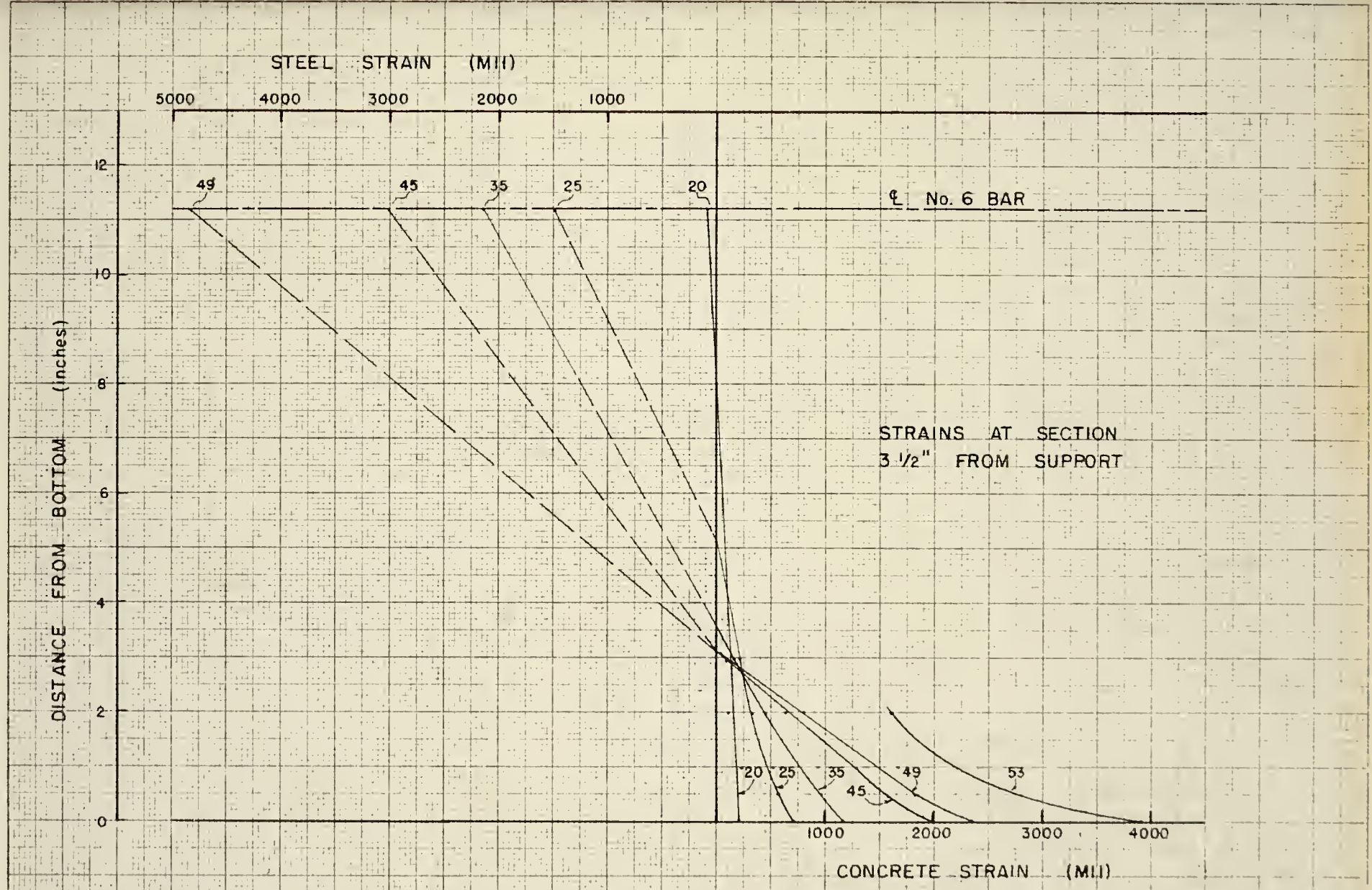

FIGURE 41. STRAIN DISTRIBUTION — BEAM IIIT-3

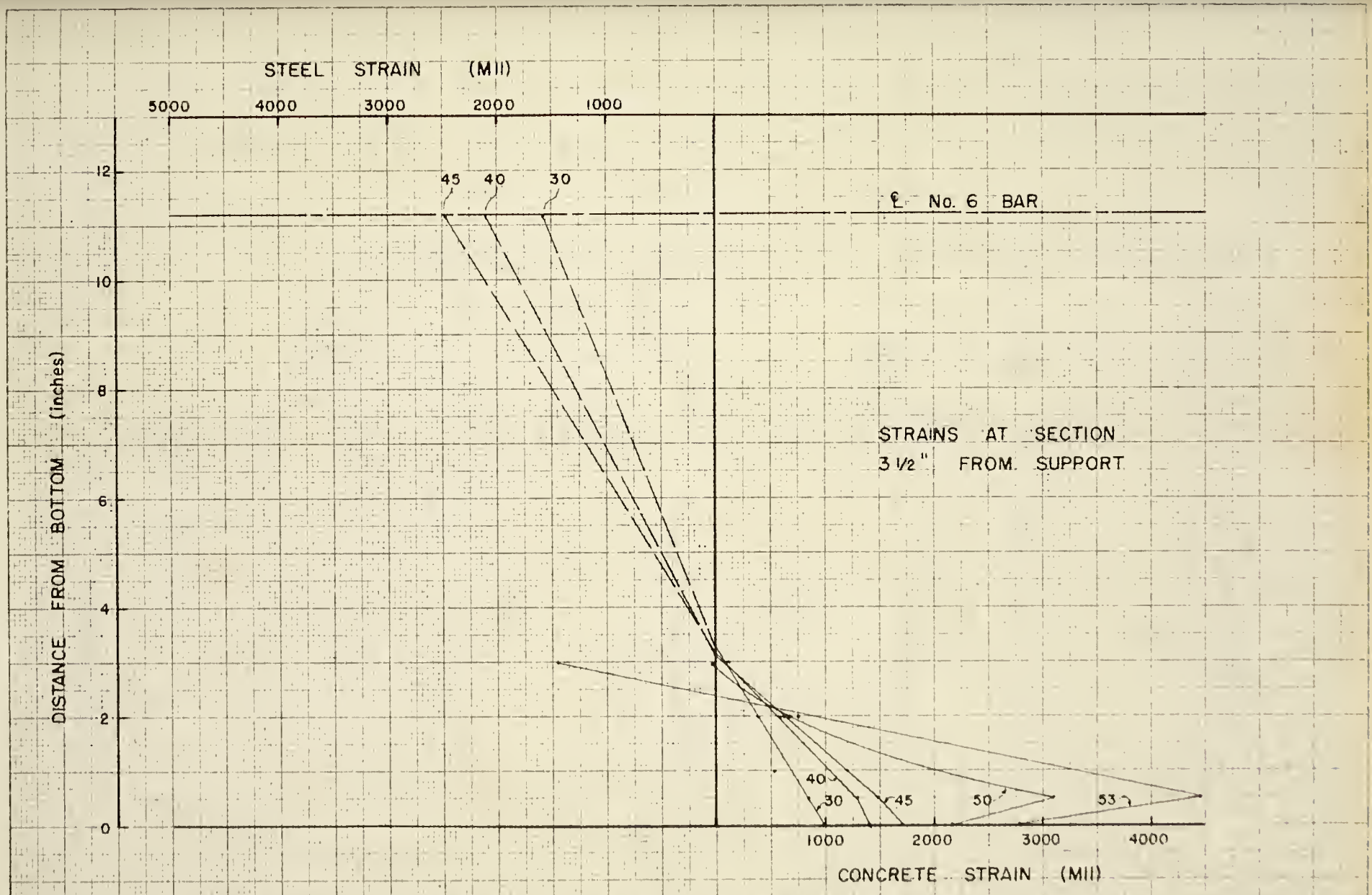

FIGURE 42. STRAIN DISTRIBUTION — BEAM IIIT-4

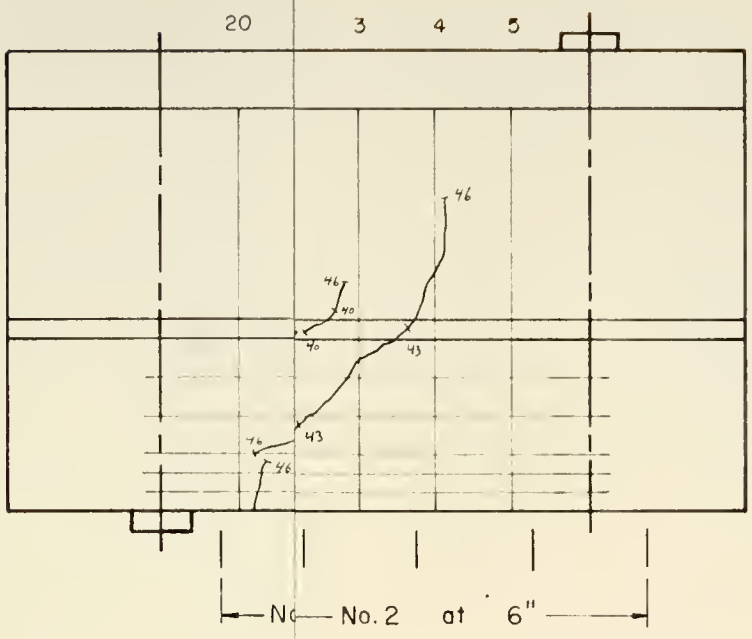

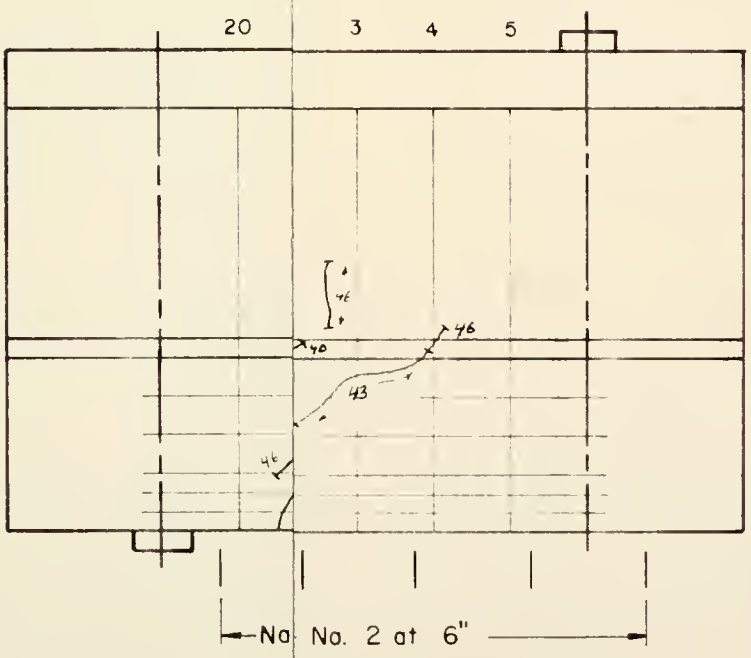

or to failure

SR — ning wide at failure

in Gage Scale: 1" = 10"

Whit

RE 43. BEAM III T — 1

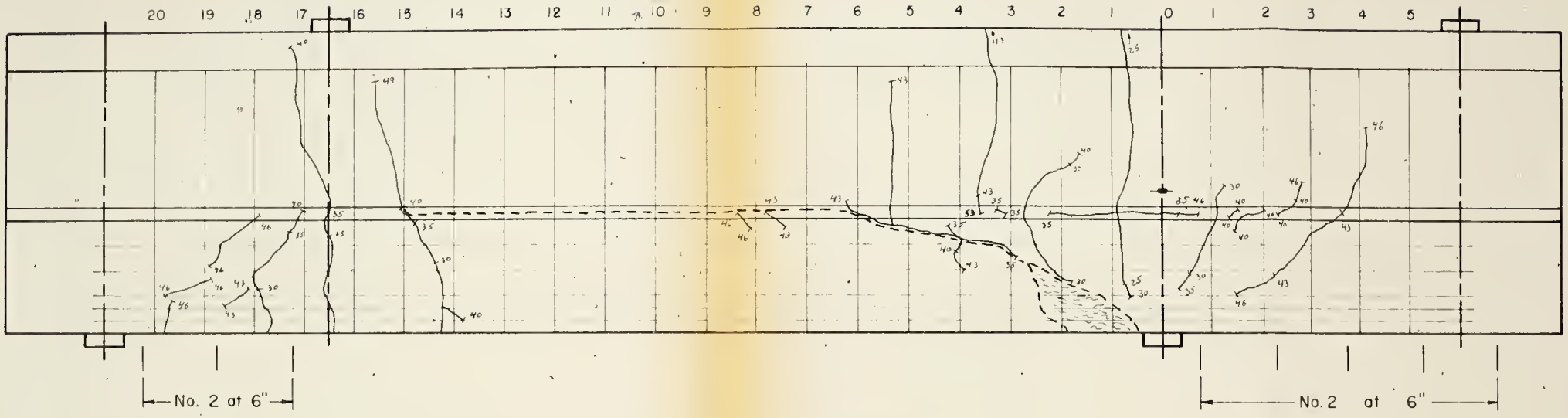

EAST SIDE (As seen from west side)

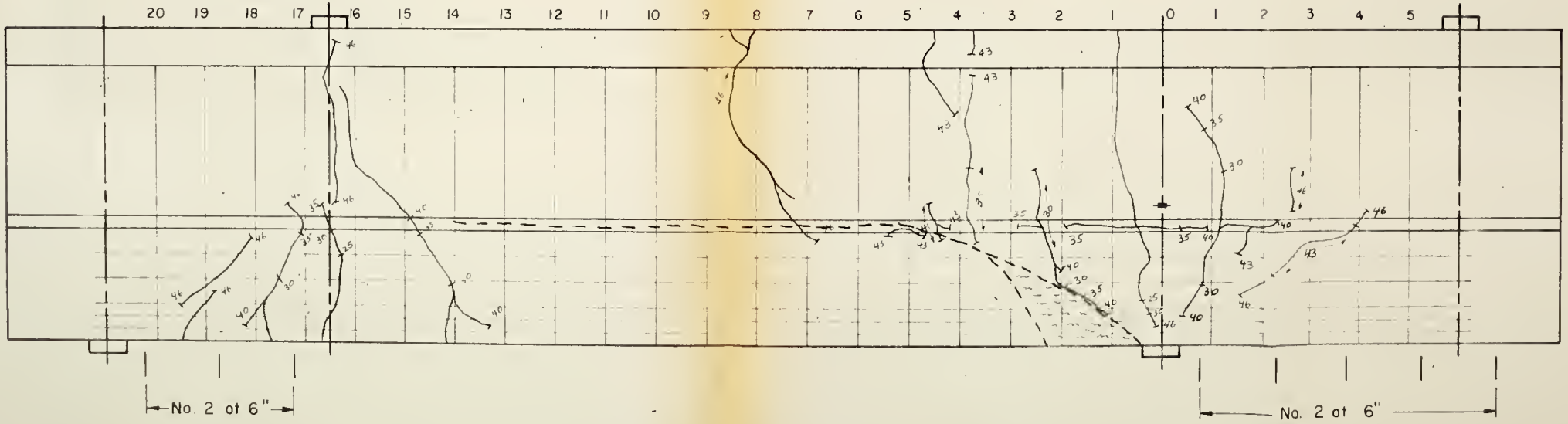

WEST SIDE

SR-4 Gage Locations:
No. 6 Bar — At support (W)

Whittemore Gage Locations:
0, 0.5", 1", 2", 3" from bottom; 3.5" from support (W)

Cracks prior to failure
Cracks opening wide at failure
SR-4 Strain Gage

Scale 1" = 10"

FIGURE 43. BEAM III T — 1

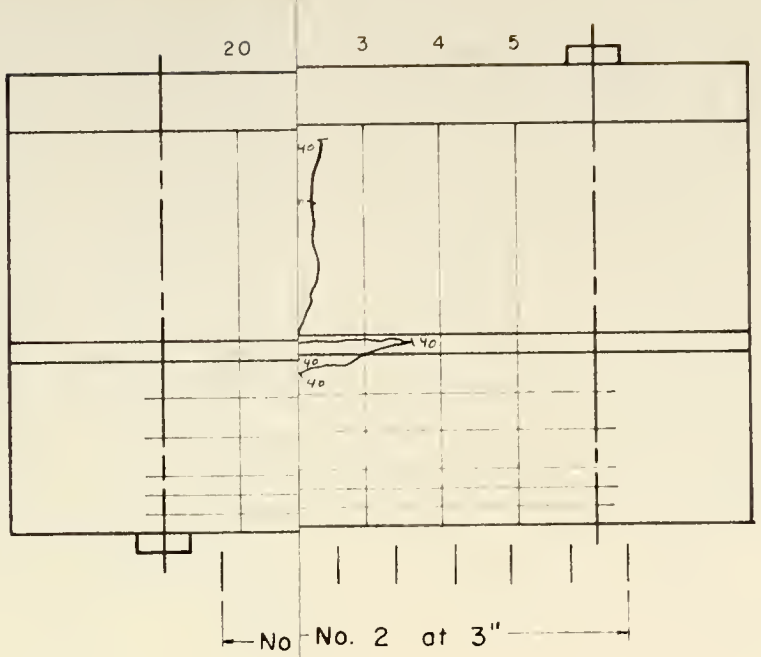

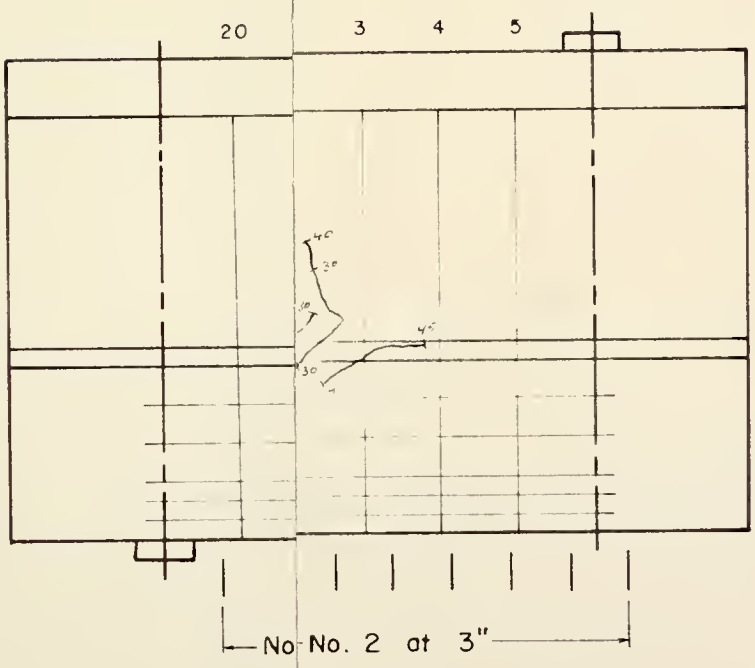

SR -

RE 44. BEAM III T - 2

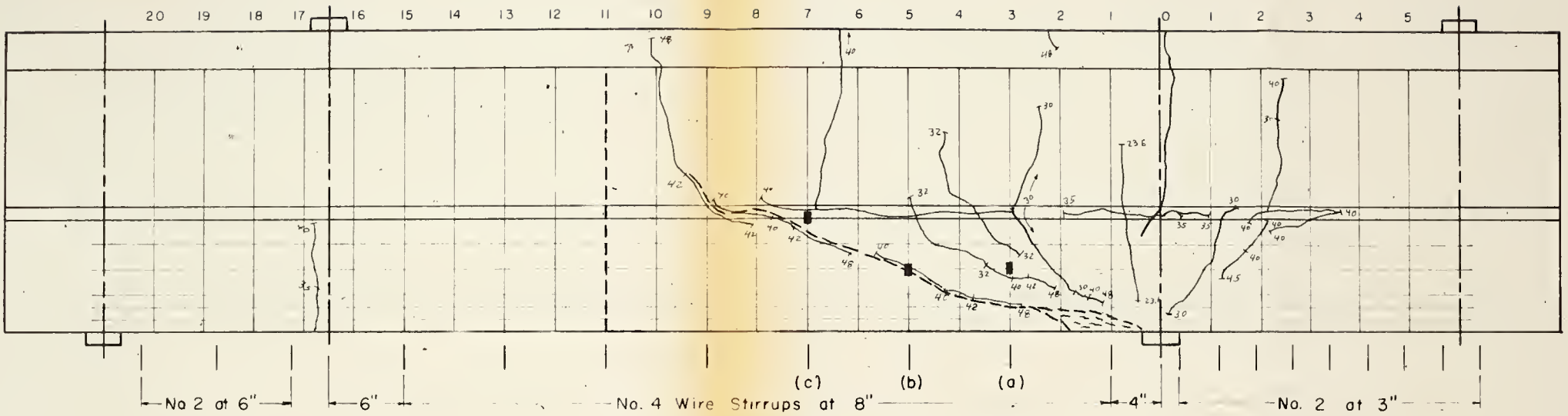

EAST SIDE (As seen from west side)

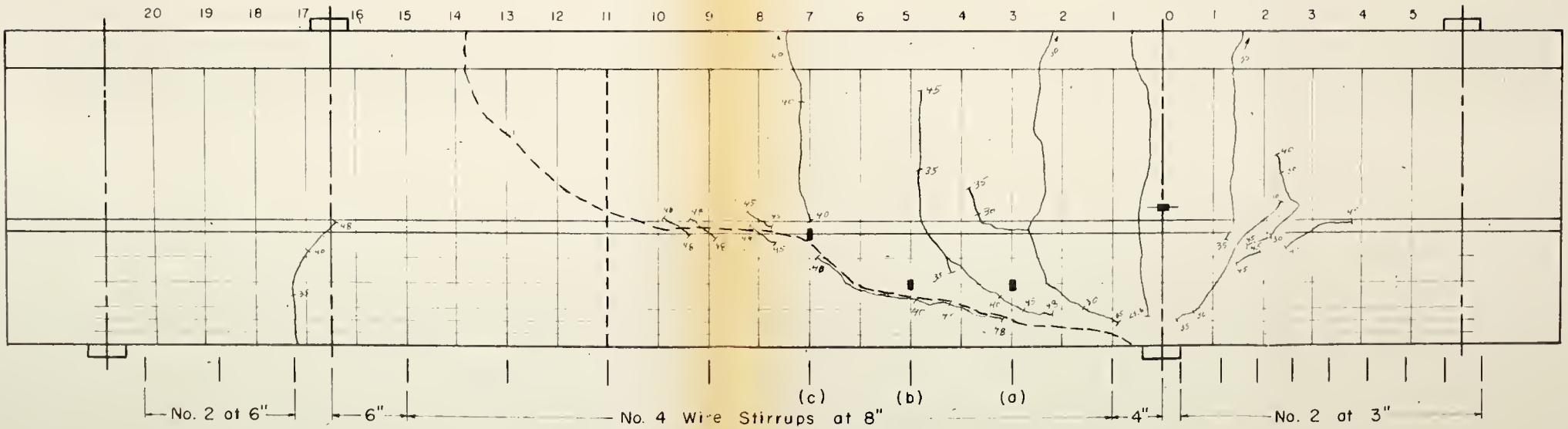

WEST SIDE

SR - 4 Gage Locations.

No 6 Bar — At Support (W)
Stirrup (a) — 5" from bottom (W)
" (b) — 5" " " "
" (c) — 9" " " "

Whittemore Gage Locations:

0, 0.5", 1", 2", 3" from bottom (W), 3.5" from support

FIGURE 44. BEAM III T – 2

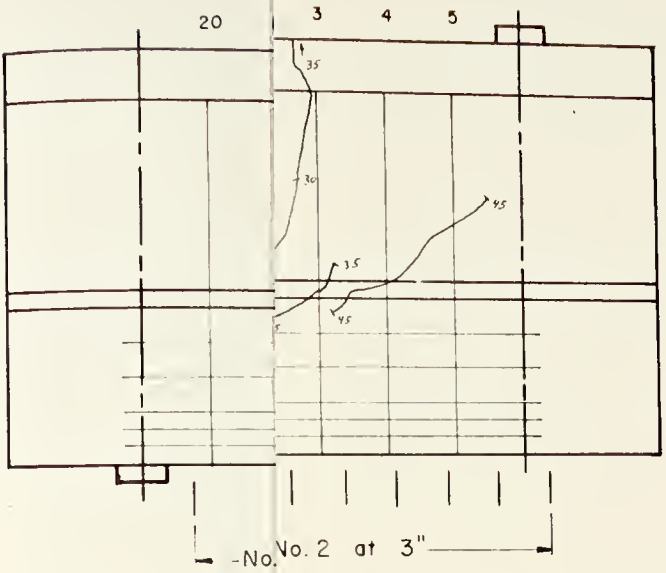

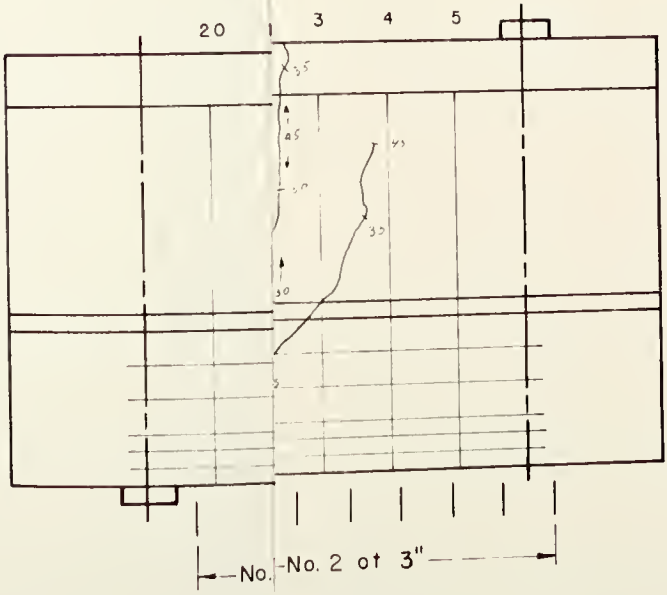

SR -

RE · 45. BEAM III T – 3

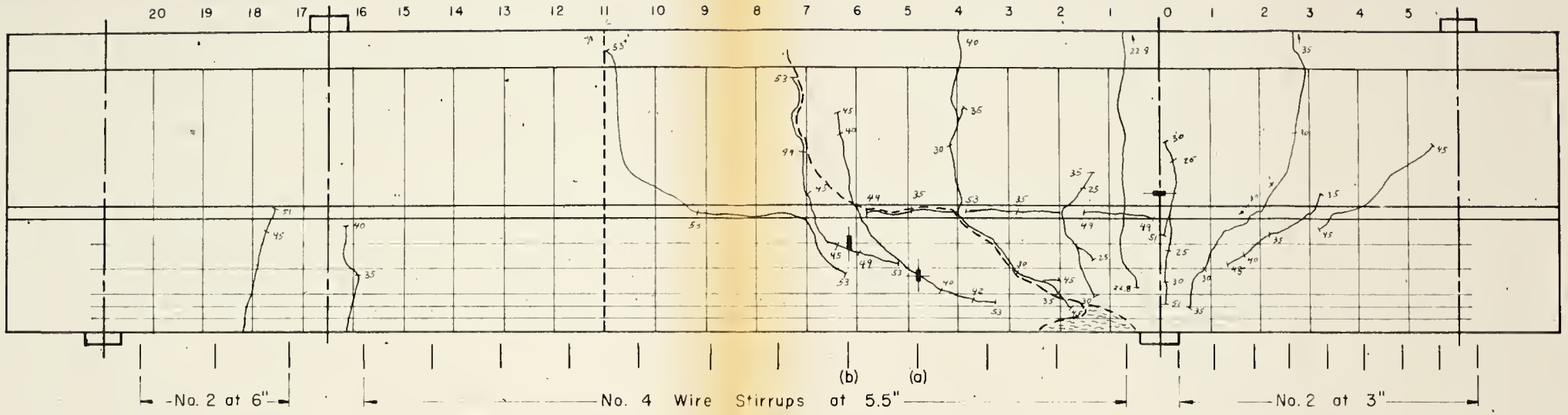

EAST SIDE (As seen from west side)

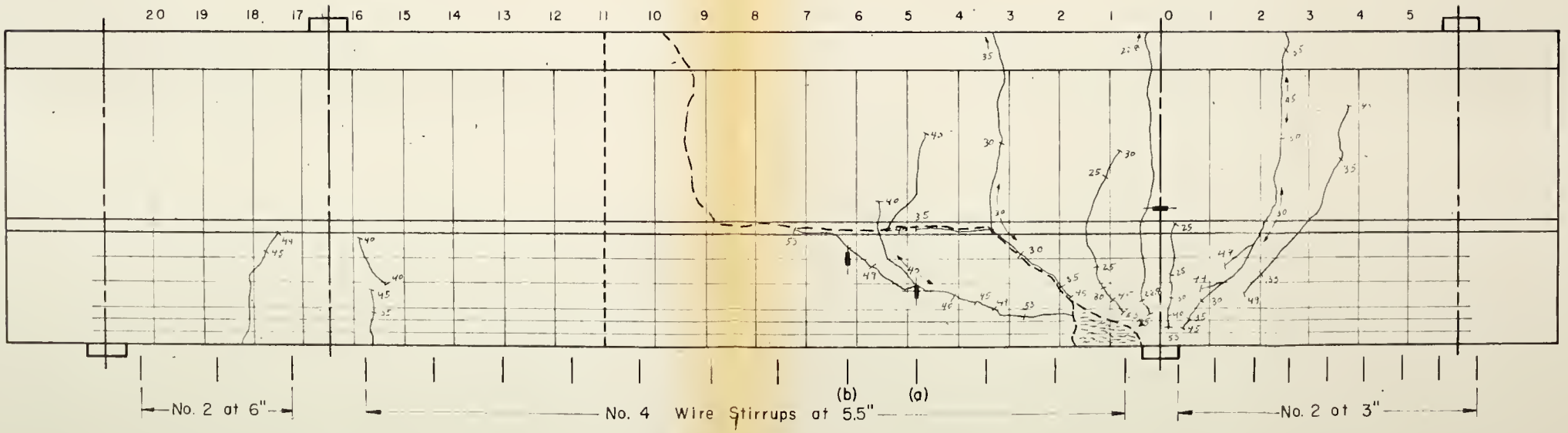

WEST SIDE

SR - 4 Gage Locations:

No. 6 Bar — At support (W).
Stirrup (a) — 4.5" from bottom (W)
" (b) — 7" " " "

Whittemore Gage Locations:
0, 0.5", 1", 2", 3" from bottom (W), 3.5" from support.

FIGURE 45. BEAM III T — 3

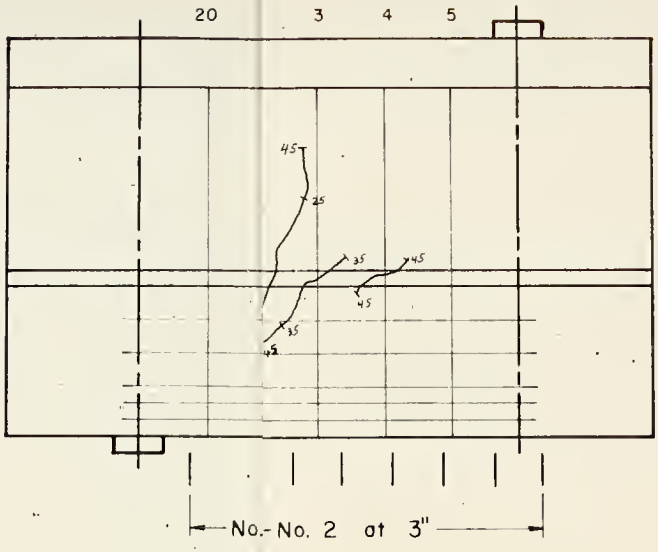

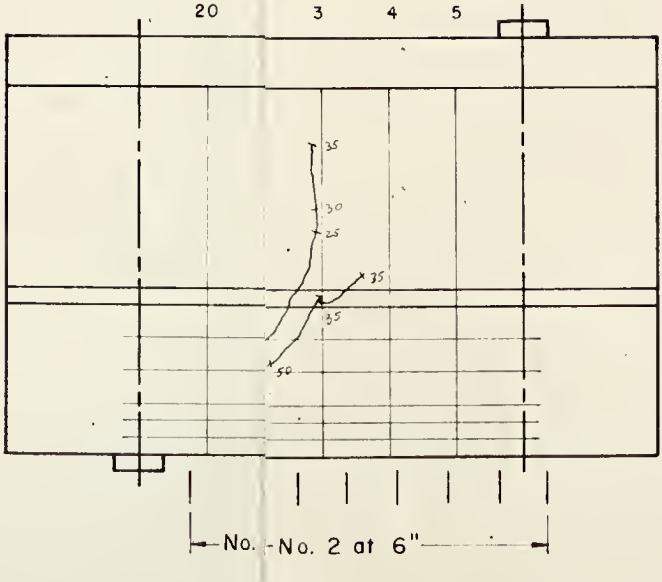

SR-

IRE . 46. BEAM III T - 4

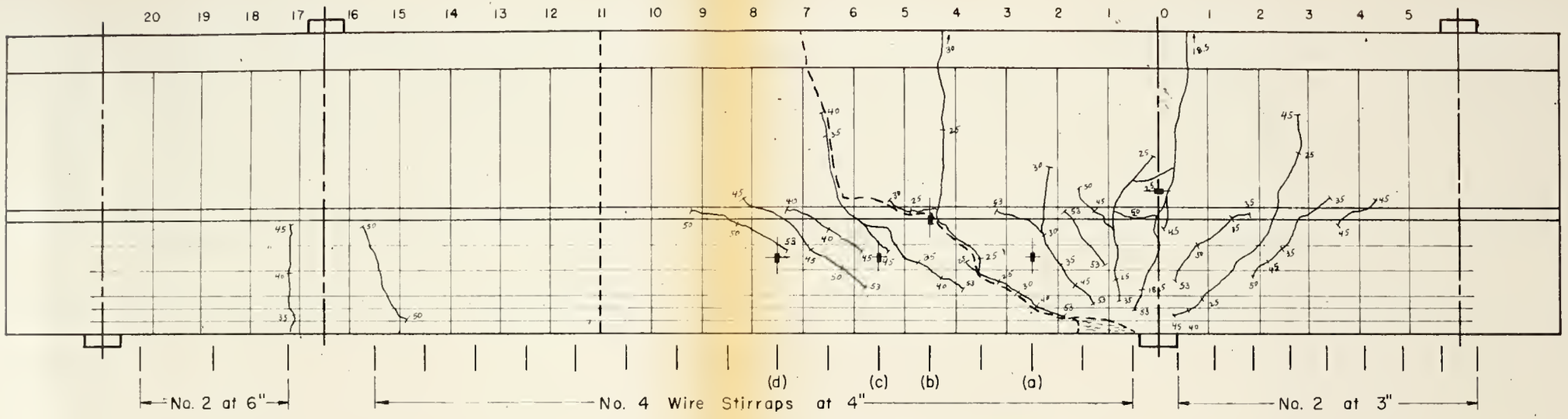

EAST SIDE (As seen from west side)

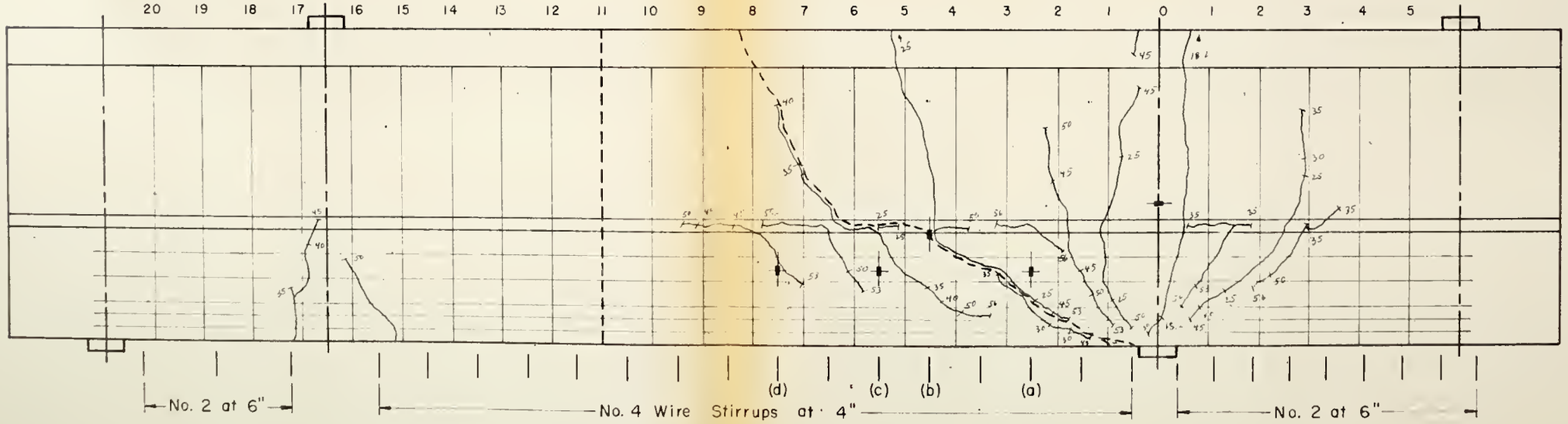

WEST SIDE

SR-4 Gage Locations:

No 6 Stirrup	Bar — At (a) — 6"	support (W) from bottom (W)		
"	(b) — 9"	"	"	"
"	(c) — 6"	"	"	"
"	(d) — 6"	"	"	"

Whittemore Gage Locations:
0,0.5",1",2",3" from bottom (W), 3.5" from support

FIGURE 46. BEAM III T-4

Series IV T

This series had an a/d ratio of 5.00 and a shear span of 56 inches. The web reinforcement was varied as shown in Table 5. All other parameters were held the same as in Series II T and Series III T. A new supply of soft stirrup steel was needed for this series and it was found to have a lower yield point. Note: Figure 14 shows the increasing number of cracks within the flange as the carrying capacity of the beams increased.

Beam IV T - 1 (No Stirrups)

At a load of 25^{k} the first flexural crack appeared in the flange penetrating to within 3 inches of the bottom on the west side and to within 8 inches on the east side. With increased load, inclined cracks began to form in the shear span. As the load increased to 36^{k}, a diagonal crack penetrated to within 3 inches of the bottom on the west side, with a new crack opening near the flange at the same load on both sides of the beam. This new crack penetrated to within 1.5 inches of the compression face on the east side by a load of 45^{k}. The beam failed in diagonal tension suddenly at a load of 48^{k} and this crack opened wide, extending back along the chamfer to within 15 inches of the second load on the west side and 30 inches on the east side.

The strain distribution (Figure 51) indicates a slight concentration of strain above the extreme compression fiber, showing the effect of the diagonal crack.

Beam IV T - 2 (Stirrups at 12")

The first inclined cracks to appear in this test were at essentially the same loads as in Beam IV T - 1 but were farther from the support. By a load of 39^{k}, a critical diagonal crack had penetrated to within 2.5 inches of the bottom on the east side. At this same load, a new crack formed at the flange and, with increased load, penetrated into the compression zone to within 1.5 inches of the beam face by a load of 57^{k}. By 60^{k} some concrete was beginning to crush at the support on the east side. This crushing continued until a load of 61.3^{k} was reached, at which time the load dropped off and the crack opened wider. The critical crack was in nearly the same location as in Beam IV T - 1.

Stirrup (a) began picking up strain at a load of 42^{k}; subsequent increases in load caused only a small increase in strain, with a total of only 550 MII at failure. The strain distribution, Figure 52 shows a strain concentration 1/2 inch from the extreme fiber; this again indicates the effect of shear on the beam.

Beam IV T - 3 (Stirrups at 8")

The initial crack pattern of this beam was essentially the same as that of Beam IV T - 2. By a load of 42^{k} a diagonal crack had penetrated to within 2 inches of the bottom surface. By 57^{k} another crack, farther from the support, had extended to within 1.5 inches of the bottom.

With an increase of load to 61.3^{k}, the beam failed by crushing of the concrete at the head of this latter crack. The failure was a shear compression - flexural tension type.

The concrete strains remained nearly linear until just prior to failure. At 57^{k} the strain at the surface increased out of proportion to the remainder of the compression area, as can be seen in the increase in slope of the concrete strain plot in Figure 49. The stirrup strain plot (Figure 50) shows that none of the stirrups picked up a large amount of strain, during the loading program. The maximum indicated strain was in stirrup (b), with about 1,000 MII of strain, which was beyond the yield point but the soft wire did not behave as if it were yielding. Note, the yield strain for this wire was approximately 700 MII. The tension steel began yielding at a load of 54^{k}.

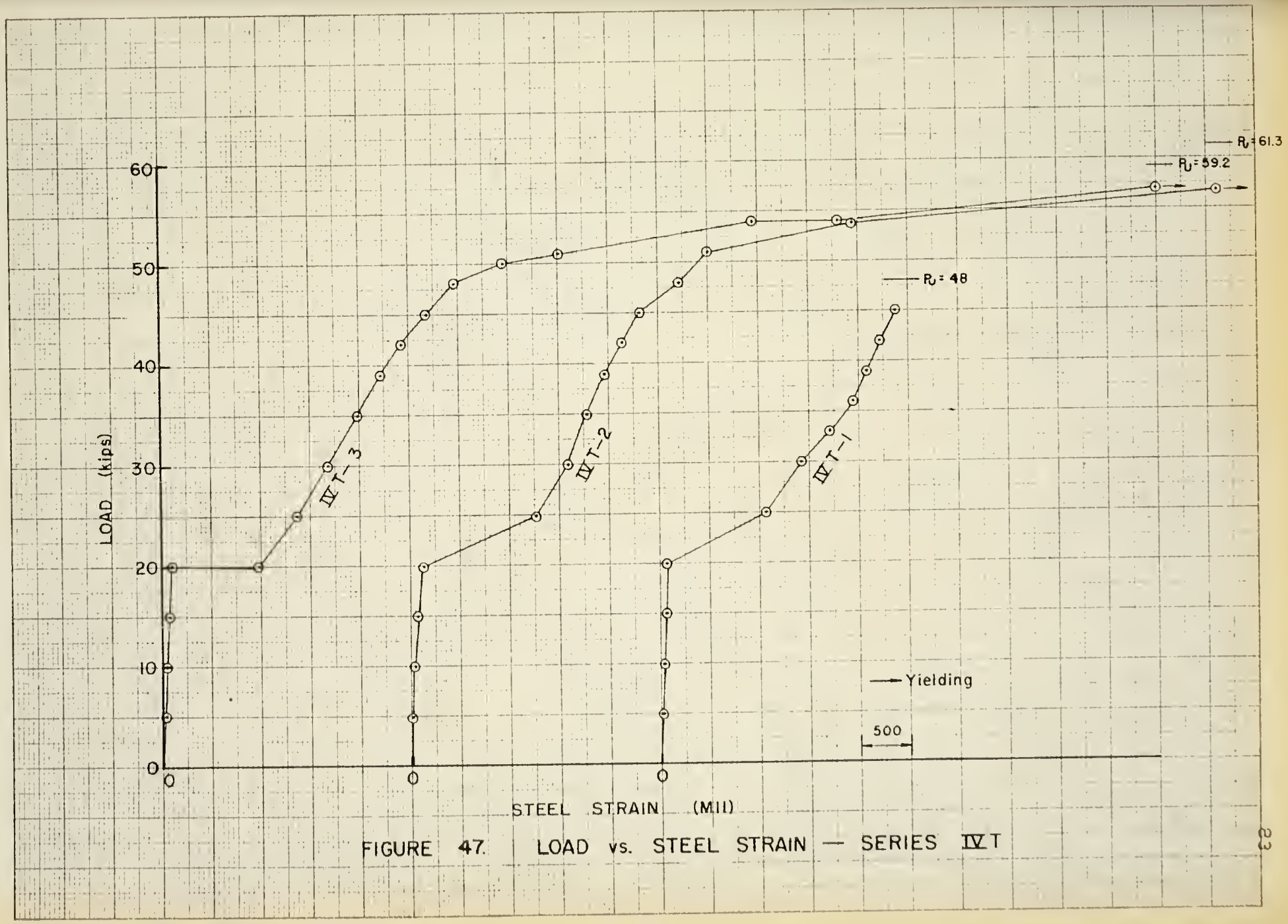

FIGURE 47. LOAD vs. STEEL STRAIN — SERIES IV T

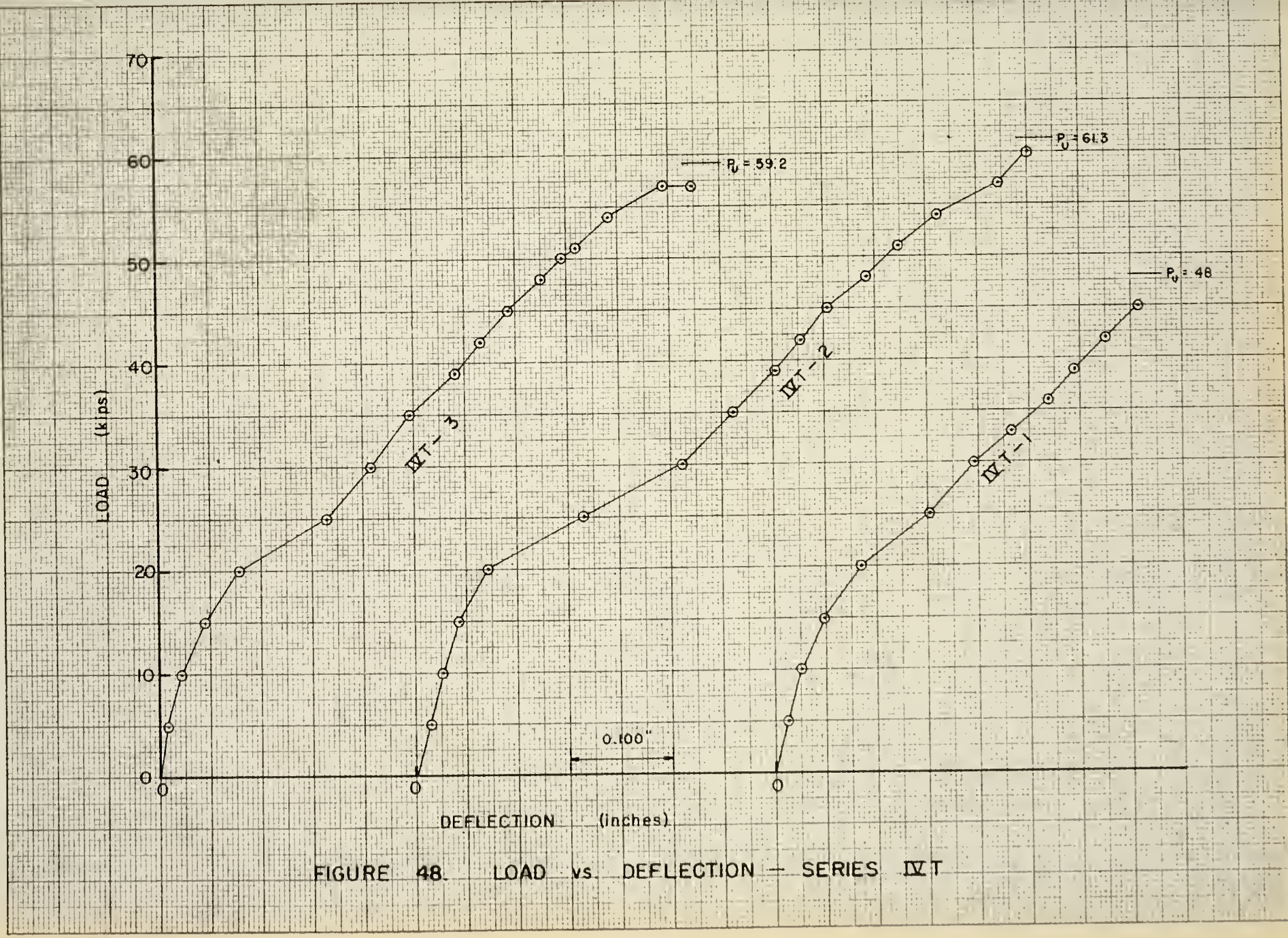

FIGURE 48. LOAD vs. DEFLECTION — SERIES IVT

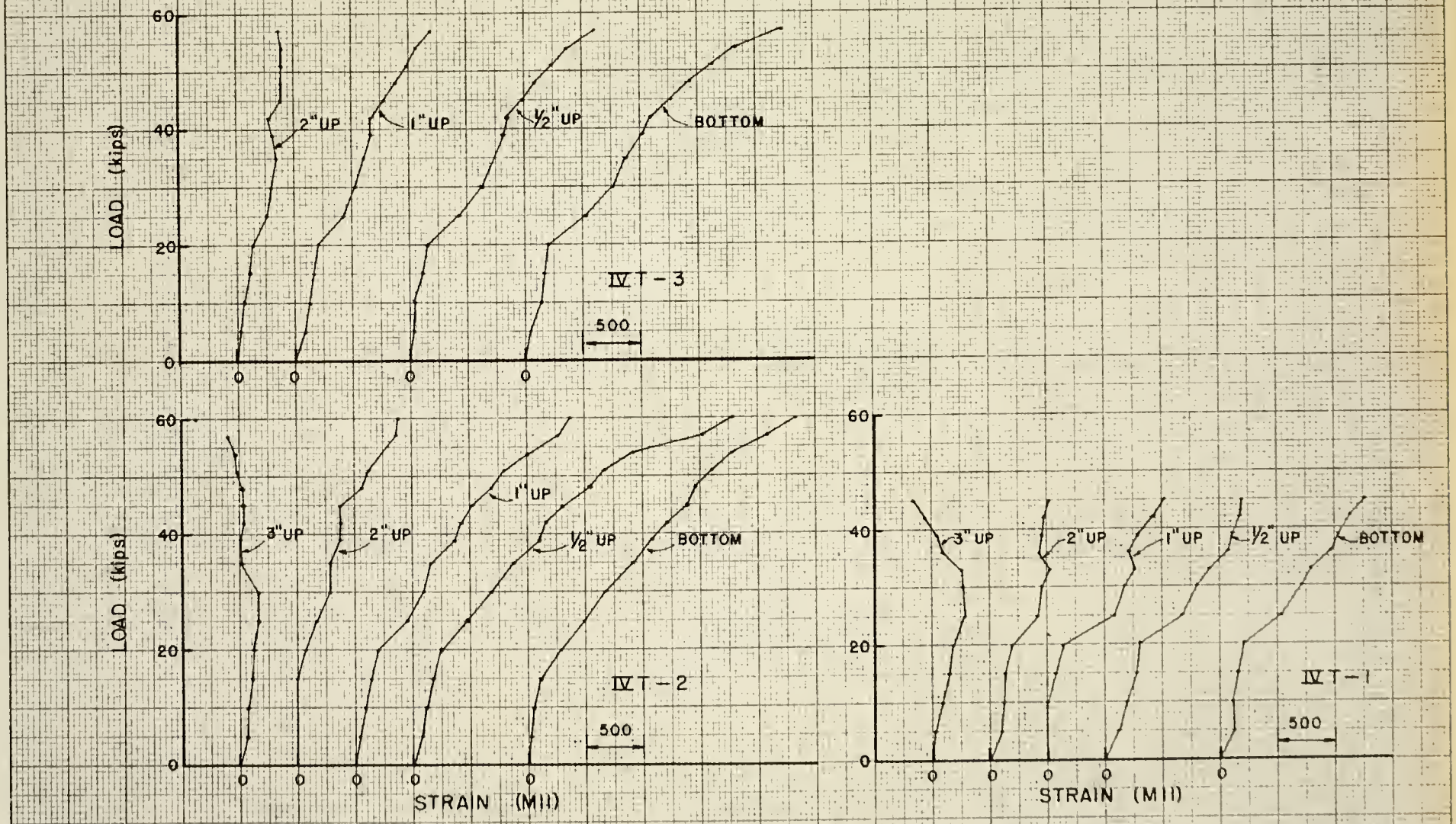

FIGURE 49. LOAD vs. CONCRETE STRAIN — SERIES IVT

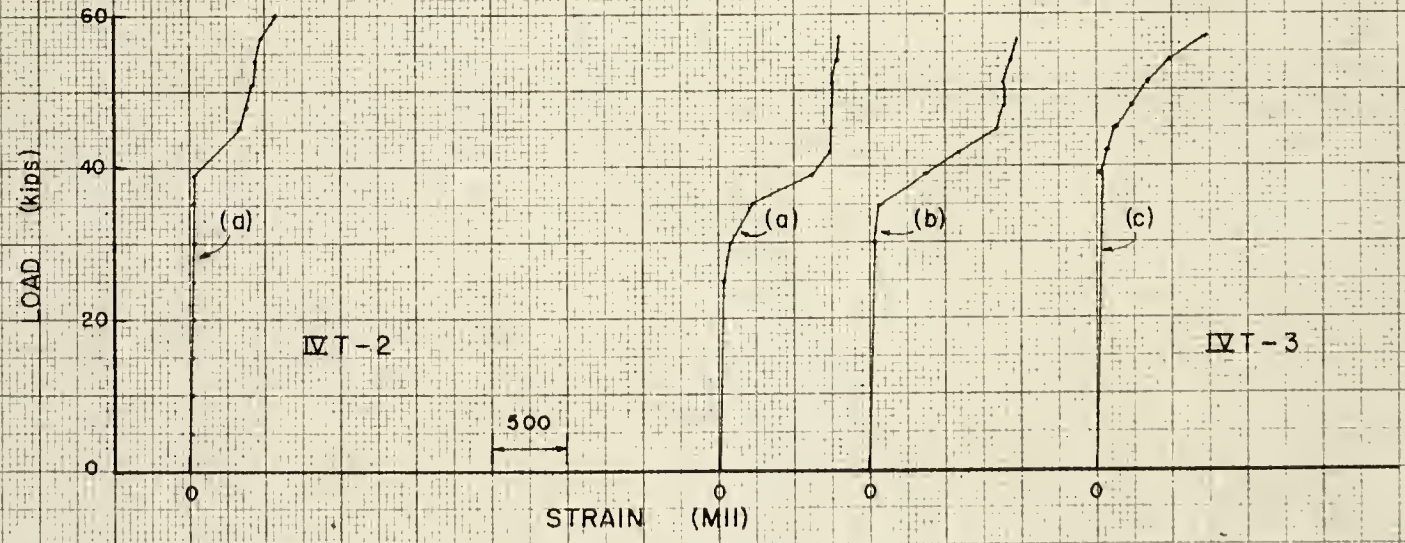

FIGURE 50. LOAD vs. STIRRUP STRAIN — SERIES IVT

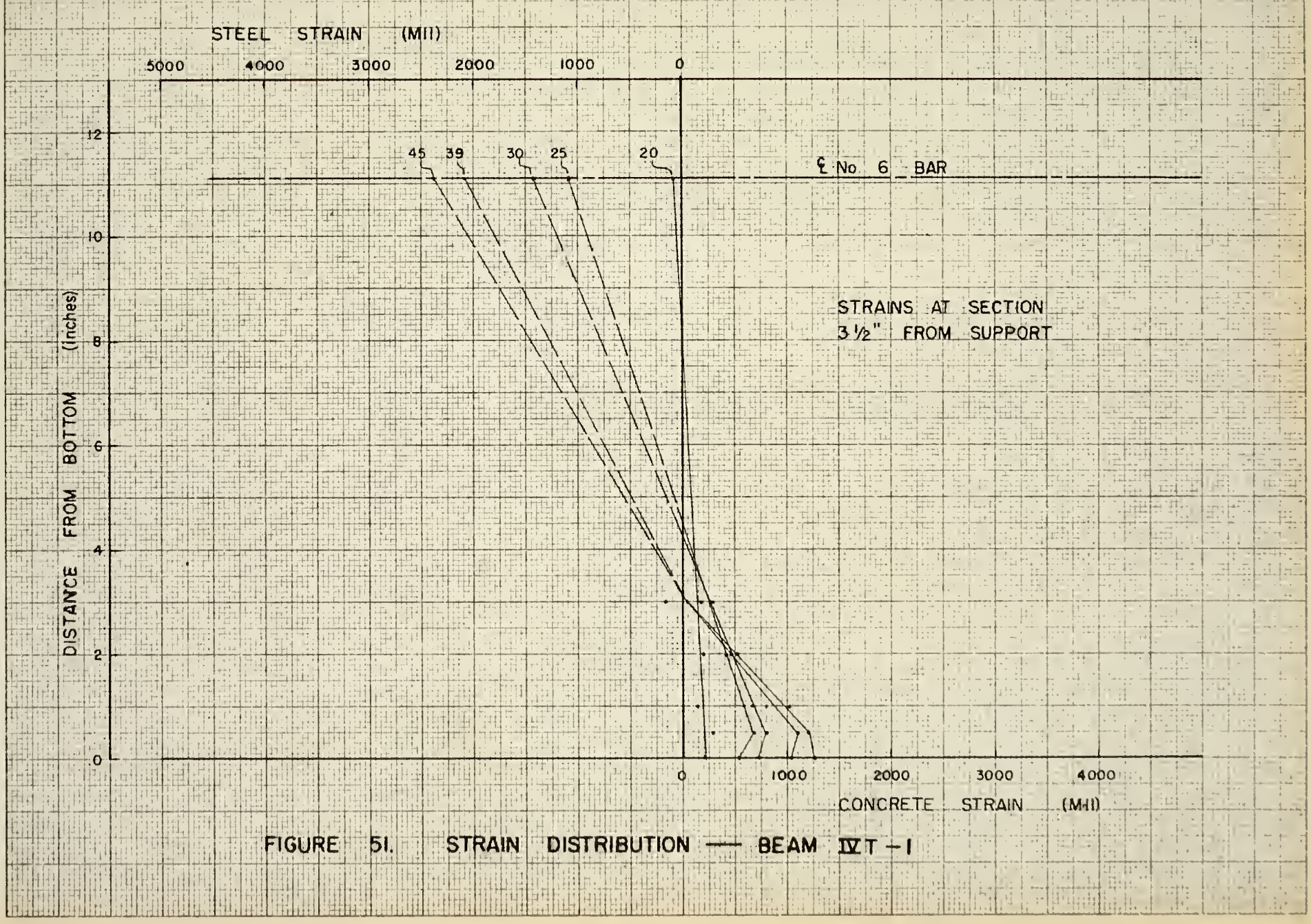

FIGURE 51. STRAIN DISTRIBUTION — BEAM IVT-1

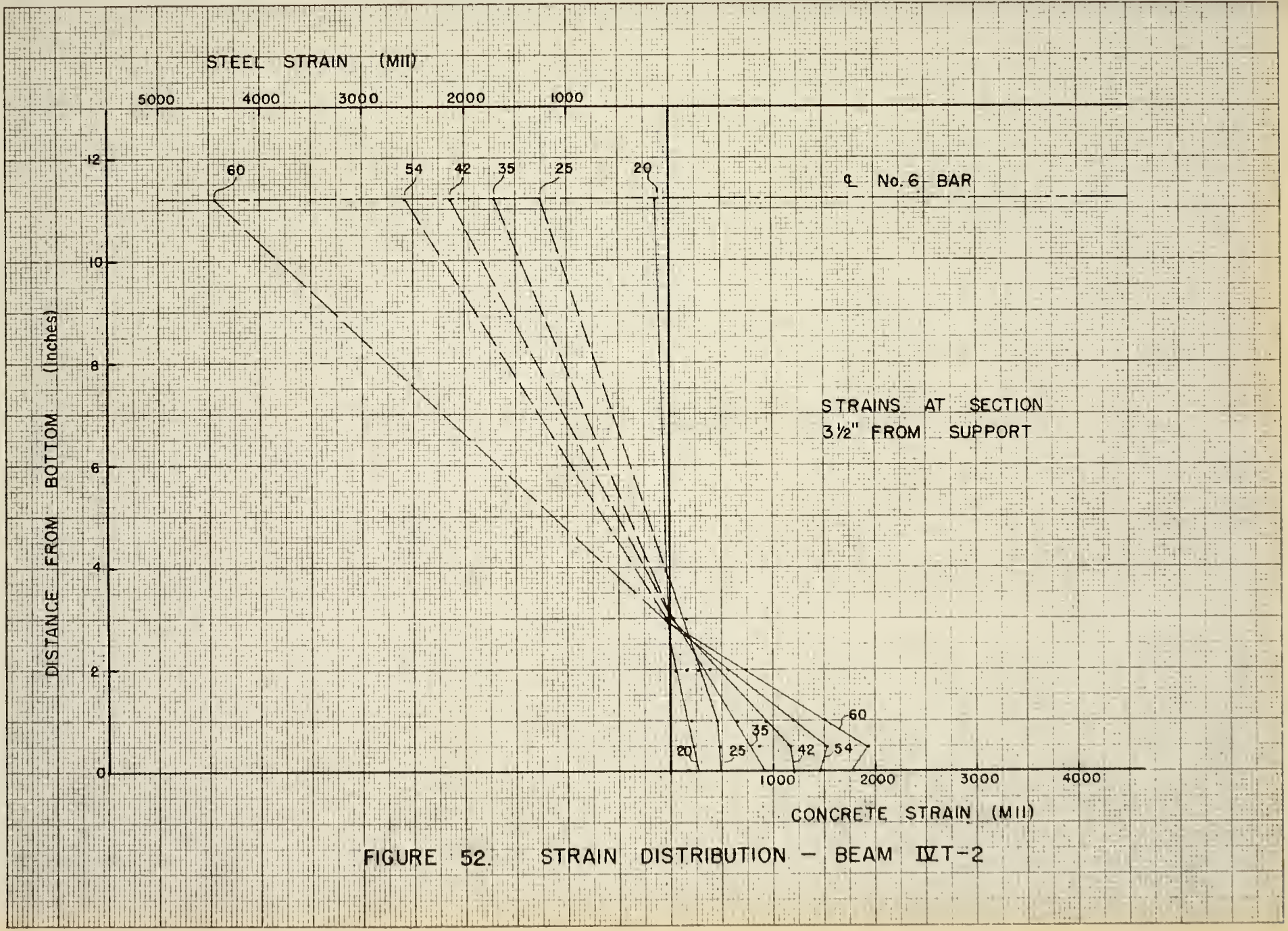

FIGURE 52. STRAIN DISTRIBUTION — BEAM IVT-2

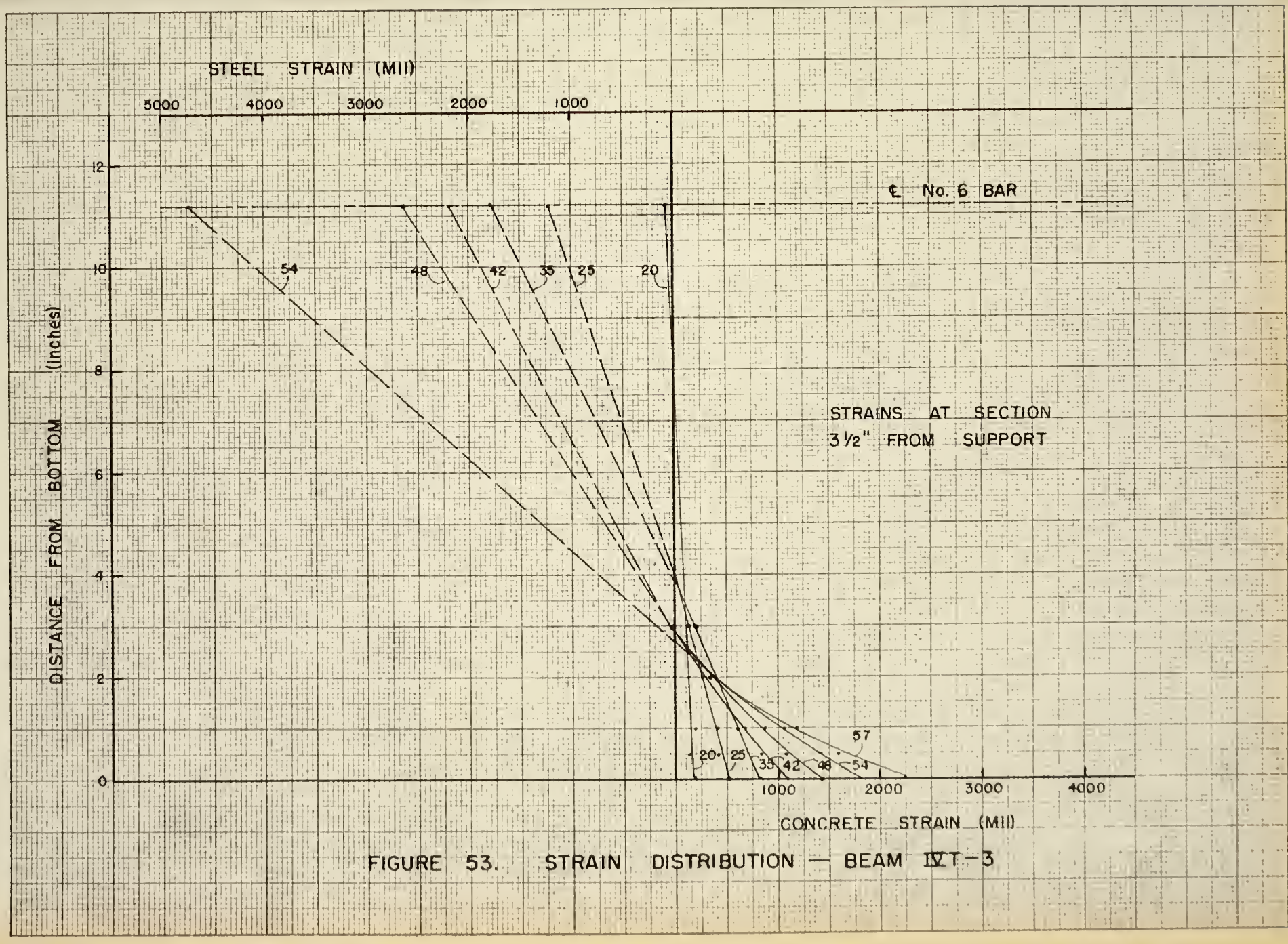

FIGURE 53. STRAIN DISTRIBUTION — BEAM IVT-3

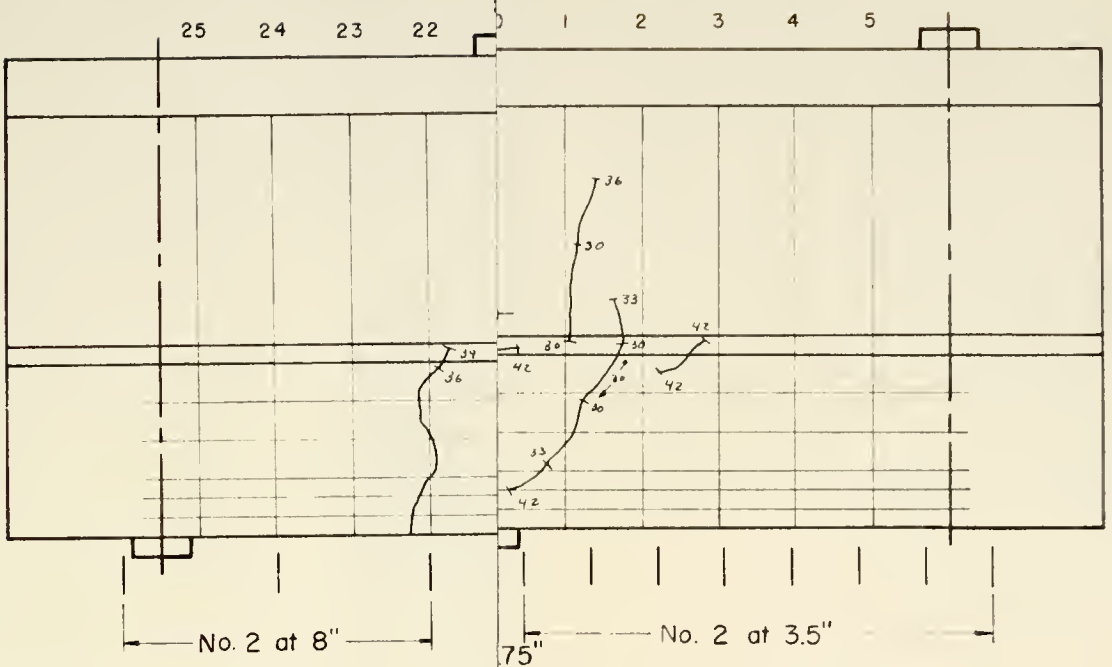

.75"

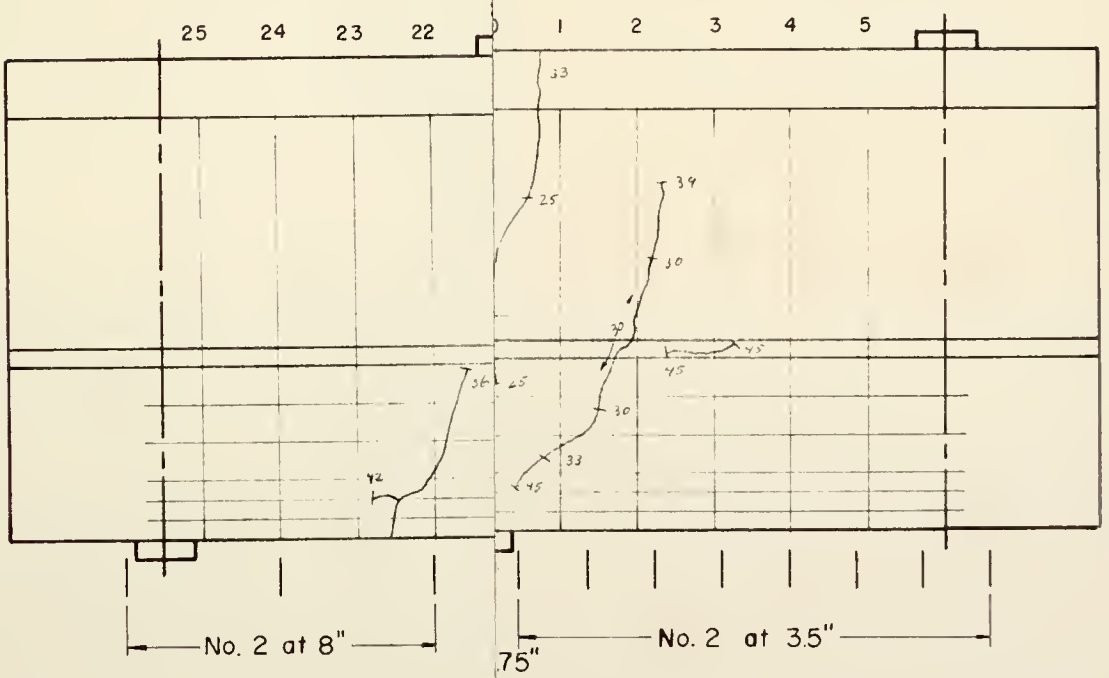

.75"

SR –

Whit BEAM IV T–1

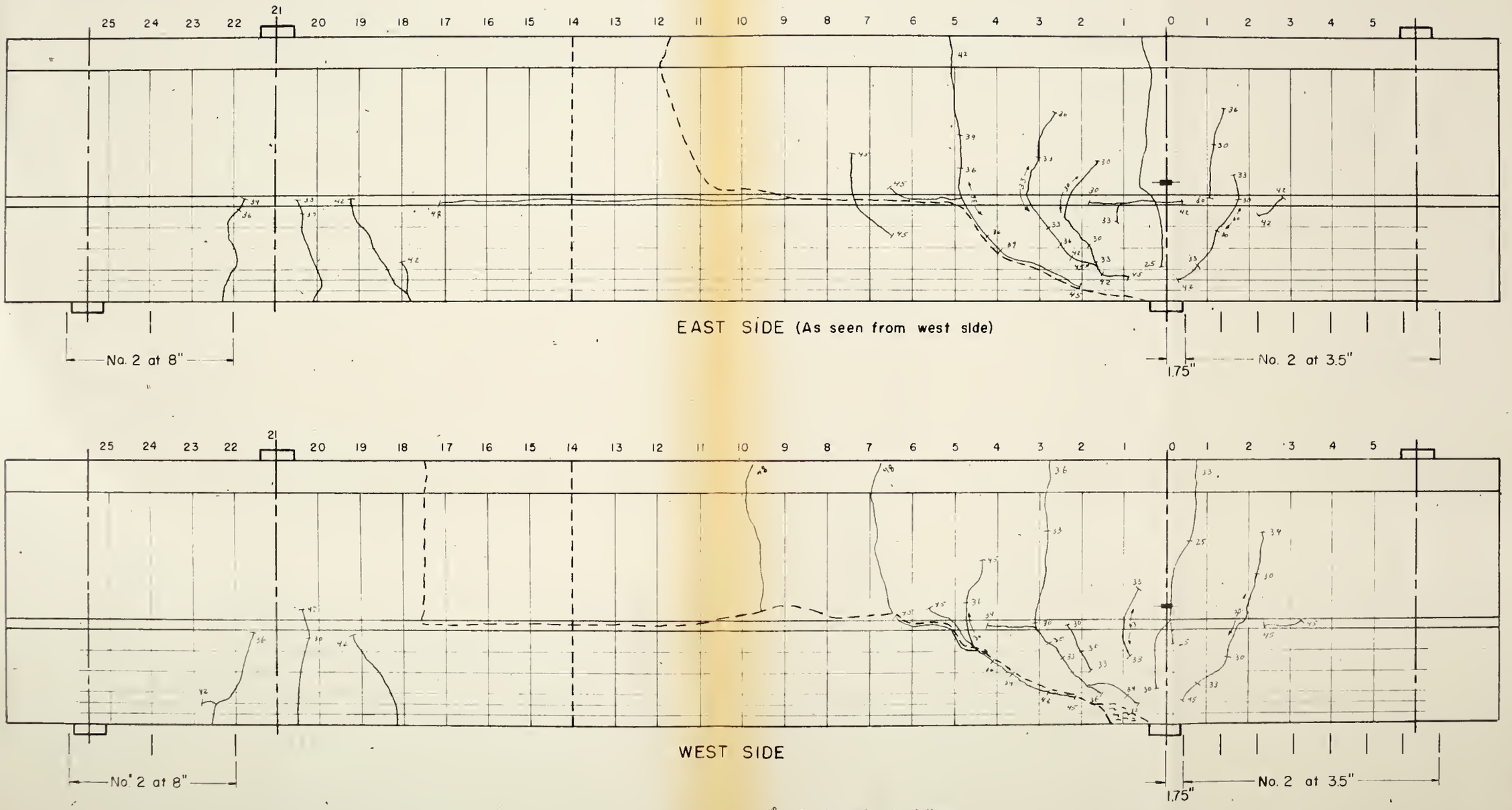

SR – 4 Gage Locations:

No. 6 Bar — At support (E & W)

Whittemore Gage Locations:

0, 0.5", 1", 2", 3" from bottom; 3.5" from support

Cracks priar to failure

Cracks opening wide at failure

SR – 4 Strain Gage

Scale: 1" = 10"

FIGURE 54. BEAM IV T–1

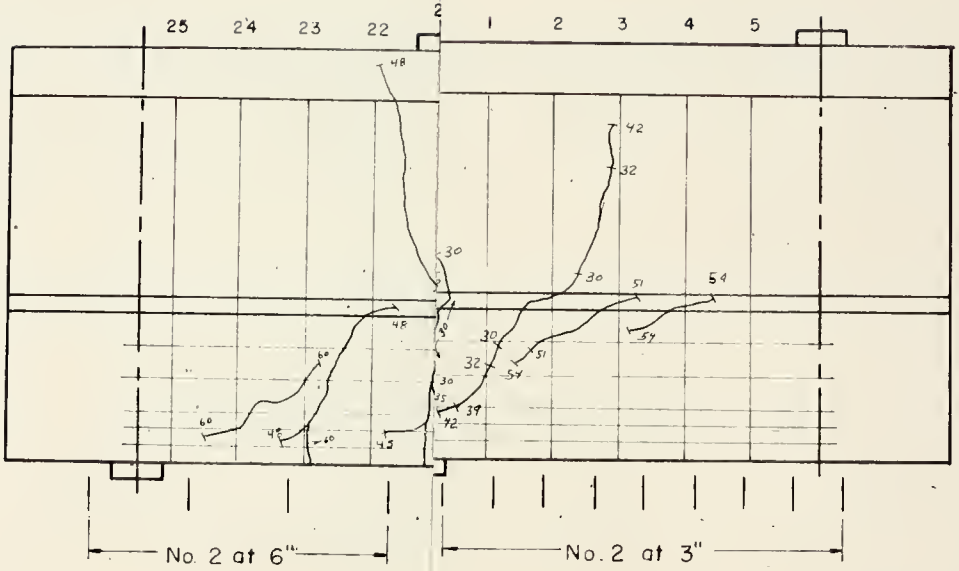

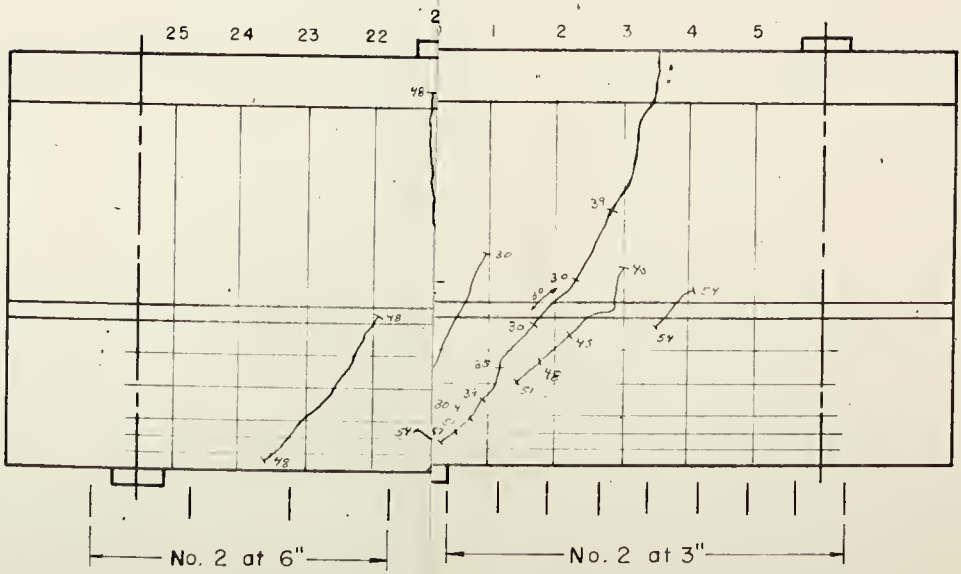

SR—

Whitt BEAM IV T—2

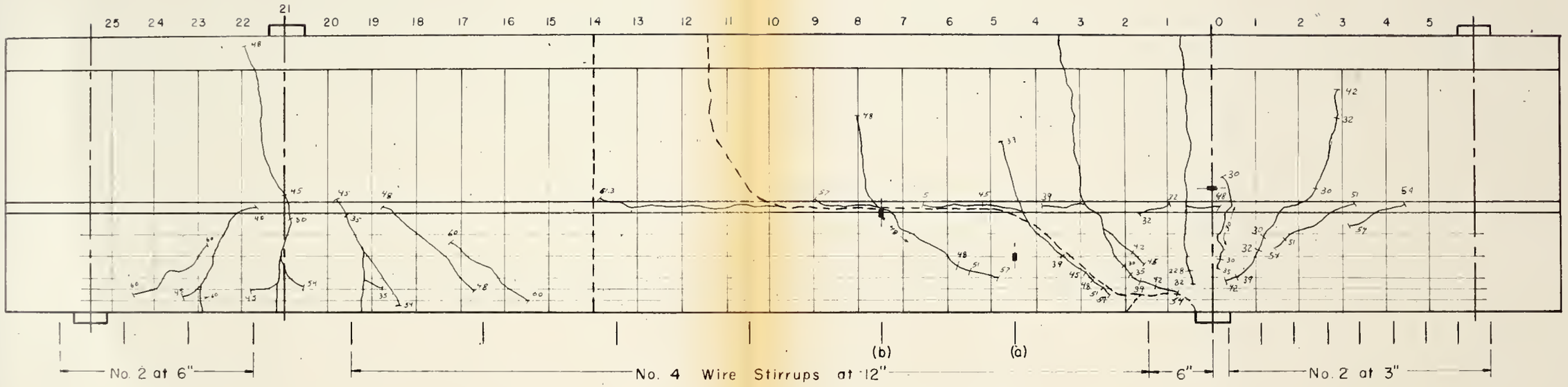

EAST SIDE (As seen from west side)

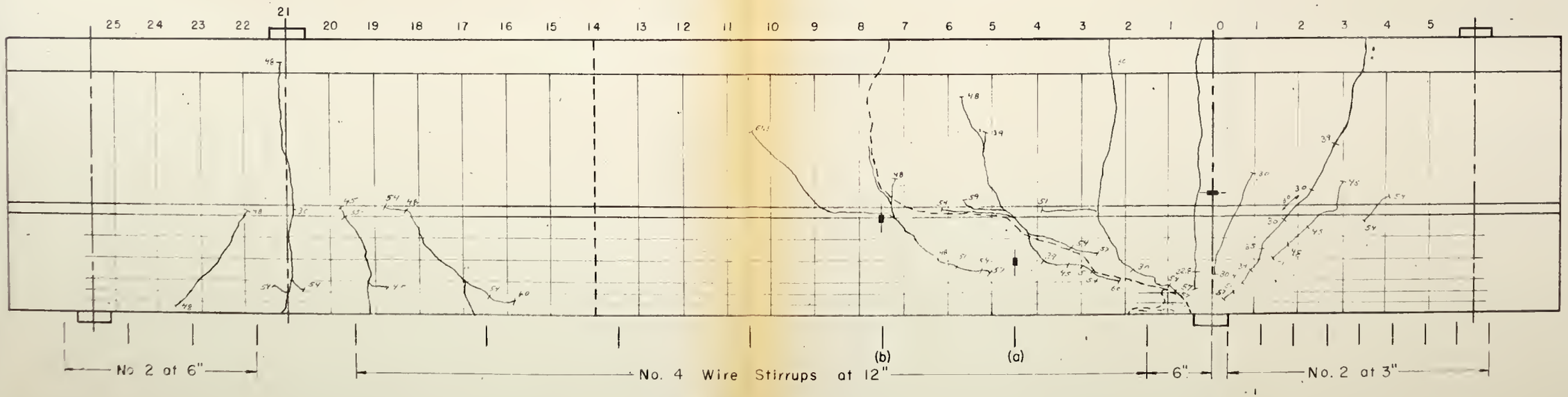

WEST SIDE

SR-4 Gage Locations:

No. 6 Bar — At support (E & W) ; Stirrup (b) — 9" from bottom (W)
Stirrup (a) — 5" from bottom (W)

Whittemore Gage Locations:

0, 0.5", 1", 2", 3" from bottom ; 3.5" from support

FIGURE 55. BEAM IV T-2

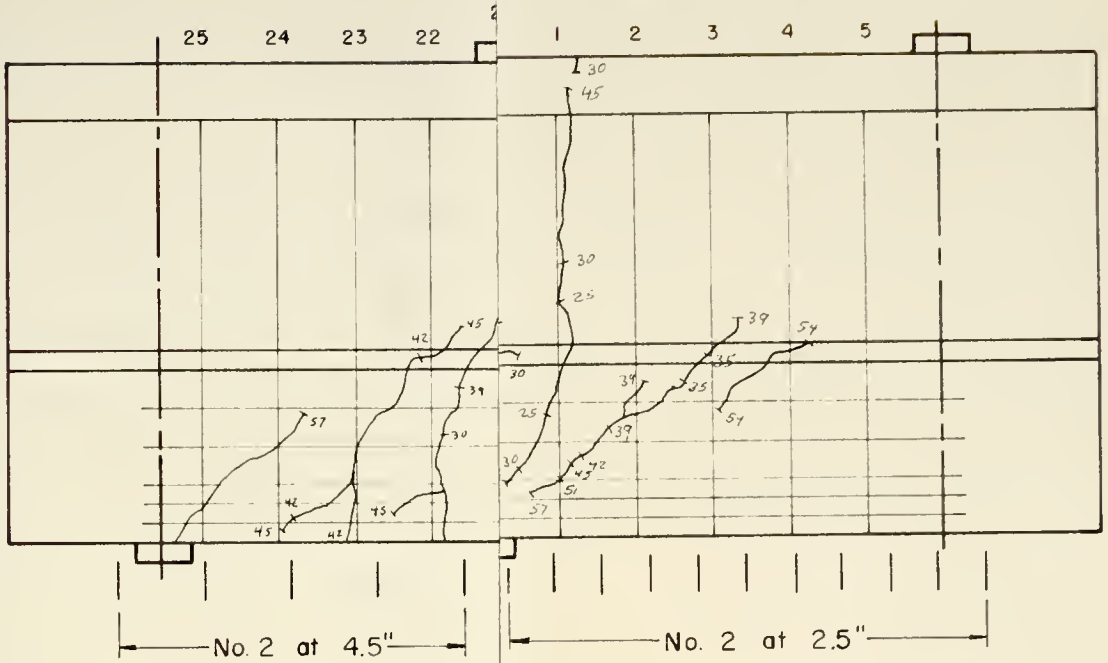

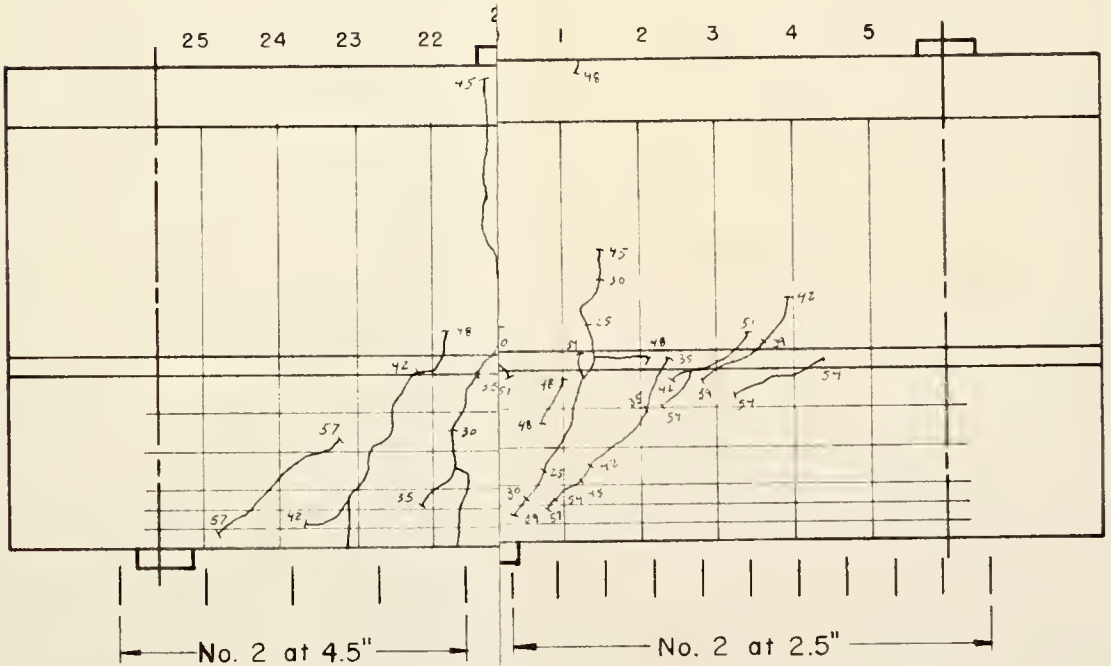

SR—

Whitt BEAM IV T—3

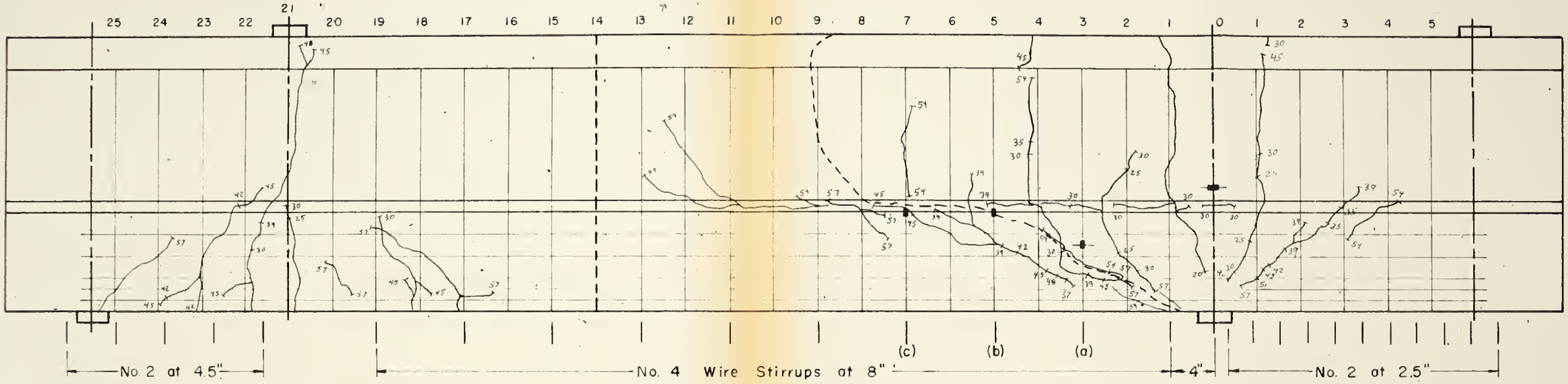

EAST SIDE (As seen from west side)

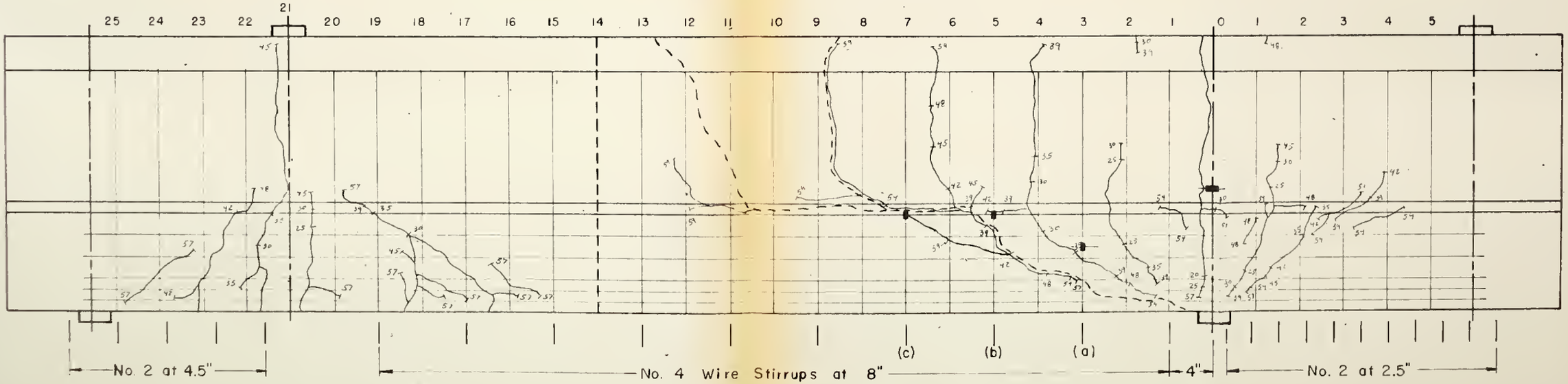

WEST SIDE

SR-4 Gage Locations:

No. 6 Bar — At support (E & W); Stirrup (b) — 9" from bottom (W)
Stirrup (a) — 6" from bottom (W); Stirrup (c) — 9" " " "

Whittemore Gage Locations:

0, 0.5", 1", 2", 3" from bottom; 3.5" from support

FIGURE 56. BEAM IV T-3

DISCUSSION OF TEST RESULTS

Modes of Failure

All beams in Series SS failed by diagonal tension. This behavior has also been observed by several other investigators (16) to be typical for simply supported T-beams. The stable compressive area eliminates the possibility of a shear-compression failure. The T-beams behaved essentially the same as the rectangular beam (SS - 4). The major difference was that the critical diagonal tension crack was pushed closer to the support in the T-beams than in the rectangular beam.

No definite relationship between type of failure and a/d ratio could be observed for the restrained series. The effect of the diagonal tension crack was apparent in beams which reached their flexural capacity.

The critical diagonal cracking load for all three restrained series was fairly constant unless a large amount of web reinforcement was present. When a large amount of web reinforcement was present, it was difficult to define the critical diagonal cracking load.

Beams II T - 3, III T - 4, IV T - 2, and IV T - 3 failed by crushing of the concrete at the support after significant yielding of the longitudinal steel had taken place.

Factors Affecting Beam Behavior

There are four major factors which affect shear strength of reinforced concrete beams: concrete strength; percentage of tension reinforcement; shear span to depth ratio; and the amount of web reinforcement present. It was intended that the first two parameters be held constant in this research. Some unintentional variation in concrete strengths occurred, however. The shear span to depth ratio and the amount of web reinforcement were the major variables investigated.

Shear Span to Depth Ratio

The summary of test results in Table 5 indicates a decrease in average shearing stress as the a/d ratio increases. The beams having nearly the same concrete strength and the same tension steel show the following results:

Series	a/d	Avg.* v_c = V/bd(psi) (diagonal tension cracking)	Avg.* v_c = V/bd (ultimate load)
II T	2.86	205	298
III T	3.93	128	194
IV T	5.00	145	171

*Avg. of all beams in each series.

The last series (IV T) shows an increase in shear stress over Series III T at diagonal tension cracking. This is due to the difficulty of defining the diagonal tension cracking load for Series IV T. The ultimate shear stress,

however, decreases as the a/d ratio increases.

Percentage of Web Reinforcement

The most noticeable effect produced by the addition of stirrups (besides the increase in strength of the beam,) was the penetration of the diagonal cracks. As the amount of web reinforcement was increased, the diagonal cracks penetrated deeper into the compression zone before the stirrups yielded, prior to failure of the beam. This, of course, was due to the increase in load required to fail the member because of the presence of the stirrups.

As the web reinforcement was increased, the shear strength of the beams in Series III T did not increase as markedly as in Series II T and Series IV T. For instance, Beam IV T - 3 had a percentage of web reinforcement of 0.158 but did not resist as great a load as Beam IV T - 2, with a percentage of 0.105. This was due to the fact that the flexural capacity of Beam IV T - 2 was exceeded by the shear capacity.

ANALYSIS OF TEST DATA

Nominal Shearing Stress at Diagonal Cracking

The Joint ACI - ASCE Committee 326 (1) presented a semi-empirical formula for predicting the resistance to diagonal tension cracking. This equation reads:

$$v_c = \frac{V_c}{bd} = 1.9 \sqrt{f'_c} + 2500 \frac{pVd}{M} \qquad (6)$$

This equation is intended to predict the average shearing stress required to produce diagonal cracking at the section under consideration. In the beams tested, the critical section was one effective depth (d) from the support. Hence, V/M = 1/a-d for the beams in the restrained series and V/M = 1/d for the beams in the simply supported series. Using the above equation, test results are compared in Table 6.

This formula was quite conservative for Series II T, which had an a/d ratio of 2.86; for the remaining series, it gave a good prediction of the average diagonal cracking load.

Nominal Shearing Stress at Ultimate Load

A comparison of the measured values and the calculated values for ultimate shearing stress is given in Table 6. For members with web reinforcement, the Joint Committee 326 recommended the following formula for ultimate shear strength:

Table 6. Comparison of Test Strengths with ACI and ASCE Committee Recommendations (1)

Beam	a/d	Diagonal Cracking Strength			Ultimate Shear Strength			
		v_c test (psi)	v_c calc.* (psi	$\frac{v_c \text{ test}}{v_c \text{ calc.}}$	v_u test (psi)	Krf_{vy} (psi)	v_u calc.** (psi)	$\frac{v_u \text{test}}{v_u \text{ calc.}}$
SS-1	4.0	152	154	.99	152	---	154	.99
SS-2	4.0	173	162	1.07	173	---	162	1.07
SS-3	4.0	152	158	.96	152	---	158	.96
SS-4	4.0	152	146	1.04	166	---	146	1.14
II T-1	2.86	226	136	1.66	226	---	136	1.66
II T-2	2.86	176	139	1.27	314	77.2	216	1.45
II T-3	2.86	305	135	2.25	355	132.5	268	1.32
III T-1	3.93	129	127	1.01	180	---	127	1.41
III T-2	3.93	147	137	1.07	188	57.8	195	.96
III T-3	3.93	129	134	.96	195	84.2	218	.89
III T-4	3.93	146	127	.87	213	115.2	242	.88
IV T-1	5.00	128	135	.95	146	---	135	1.08
IV T-2	5.00	165	138	1.19	187	21.3	159	1.18
IV T-3	5.00	146	127	1.15	181	32.1	159	1 14

* $v_c = v_c/bd = 1.9\sqrt{f'_c} + 2500 \quad vd/M. \qquad v_c = v_u$ for beams without stirrups.

** $v_u = v_u/bd = v_c + Krf_{vy}$ for beams with stirrups.

$$v_u = \frac{V_u}{bd} = v_c + v_s$$

In this equation, v_s is the portion of the total shear assumed to be carried by the stirrups, as given by the truss analogy. Thus, $v_s = k\, A_v/bs\, f_{vy}$, or in this case where $K = 1$, $v_s = Krf_{vy}$ (vertical stirrups). Therefore,

$$v_u = 1.9\sqrt{f'_c} + 2500\,\frac{pVd}{M} + Krf_{vy} \qquad (7)$$

This formula gave good results for Series IV T (with large a/d ratio); it was quite conservative for small a/d ratics. Series III T gave test values of only 90% of the predicted values. For beams with no stirrups, the formula predicted the average shear strength of simply supported beams reasonably well.

In Table 7 the test results are compared to the current design criteria of the "Standard Specifications for Highway Bridges [5]. These specifications state that the allowable shearing stress (v_a) for beams without stirrups is .03 f'_c and no greater than 90 psi. The shear stress is computed, using $v_c = V/bjd$. For beams with stirrups, the allowable shear stress is given by

$$v_a = \frac{V}{bjd} = 90 + r\, f_v \qquad (8)$$

In this equation, f_v is the working stress of the stirrup steel. The stirrup steel used in the first two restrained series was of structural grade which met the ASTM yield

Table 7. Comparison of Test Strengths with AASHO "Standard Specifications for Highway Bridges" (5)

Beam	v_u ** test (psi)	r f_v (psi)	v_a * (psi)	$\frac{v_u \text{ test}}{v_a}$
SS-1	152	---	90	1.69
SS-2	173	---	90	1.92
SS-3	152	---	90	1.69
SS-4	166	---	90	1.85
II T-1	226	---	90	2.51
II T-2	314	38.0	128	2.45
II T-3	355	65.1	155	2.29
III T-1	180	---	90	2.00
III T-2	188	28.5	119	1.58
III T-3	195	41.4	131	1.49
III T-4	213	56.9	147	1.45
IV T-1	146	---	90	1.62
IV T-2	187	10.5	101	1.85
IV T-3	181	15.8	106	1.71

* $v_a = 90$ psi for beams without stirrups;

$v_a = 90 + r\ f_v$ for beams with stirrups.

** v_u test $= V_u/bjd$ or practically $8V_u/7bd$.

strength requirements. Therefore, the allowable stirrup working stress for those series was f_v = 18,000 psi. The stirrup steel used in the last restrained series, however, was a softer steel with a yield point of 20,000 psi; therefore, a working stress of 10,000 psi was used.

The smaller shear span-to-depth ratio had the largest factor of safety. This factor of safety decreased as the shear span-to-depth ratio increased.

Moment at Shear-Compression Failure

Earlier studies (13), (14), (15), (18) have shown that the load at shear failure may be correlated on the basis of the failure moment at the critical section. With the notation from Figure 57, an analytical expression for the shear moment capacity may be derived from two equations of statical equilibrium.

From equilibrium of longitudinal forces:

$$T = C_c + C_s$$

or

$$Pbdf_s = k_1 k_3 f'_c bd k_s + A'_s f'_s \qquad (9)$$

From equilibrium of moments about a point "O":

$$M_s = c(d - k_2 k_s d) - A'_s f'_{su} (d - d') \qquad (10)$$

where

k_1 = coefficient defining the magnitude of the force C in the concrete in a beam at failure,

k_2 = coefficient defining the position of the force C in a beam at failure

k_3 = ratio of the compressive strength of concrete in a beam to f'_c

k_s = ratio of the depth of the compressive zone at the critical section in a beam at shear failure to the effective depth of the beam.

Assuming the tension crack has penetrated sufficiently that the compression steel stress is negligible, Equations 9 and 10 can be combined to give:

$$\frac{M_s}{f'_c b d^2} = p \frac{f_{su}}{f'_c} \left(1 - \frac{k_2}{k_1 k_3} \frac{p f_{su}}{f'_c}\right) \quad \text{where } p = \frac{A_s}{bd} .$$

The only unknowns are f_{su} (stress in the longitudinal steel at failure) and k_2/k_1k_3 (properties of the concrete stress block).

For the case of flexural compression failure the steel stress at failure may be determined from the compatibility condition for strains. Similarly, the shear compression failure stresses must come from strain compatibility. However, the strain distributions for the two cases are different in that, for the flexural case the strain distribution is linear and continuous. The shear compression case is probably nonlinear or discontinuous. Hypothetical strain distributions have been proposed by several researchers, two of which are presented in Figure 57 .

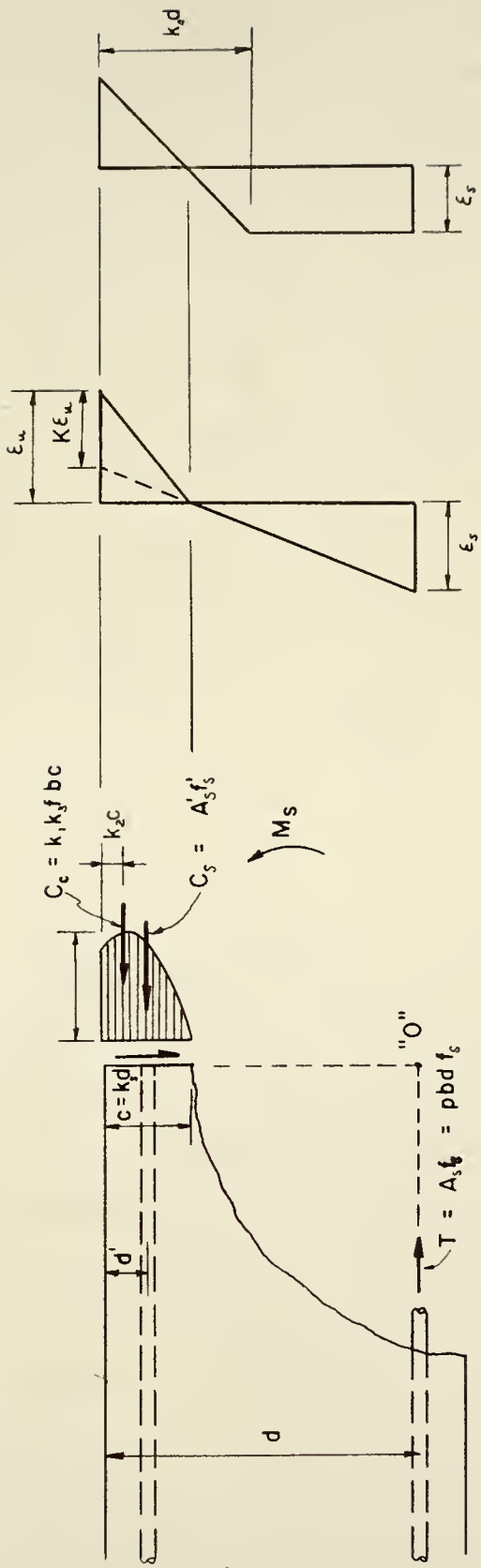

FIGURE 57. CRITERION FOR SHEAR—MOMENT CAPACITY

Morrow[15] and Moody[14] have each developed an empirical expression for steel stress based on their proposed strain distributions. Morrow's expression was obtained from a consideration only of beams without web reinforcement while Moody considered some beams with web reinforcement and other beams without web reinforcement. Both developments were based on rectangular beams but will be applied to T-beams here, on the basis of the standard design procedures.

When the strain distribution proposed by Morrow[15] was used, the calculated loads were conservative, but when the measured steel stress was used the calculated values were much higher than test values. The calculated values, using the strain distribution proposed by Moody[14], were very close to the test values for the beams without stirrups but were unconservative for beams with stirrups. In both cases the measured values of steel strain at failure were significantly higher than the calculated values.

The beams in Series IIT and IIIT were identical except for the addition of flanges to the beams of Series IIB and IIIB in Harvey's research[10]. The beams in Series IIT and IIB, when compared, are found to have quite similar ratios for P_{test}/P_{calc}; however, for Series IIIT the ratio is approximately twenty percent lower than for corresponding beams in Harvey's Series IIIB.

When Morrow's proposed strain distribution was used, the Beams IIT-1 and IIIT-1 had a slightly higher P_{test}/P_{calc} ratio than companion beams from Harvey's research. This

Table 8. Moment at Shear-Compression Failure (Test vs. Calculated from Equations of Reference 15).

Beam	Calculated*			Measured		$\frac{P_{test}}{P_{calc.}}$	Calculated Using Measured f_s **		
	f_{su} (psi)	M_s (in-kips)	P_{calc}* (kips)	f_s (psi)	P_{test} (kips)		M_s	$P_{calc.}$	$\frac{P_{test}}{P_{calc}}$
IIT-1	40,200	372.5	39.9	69,000	49	1.23	613	65.8	.740
IIIT-1	36,600	340.0	32.8	73.000	49	1.49	639	61.6	.795
IVT-1	38,400	360.0	32.5	67,500	48	1.48	613	55.2	.870

* P_{calc} based on M_s developed at edge of support block.
Series II T: $P = M_s/9.32$; Series III T: $P = M_s/10.38$; Series IV T: $P = M_s/11.08$
(neglecting influence of compression steel)

$$M_s = pf_s \left(1 - \frac{k_2}{k_1 k_3} \frac{pf_s}{f'_c}\right) bd^2 = A_s f_s \left(1 - \frac{k_2}{k_1 k_3} \frac{pf_s}{f'_c}\right) d$$

$$\frac{k_2}{k_1 k_3} = 0.44 \quad k_1 k_3 = \frac{8.00 + f'_c}{70 + f'_c}$$

$$f_s = 1/2 E_s K_{\epsilon_u} \left(-1 + \sqrt{1 + \frac{4 k_1 k_3 f'_c}{p E_s K_{\epsilon_u}}}\right)$$

$$10^4 K_{\epsilon_u} = \frac{1.116\, a/d + .174}{a/d - .872}$$

** See Appendix C for sample calculations.

Table 9. Moment at Shear Compression Failure. (Test vs. Calculated from Equations of Reference 14).

Beam	Calculated* f_{su} (psi)	M_s (in-kips)	P_{calc} (kips)	Measured f_s (psi)	P_{test} (kips)	$\frac{P_{test}}{P_{calc.}}$
IIT-1	51,900	472	50.7	69,000	49	.97
IIT-2	---	737	79.1	80,500	68	.86
IIT-3	---	798	85.7	---	77	.90
IIIT-1	53,700	487	47.0	73,000	49	1.04
IIIT-2	---	793	76.4	83,000	51.3	.67
IIIT-3	---	848	81.7	83,000	53	.63
IIIT-4	---	914	88.2	---	57.9	.66
IVT-1	61,500	561	50.7	67,500	48	.95
IVT-2	---	847	76.6	---	61.3	.80
IVT-3	57,500	923	83.5	---	59.2	.70

(neglecting influence of compression steel)

Beam without stirrups:

$$M'_s = pf_s\left(1 - \frac{k_2}{k_1k_3}\frac{pf_s}{f'_c}\right) bd^2 = A_sf_s\left(1 - \frac{k_2}{k_1k_3}\frac{pf_s}{f'_c}\right)d \quad \text{Eq. (3a) Ref. 14.}$$

$$k_2 = 0.42 \qquad k_1k_3 = 1.121 - 0.0485\, f'_c/1000 \qquad \text{Eqs. (5a, 5b) Ref. 14.}$$

$$f_s = \frac{\frac{3M}{Vd} - 0.45}{\frac{3M}{Vd} + 0.55}\left[6.9 \times 10^{-4} E_s \left(-1 + \sqrt{1 + \frac{1450}{pE_s/k_1k_3f'_c}}\right)\right] \quad \text{Eq. (6a) Ref. 14.}$$

Beams with vertical stirrups:

$$M_s = A_1M'_s + A_2A_3\,(rf_{vy})(a''/d)^2\, bd^2 \quad \text{Eq. (7) Ref. 14}$$

where M'_s = shear moment capacity of same beam without stirrups

$A_1 = 1.38$, $A_2A_3 = .08$, which are empirical constants

Table 9. (continued)

· a'' = the distance from the section of maximum negative moment to the section of maximum positive moment.

* See Appendix C for sample calculations.

would suggest that the flange does not add to the shear strength in the case of restrained beams.

Ultimate Strength in Flexure

Strains in tension steel for Beams IIT-3, IIIT-4, IVT-3 and IVT-4 indicate that the section was at or near its ultimate capacity in flexure. By Whitney's ultimate strength approach (using $f_y = 75{,}000$ and $f'_c = 4{,}000$ psi),

$$M_u = A_s f_y \left(d - \frac{a}{2}\right) \quad \text{where } a = \frac{A_s f_y}{.85 f'_c b}$$

$M_u = 632{,}000$ in-lbs. (neglecting the compression steel).

For ultimate crushing adjacent to the support block, this yields:

	Calculated Values	Test Values
Beam IIT-3:	$P = \frac{632}{9.32} = 67.8$ k	P = 77
Beam IIIT-4:	$P = \frac{632}{10.38} = 60.8$ k	P = 57.9
Beams IVT-2 : IVT-3	$P = \frac{632}{11.08} = 57.1$ k	P = 61.3 P = 59.2

As can be seen in the above comparison, Beams IIT-3, IVT-2 and IVT-3 withstood loads greater than the predicted flexural ultimate strength. While the load vs. steel strain curve (Figure 36) indicates definite signs of yield, Beam IIIT-4 failed below the predicted flexural strength. This

was probably due to the effects of the diagonal tension crack. Some of the difference between calculated and test values may be eliminated if the possibility of strain hardening is considered.

Comparison of Shear Strength of Rectangular Section and T-Section

The beams in Series IIT and IIIT are essentially identical to beams in Series IIB and IIIB in a recent investigation by Harvey[10], with the exception of the addition of a 3-inch thick flange in the IIT and IIIT Series.

Table 10 indicates the diagonal cracking and ultimate loads for the rectangular beams were essentially the same as those for the T-beams. The last two beams listed in Table 10 failed by a shear-compression-flexural tension mode for the T-beam Series, thus explaining the low ratio. This may also be due to the two beams in the T-beam study having approximately 450 psi lower compressive strength than the two beams in the rectangular beam study.

In comparing the behavior of the stirrups in companion beams of Series IIT and Series IIB[10], one can see that once a stirrup began picking up strain, the behavior was essentially the same in both rectangular and T-beams. However, in order to develop equivalent strain values in the stirrups of IIT and IIB, a higher load was required for T-beams than for rectangular beams. Consider, for example, Beam IIB-2 (Figure 58) and Beam IIT-2 (Figure 28). The

stirrups in Beam IIB-2 began yielding at a load of approximately 40^{k} while the stirrups in Beam IIT-2 did not yield until a load of 59^{k} was reached. The ultimate loads for these two beams were essentially the same value, which would indicate that the rectangular beam had additional resistance to shear after the stirrups began to yield while the T-beam had very little additional resistance. Basically the same behavior was observed in comparing Beams IIB-3 and IIT-3.

Table 10. Comparison of T-Beams and Rectangular Beams (10)

Beam		Diagonal Cracking Shear Stress (psi) T-Beams v_T	Rect. Beams v_R	$\frac{v_T}{v_R}$	Ultimate Strength Shear Stress (psi) T-Beams v_T	Rect. Beams v_R	$\frac{v_T}{v_R}$
IIT or IIB	1	226.0	157	1.44	226.0	221	1.02
	2	175.7	156	1.05	314.0	292	1.08
	3	304.5	163	1.88	355.0	312	1.15
IIIT or IIIB	1	128.7	136	.97	180.0	140	1.32
	2	147.2	136	1.11	188.0	179	1.07
	3	128.2	---	----	195.0	263	.74
	4	110.2	---	----	213.0	258	.83

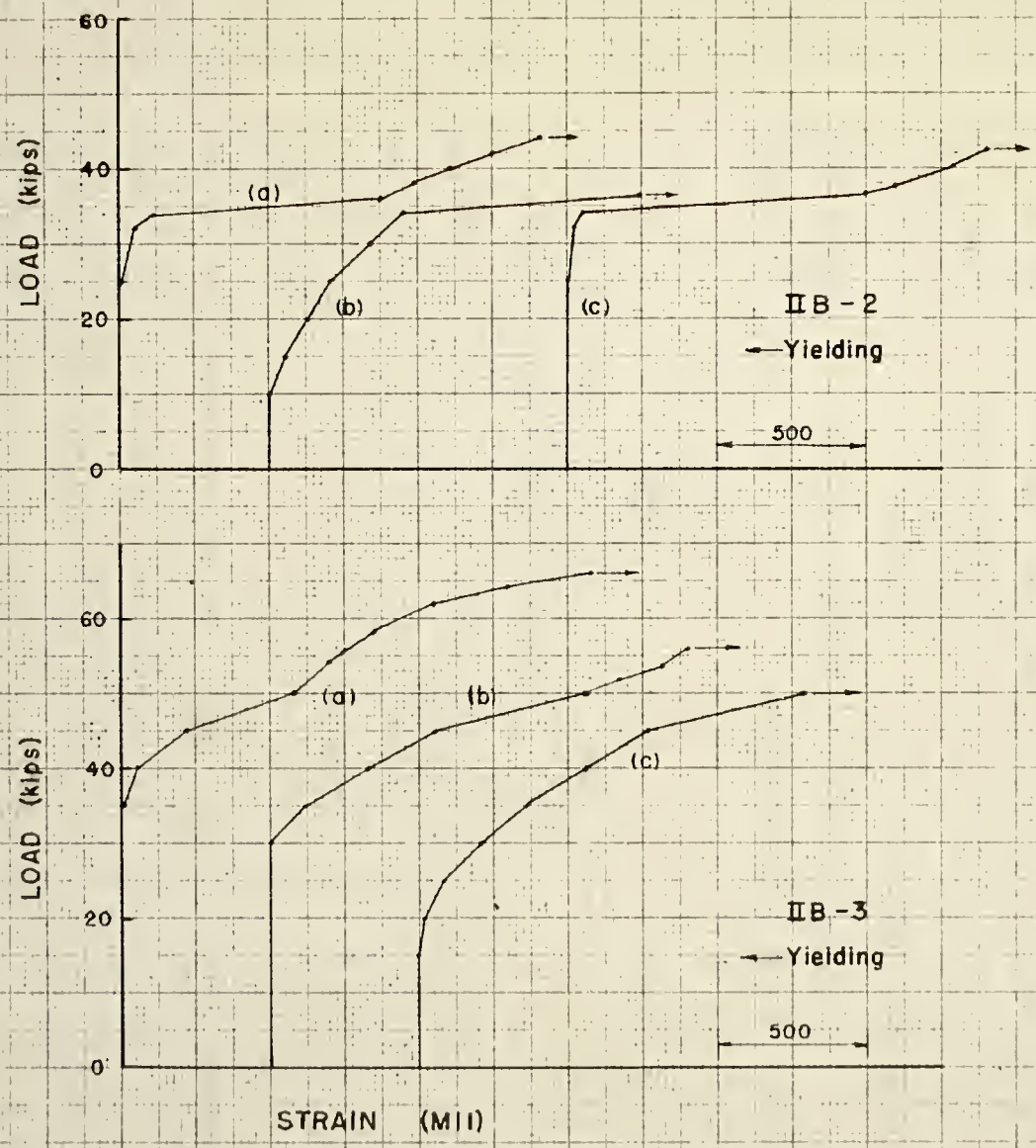

Note: Graphs taken from Figure 24 of Reference 10.

FIGURE 58. LOAD vs. STIRRUP STRAIN — SERIES II

SUMMARY AND CONCLUSIONS

1. The beam tests reported herein indicate two general modes of shear failure in reinforced concrete T-beams without shear reinforcement:
   a. A "shear compression" failure occurring at the section of maximum moment and shear at loads substantially greater than the load at which the diagonal crack first penetrated the compression zone. Failure was by crushing of the reduced compression zone adjacent to the support, following significant redistribution of internal strains.
   b. A "diagonal tension" failure occurring generally at some distance away from the support at a load equal to or only slightly greater than the load at which the critical diagonal tension crack formed. Such failure was sudden, occurring with little warning.
2. For beams with small percentages of stirrups, the failure mode was essentially the same as for beams without stirrups, after yielding of stirrups crossed by the critical crack.
3. Beams with high percentages of stirrups behaved essentially the same as beams failing in flexure, but with a diagonal crack opening upon failure and with crushing of the concrete at the head of this crack.

4. The semi-empirical formula for shear stress at diagonal cracking presented by the Joint ACI-ASCE Committee 326 gave conservative values for the series with a/d ratio of 2.86, but for all other series (with greater a/d ratios) the values were quite accurate.
5. The factor of safety (ratio of ultimate shear stress to allowable shear stress) for beams, using the AASHO "Standard Specifications for Highway Bridges," (1961) ranged from 2.51 for the smaller a/d ratio down to approximately 1.5 for larger a/d ratios.
6. The shear stress at failure decreased with increasing a/d ratio, but the series with a/d ratio equal to 5.00 had a higher shear stress at diagonal cracking than the Series with a/d ratio of 3.93. This could have been due to the difficulty of defining the diagonal cracking load for the larger a/d.
7. Applying Morrow's proposed strain distribution to the shear-compression failure theory gave good predictions for failure load but the calculated steel strains were only about half of the measured strains. When Moody's strain distribution was applied, the predicted values for ultimate load were unconservative, but the calculated steel strains were closer to measured values than Morrow's predictions.

8. For the limited number of specimens tested, the comparison of rectangular and T-beams indicates that the practice of computing the shear strength of restrained T-beams by considering only the web of the beam is justified.

BIBLIOGRAPHY

BIBLIOGRAPHY

1. ACI-ASCE Committee 326, "Shear and Diagonal Tension," ACI Journal, Jan., Feb., Mar. 1962 Proceedings Vol. 59.

2. ACI Committee 318, "Building Code Requirements for Reinforced Concrete (ACI 318-56)," ACI Journal, May 1956 Proceedings Vol. 52, pp. 913-86.

3. ACI Committee 318, "Building Code Requirements for Reinforced Concrete (ACI 318-63)," ACI Standard, June 1963.

4. Al-Alusi, A. F., "Diagonal Tension Strength of Reinforced Concrete T-Beams with Varying Shear Span," ACI Journal, May 1957 Proceedings, Vol. 53, pp. 1067.

5. American Association of State Highway Officials, "Standard Specifications for Highway Bridges," 1961.

6. Bower, J. E. and Viest, I. M., "Shear Strength of Restrained Concrete Beams without Web Reinforcement," ACI Journal, July 1960 Proceedings Vol. 57, pp. 73.

7. Elstner, R. C., Moody, K. G., Viest, I. M. and Hognestad, E., "Shear Strength of Reinforced Concrete Beams. Part 3 - Tests of Restrained Beams with Web Reinforcement," ACI Journal, Feb. 1955 Proceedings Vol. 51, pp. 525-40.

8. Ferguson, P. M. and Thompson, J. N., "Diagonal Tension in T-Beams without Stirrups," ACI Journal, Mar. 1953 Proceedings Vol. 49, pp. 665.

9. Guralnick, S. A., "High Strength Deformed Steel Bars for Concrete Reinforcement," ACI Journal, Sept. 1960 Proceedings Vol. 57, pp. 241.

10. Harvey, W. N., "A Study of Diagonal Tension Failure in Reinforced Concrete Beams," M. S. Thesis, Purdue University, 1964.

11. Hognestad, E., "What Do We Know About Diagonal Tension and Web Reinforcement in Concrete?" Circular Series No. 64, University of Illinois Engineering Experiment Station, Mar. 1952.

12. Hognestad, E., Hanson, N. W., Magura, D. D. and Mass, M. A., "Shear Strength of Slender Continuous Reinforced Concrete T-Beams," PCA Journal, Sept. 1963, Vol. 5, No. 3.

13. Laupa, A., Siess, C. P. and Newmark, N. M., "Strength in Shear of Reinforced Concrete Beams," Bulletin No. 428, University of Illinois Engineering Experiment Station, 1955.

14. Moody, K. G. and Viest, I. M., "Shear Strength of Reinforced Concrete Beams - Part 4 - Analytical Studies," ACI Journal, Mar. 1955 Proceedings Vol. 51, pp. 697.

15. Morrow, JoDean and Viest, I. M., "Shear Strength of Reinforced Concrete Frame Members without Web Reinforcement," ACI Journal, Mar. 1957 Proceedings Vol. 53, pp. 833.

16. Taub, J. and Neville, A. M., "Resistance to Shear of Reinforced Concrete Beams. Parts 1 and 2," ACI Journal, Aug., Sept., 1960 Proceedings Vol. 59, pp. 193, 315.

17. Timoshenko, S. and Goodier, J. N., Theory of Elasticity, 2nd Ed., 1951, McGraw-Hill Book Company, Inc., pp. 171-77.

18. Zwoyer, E. M. and Siess, C. P., "Ultimate Strength in Shear of Simply-supported Prestressed Concrete Beams without Web Reinforcement," ACI Journal, Oct. 1954 Proceedings Vol. 51, pp. 181.

APPENDIX A

STRESS - STRAIN PROPERTIES OF THE REINFORCEMENT

APPENDIX A

STRESS - STRAIN PROPERTIES OF THE REINFORCEMENT

Figure 59 is a typical stress-strain curve for the longitudinal steel used in each beam. Figures 60 and 61 are typical stress-strain curves for the web reinforcement used. The steelrepresented was used only in the last test series in Figure 61. Note that these are not average curves but typical curves of one of the coupons tested of each material.

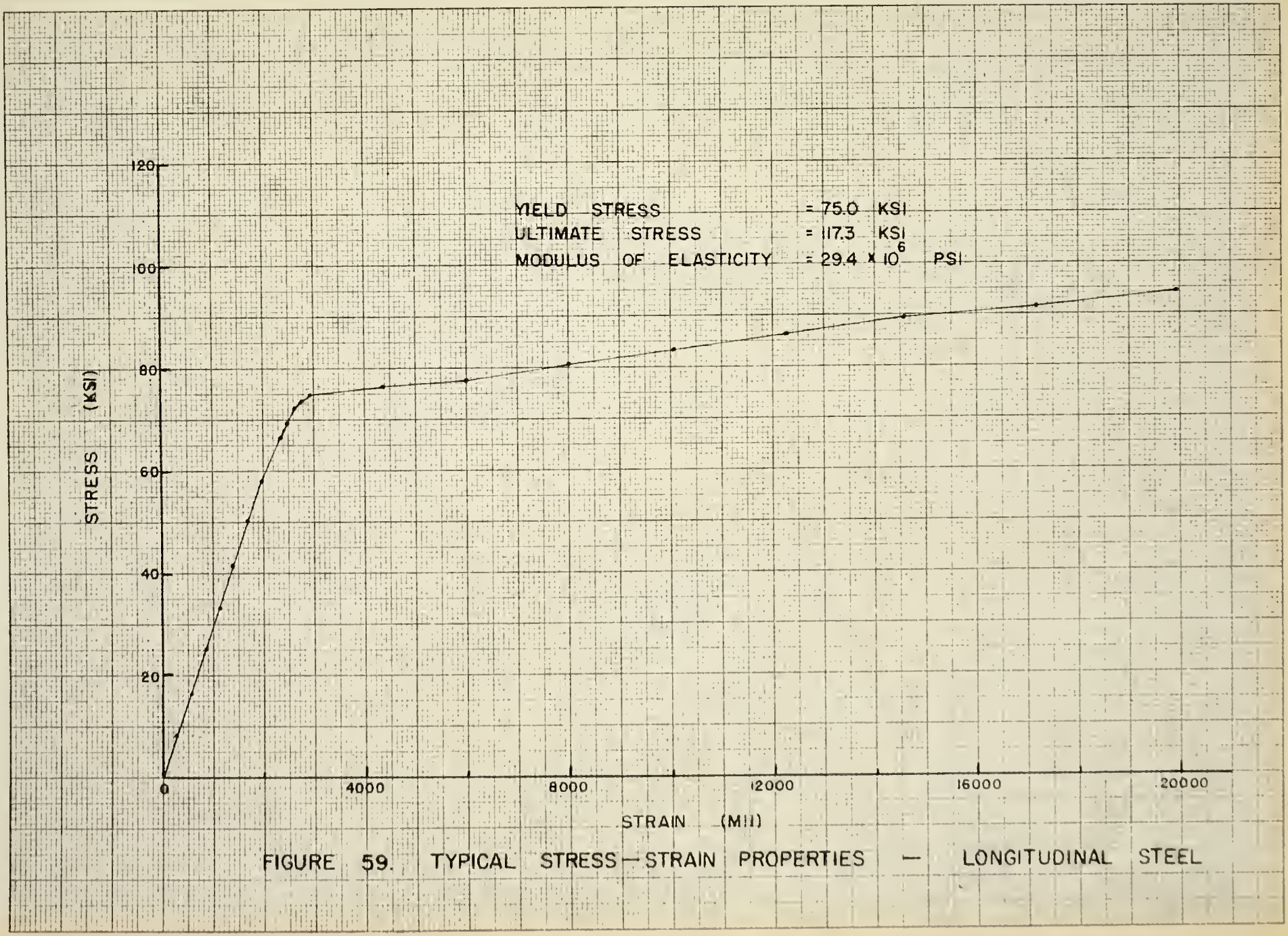

FIGURE 59. TYPICAL STRESS—STRAIN PROPERTIES — LONGITUDINAL STEEL

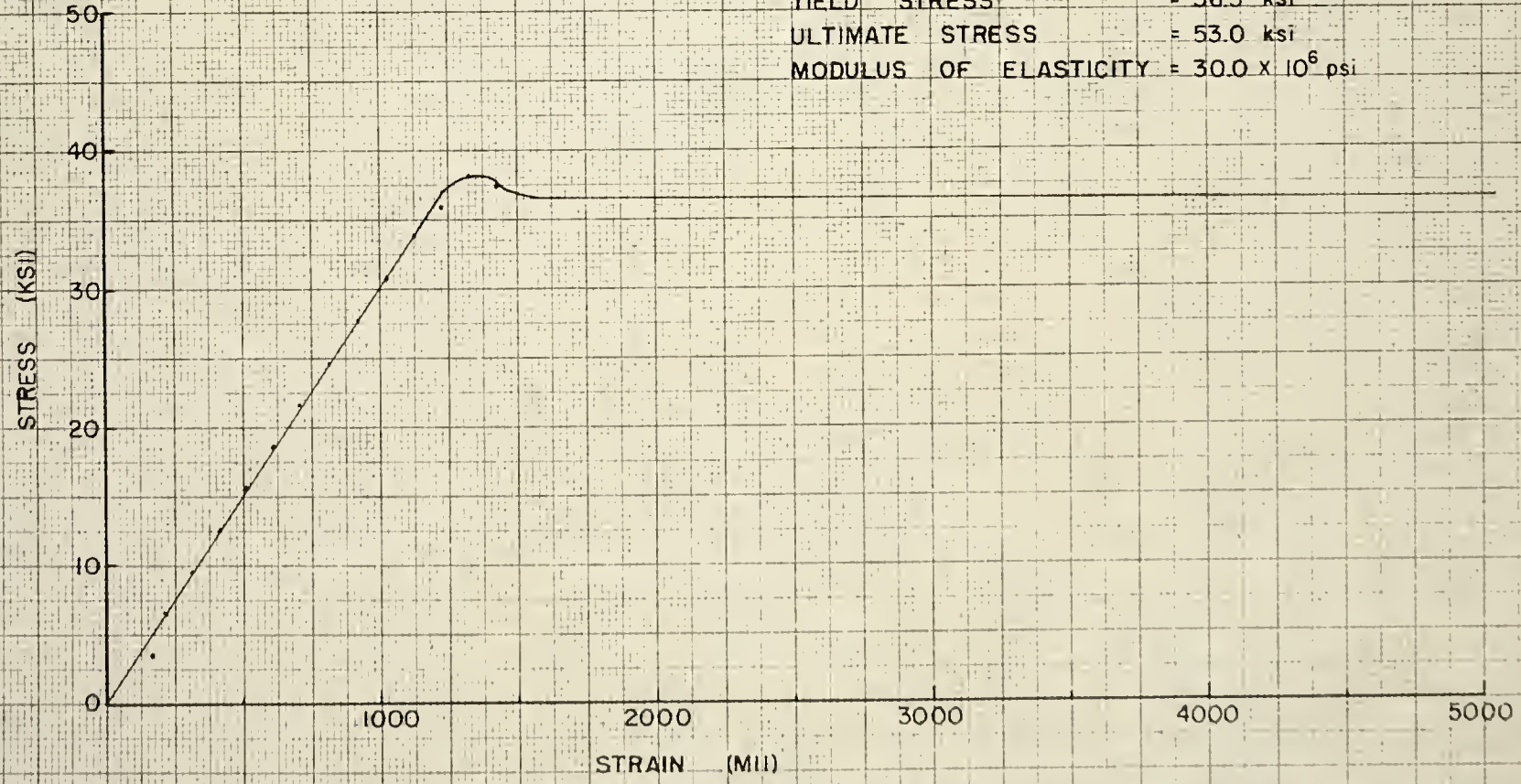

FIGURE 60. TYPICAL STRESS — STRAIN PROPERTIES — STIRRUP STEEL

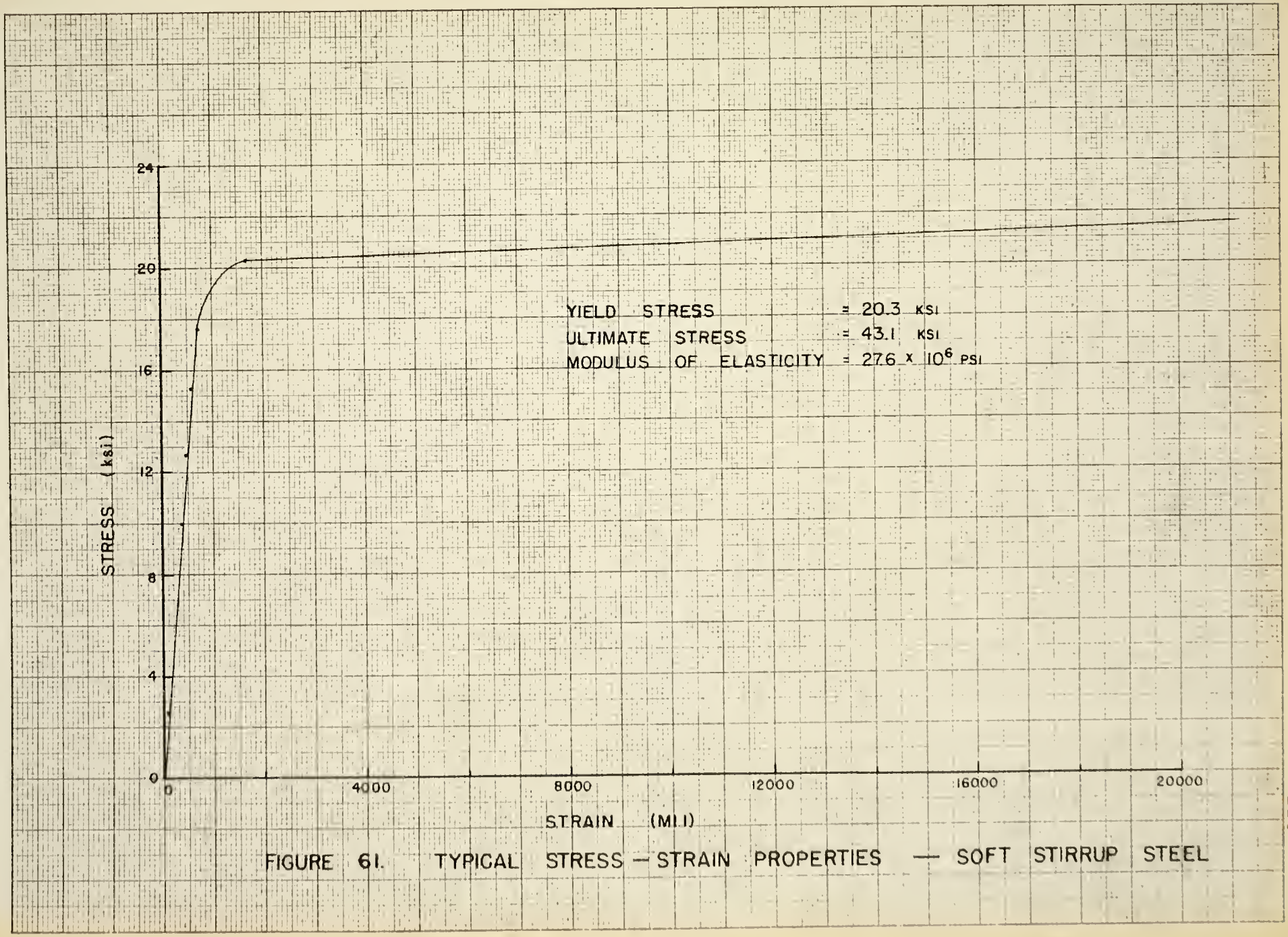

FIGURE 61. TYPICAL STRESS — STRAIN PROPERTIES — SOFT STIRRUP STEEL

APPENDIX B

PROCEDURES FOR APPLICATION AND WATERPROOFING OF THE SR-4 STRAIN GAGES

APPENDIX B

PROCEDURES FOR APPLICATION AND WATERPROOFING OF THE SR-4 STRAIN GAGES

SR-4 electric strain gages (Budd C-6-141B) were used for all beam specimens. The installation procedures used were, in general those recommended by the manufacturer and are given as follows.

Surface Preparation

The rib of the reinforcing steel was first ground off to provide a wide enough area to apply the gage and a pair of terminal pads. Fine sand paper was used to remove any deep scratches and, in general, to smooth the area where the gage was to be applied. Acetone was applied to remove any oil or grease from the bar and care was taken to prevent the gage location from becoming oily. The area was also cleaned by sanding it with 280 grit silicon carbide paper which had been dipped in metal conditioner (a mild acid solution). The metal conditioner was wiped off with a tissue. This operation was repeated with a fresh piece of sand paper. Then conditioner was applied with a cotton swab and remained on the steel about 30 seconds before being wiped off with a tissue. Neutralizer was applied with a clean swab and was

was left on for about 30 seconds. The gage location was then ready for application of the gage.

Gage Application

The metal foil gage was placed on a piece of cellophane tape so that the gage could be handled after its backing was removed. The terminal pads were placed near the terminal end of the strain gage. A coating of accelerator was applied to both the terminal pads and the gage back. This accelerator was allowed to dry for at least 4 minutes. The gage was then placed in position on the bar, held in place by the cellophane tape. A bead of Eastman 910 adhesive was placed on the bar at the point where the tape was stuck to it. With a tissue, the gage was rolled down from one end to the other. Care was taken to hold the loose end away from the bar in order to prevent the formation of air bubbles or wrinkles under the gage. Pressure was applied for one minute, after which the tape was peeled off by pulling back as close to the bar as possible. The gage was inspected to insure that it was completely bonded. The lead wire was then soldered to the terminal pad with a fine jumper wire connecting the lead wire to the gage. The excess resin from soldering was removed with a resin solvent.

Waterproofing

The gage was waterproofed by applying a thin layer of two-part epoxy waterproofing over an area slightly larger than

the gage and terminal pads. The waterproofing was extended up the lead wire for a short distance. It was purchased from the Budd Instrument Division, Box 245, Phoenixville, Pennsylvania. The waterproofed area was cured for one hour under heat lamps (at 150° to 200°F). The final gage installation was compact in size, covering an area of approximately 1½" long and 1/3 the circumference the bar with a thickness of about 1/8 inch. A typical waterproofed gage can be seen in Figure 62.

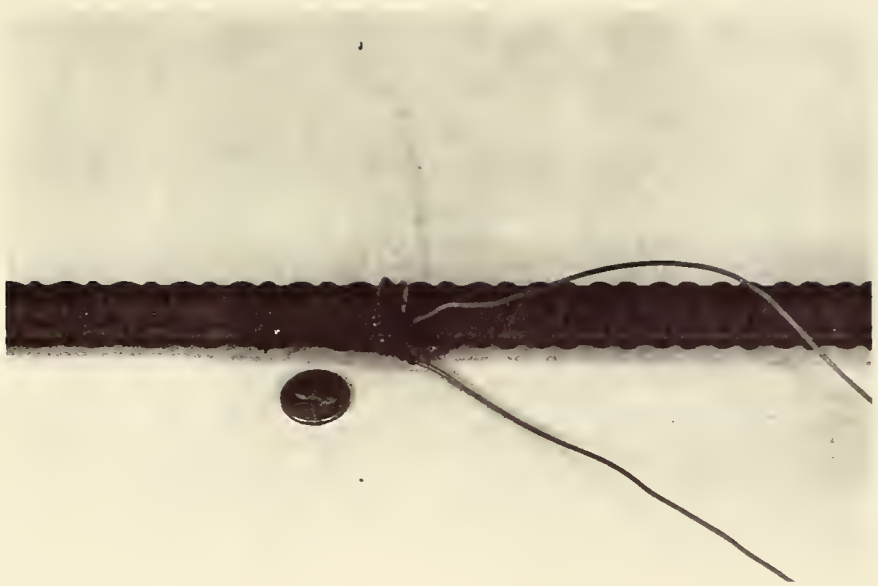

FIGURE 62. TYPICAL WATERPROOFED GAGE

APPENDIX C

SAMPLE CALCULATIONS

APPENDIX C

SAMPLE CALCULATIONS

Using strain distribution proposed by Morrow (15):

$$M_s = pf_s \left(1 - \frac{k_2}{k_1 k_3} \frac{pf_s}{f'_c}\right) bd^2 = A_s f_s \left(1 - \frac{k_2}{k_1 k_3} \frac{pf_s}{f'_c}\right) d$$

$$\frac{k_2}{k_1 k_3} = 0.44; \quad k_1 k_3 = \frac{800 + f'_c}{70 + f'_c}$$

$$f_s = \frac{1}{2} E_s K_{\epsilon u} \left(-1 + \sqrt{1 + \frac{4 k_1 k_3 f'_c}{p E_s K_{\epsilon u}}}\right)$$

$$10^4 K_{\epsilon u} = \frac{1.116\, a/d + .174}{a/d - .872}$$

Beam II T - 1

$a/d = 2.86$

$f'_c = 4010$ psi

$E_s = 29.4 \times 10^6$ psi

$$p = \frac{.88}{6(11.2)} = .01308$$

$$10^4 K_{\epsilon u} = \frac{1.116\,(2.86) + .174}{2.86 - .872} = \frac{3.366}{1.988} = 1.693$$

$$k_1 k_3 = \frac{800 + 4010}{70 + 4010} = \frac{4810}{4080} = 1.179$$

$$f_s = \frac{29.4(10^6)1.693(10^{-4})}{2} \left(-1 + \sqrt{1 + \frac{4(1.179)4010}{.01308(29.4)(10^6(1.693)(10^{-4})}}\right)$$

$$= 2510 - 1 + \sqrt{1 + 288.4}$$

$$= 2510\ (16.0) = 40{,}200 \text{ psi}$$

$$M_s = (.88)(40.2)\left[1 - \frac{(.44)(.01308)(40.2)}{4.01}\right] \qquad 11.2$$

$$= 395.3\ \left[1 - .0577\right]$$

$$= 372.5 \text{ in-kips}$$

$$P = \frac{M_s}{9.32} = \frac{372.5}{9.32} = 39.9k$$

Using strain distribution proposed by Moody (14).

$$M_s = pf_s\left(1 - \frac{k_2}{k_1 k_3}\ \frac{pf_s}{f'_c}\right) bd^2$$

$$k_2 = 0.42; \quad k_1 k_3 = 1.121 - 0.0485\ \frac{f'_c}{1000}$$

$$= 1.121 - 0.0485\ \frac{(4010)}{1000}$$

$$= .927$$

$$f_s = \frac{\frac{3M}{vd} - 0.45}{\frac{3M}{vd} + 0.55}\left[6.9 \times 10^{-4} E_s\left(-1 + \sqrt{1 + \frac{1450}{E_s k_1 k_3 f'_c}}\right)\right]$$

$$\frac{M}{vd} = \frac{9.32\ P}{(.310\ P)11.2} = 2.68$$

$$f_s = \frac{3(2.68) - 0.45}{3(2.68)+0.55}\left[6.9 \times 10^{-4}\ (29.4)(10^6)\ (-1 + \sqrt{1 + \frac{1450(.927)(4010)}{(.01308)(29.4)(10^6)}})\right]$$

$$= .883\left[58,800\right] = 51,900 \text{ psi}$$

$$M'_s = .01308(51,900)(1 - \frac{0.42(.01308)(51,900)}{0.927(4010)})(6)(11.2)^2$$

$$= 511\ (1 - .0769)$$

$$= 511\ (.9231) = 472 \text{ in-kips}$$

$$P = \frac{M_s}{9.32} = \frac{472}{9.32} = 50.7$$

APPENDIX D

LOAD - STRAIN DATA

APPENDIX D LOAD - STRAIN DATA

Table D.1. Steel and Concrete Strains - Beam SS-1*

Load kips	No. 6 Bar (MII) at ℄	Compression Zone (at Centerline of Span)										Remarks
			Top of Flange				Edge of Flange		Bottom of Flange			
			6" from ℄	12" from ℄	15" from ℄	17" from ℄	1" from top	2" from top	17" from ℄	15" from ℄	6" from ℄	
3	45	10	140	40	40	60	10	0	40	50	60	
6	425	150	120	220	120	180	110	40	80	20	0	
9	653	330	240	240	20	270	230	30	180	90	30	
12	1953	440	340	370	-120	380	190	10	220	160	70	
15	1270	550	500	450	-180	460	250	10	270	200	80	
18	1530	650	460	540	-340	590	270	20	320	250	160	
20	1705	-	-	-	-	-	-	-	-	-	-	
21.3	-	-	-	-	-	-	-	-	-	-	-	ultimate 21.3k

*See Figure 20 for gage locations.

Table D.2. Steel and Concrete Strains - Beam SS-2*

Load kips	No. 6 Bar (MII) at $\mathbb{C}_L$		Compression Zone (at Centerline of Span) Top of Flange 6" from $\mathbb{C}_L$	9" from $\mathbb{C}_L$	12" from $\mathbb{C}_L$	14" from $\mathbb{C}_L$	Edge of Flange 1" from Top	2" from Top	Bottom of Flange 14" from $\mathbb{C}_L$	12" from $\mathbb{C}_L$	9" from $\mathbb{C}_L$	6" from $\mathbb{C}_L$	Remarks
3	50	80	70	90	40	100	120	120	-120	-100	-140	-200	
6	217	240	380	200	220	200	260	200	-100	-120	-200	-180	
9	565	390	400	380	360	380	340	200	- 80	20	-180	- 80	
12	862	530	500	480	440	500	400	200	- 40	60	-200	- 60	
15	1177	650	580	610	560	700	460	220	- 20	80	10	20	
18	1425	730	720	710	640	720	480	280	- 10	140	140	120	
21	1685	810	820	860	740	800	580	260	40	180	80	120	
22.85													ultimate 22.85k

*See Figure 21 for gage locations

Table D.3. Steel and Concrete Strains - Beam SS-3*

Load kips	No. 6 Bar (MII) at C_L		Compression Zone (at Centerline of Span)									Remarks
			Top of Flange				Edge of Flange		Bottom of Flange			
			3" from C_L	6" from C_L	9" from C_L	11" from C_L	1" from top	2" from top	11" from C_L	9" from C_L	6" from C_L	
3	50	70	60	40	60	20	30	30	- 40	- 40	- 30	
6	460	220	220	190	200	160	110	90	- 20	- 30	0	
8	670	320	300	290	270	250	180	90	40	30	30	
10	860	420	440	410	400	290	250	90	110	40	100	
12	1175	540	560	520	500	450	300	80	130	120	140	
14	1345	650	640	630	600	570	330	90	190	170	170	
16	1515	720	730	700	660	650	400	110	170	200	260	
18	1700	800	830	800	750	750	430	110	260	260	250	
20	1870	890	910	870	860	830	480	130	300	270	320	ultimate.

*See Figure 22 for gage locations.

Table D.4. Steel and Concrete Strains - Beam SS-4*

Load kips	No. 6 Bar (MII) at Centerline	Compression Zone (at Centerline of Span)				Remarks
		Top	1/2" Down	1" Down	2" Down	
2	45	100	140	100	60	
4	205	260	230	220	140	
6	520	420	410	350	210	
8	750	680	580	510	330	
10	980	930	770	650	400	
12	1210	1130	940	780	500	
14	1470	1360	1070	930	570	
16	1700	1400	1180	1070	650	
17	1820	1760	1360	1170	700	
18	1930	1860	1480	1250	760	
19	2050	2020	1510	1310	770	
20	2185	2150	1650	1380	840	
21	2315	2270	1740	1460	890	Ultimate

*See Figure 23 for gage locations.

Table D.5. Steel and Concrete Strains - Beam IIT-1.*

Load kips	No. 6 Bar (MII) at Support	Compression Zone 3-1/2" From Support					Remarks
		3" Up	2" Up	1" Up	1/2" Up	Bottom	
5	20	100	--	40	60	--	
10	44	140	--	40	80	180	
15	64	160	--	100	180	280	
20	96	240	60	120	180	260	
25	157	260	100	120	240	300	
26.7	1307						Flange cracked
30	1482	280	240	460	540	520	
35	1732	340	320	560	680	640	
40	1980	260	360	700	820	800	
43	2128	320	420	860	480	820	
46	2283	280	500	940	1120	960	
49	2449	400	560	1140	1320	1140	Ultimate

*See Figure 32 for gage locations.

Bottom	Remarks
70	
120	
260	
410	Flange cracked at 22^{k}
510	
660	Unload & reload to 31^{k}
530	
570	
580	
850	
890	
930	
1030	
1280	
1390	Loud cracking noises
1480	
1670	
1700	
1840	Ultimate

Table D.6. Steel and Concrete Strains - Beam II T-2*

Load (kips)	No. 6 Bar (MII) at Support	Stirrups (MII) (a)	(b)	(c)	Compression Zone 3-1/2" From Support 3" Up	2" Up	1" Up	1/2" Up	Bottom	Remarks
6	14	8	1	2	60	- 20	40	40	70	
11	26	11	1	2	140	- 80	100	80	120	
17	52	14	- 2	- 2	220	- 140	120	120	260	
22	767	5	- 10	- 4	180	120	120	140	410	Flange cracked at 22^k
28	1100	16	- 9	- 2	240	180	240	300	510	
31	1248	22	- 10	- 3	260	220	320	360	660	Unload & relcad to 31^k
31	1194	8	- 8	2	260	240	320	380	530	
34	1300	8	- 9	- 2	260	260	340	400	570	
36	1408	8	- 10	- 2	260	280	420	460	580	
39	1520	5	- 9	2	260	320	440	480	850	
42	1631	26	178	14	260	340	480	560	890	
45	1720	560	456	96	- 200	300	480	560	930	
48	1814	960	870	416	- 80	240	480	580	1030	
53	2112	1512	1448	946	180	260	660	820	1280	
59	2310	1492	1700	1066	320	240	700	920	1390	Loud cracking noises
61-56	2728	1622	6560	3560	500	220	860	1040	1480	
62	4890	1712	6680	21646	860	- 120	960	1120	1670	
64	6060	--	8720	21440	1060	- 20	1040	1220	1700	
67	8050	--	8718	--	1540	160	1140	1320	1840	Ultimate
69										

* See Figure 33 for gage locations.

Bottom	Remarks
30	
140	
130	
140	
110	Flange cracked 29.2^{k}
360	
550	
630	
810	
980	
1030	
1240	
1260	
1340	
1520	
1650	
1870	
2330	
2730	
3080	
3620	
5950	
6570	
--	Ultimate

Table D.7. Steel and Concrete Strains - Beam II T - 3*

Load (kips)	No. 6 Bar (MII) at Support	Stirrups (MII) (a)	(b)	(c)	Compression Zone 3-1/2" From Support 3" Up	2" Up	1" Up	1/2" Up	Bottom	Remarks
5	13	6	4	4	40	40	60	20	30	
10	27	10	7	6	60	80	120	60	140	
15	42	14	10	8	60	80	120	100	130	
20	54	15	10	6	100	120	180	160	140	
25	72	21	15	9	140	140	200	160	110	Flange cracked 29.2[k]
30	1340	16	9	2	160	200	360	280	360	
35	1595	14	11	9	120	240	460	500	550	
40	1835	38	16	21	120	260	520	620	630	
45	2047	233	17	221	120	260	600	700	810	
50	2263	619	41	656	80	280	680	800	980	
55	2544	824	127	882	0	300	700	880	1030	
60	3169	938	868	1147	120	260	740	880	1240	
62	4136	927	1024	1220	180	300	840	1060	1260	
64	8630	942	1235	1280	280	320	840	1040	1340	
66	10634	1020	1460	1298	420	320	960	1240	1520	
68	11962	1088	1394	1292	520	280	980	1320	1650	
70	13850	1250	1234	1282	700	260	1100	1560	1870	
71	14470	1348	1288	1259	980	200	1280	1900	2330	
72	15230	1317	1376	1267	1100	-160	1360	2340	2730	
73	16150	1330	1960	1278	1280	-180	1480	3040	3080	
74	17000	1426	2820	1310	1460	-160	1600	3520	3620	
75	17980	--	5800	--	1620	-240	2360	6400	5950	
76	18400	--	--	--	1780	-700	3880	--	6570	
77	26000	--	--	--	1960	-840	5500	--	--	Ultimate

*See Figure 34 for gage locations.

Table D.8. Steel and Concrete Strains-Beam IIIT-1.*

Load kips	No. 6 Bar (MII) at Support	Compression Zone 3-1/2" From Support					Remarks
		3" Up	2" Up	1" Up	1/2" Up	Bottom	
5	18	20	20	40	80	140	
10	34	80	20	80	160	---	
15	57	80	60	140	160	140	
20	84	140	120	180	240	---	
25	1244	140	160	240	380	390	Flange cracked
30	1570	320	- 140	420	560	670	
35	1810	200	- 180	520	740	760	
40	2308	- 120	- 200	680	940	920	
43	2470	40	- 220	440	1080	1120	
46	2570	660	- 20	860	1140	1290	
49	2690	---	--	---	----	----	Ultimate

*See Figure 43 for gage locations.

Bottom	Remarks
0	
--	
--	
--	Flange cracked 23.6^{k}
- 260	
560	
880	
980	
1120	
--	Ultimate 51.3^{k}
2580	

Table D.9. Steel and Concrete Strains - Beam III T - 2*

Load (kips)	No. 6 Bar (MII) at Support	Stirrups (MII) (a)	(b)	(c)	Compression Zone 3-1/2" From Support 3" Up	2" Up	1" Up	1/2" Up	Bottom	Remarks
5	24	8	7	1	20	- 80	- 160	- 80	0	
10	48	14	8	0	- 100	- 100	200	120	--	
15	74	18	12	1	- 120	- 160	240	180	--	
20	124	25	17	2	- 160	- 220	300	260	--	Flange cracked 23.6^k
25	1606	18	13	- 2	- 140	- 280	460	460	- 260	
30	1992	41	27	4	- 20	- 240	520	640	560	
35	2371	360	0	256	240	- 120	560	760	880	
40	2718	618	415	1764	360	- 160	640	880	980	
45	3585	908	1038	--	460	- 140	720	1100	1120	
48	6100	1246	1236	--	560	- 140	880	1300	--	Ultimate 51.3^k
51	10300	--	--	--	1200	120	1000	1560	2580	

* See Figure 44 for gage locations.

Table D.10. Steel and Concrete Strains - Beam III T - 3*

Load kips	No. 6 Bar (MII) at Support	Stirrups (MII) (a)	(b)	Compression Zone 3-1/2" From Support 3" Up	2" Up	1" Up	1/2" Up	Bottom	Remarks
5	23	2	6	40	--	- 80	--	50	
10	43	3	9	80	--	100	--	120	
15	73	11	27	140	- 60	200	- 20	140	
20	102	15	22	160	100	220	- 40	190	Flange cracked 22.8 k
25	1492	11	31	220	320	520	560	700	
30	1820	11	30	240	400	760	760	990	
35	2140	15	527	180	460	940	960	1150	
40	2463	128	683	120	520	1140	1240	1510	
45	2930	558	725	100	640	1260	1580	1990	
47	3215	715	813	---	---	---	---	---	
49	4842	910	814	100	800	1680	1820	2840	
51	7370	1093	876	---	---	---	---	---	Ultimate
53	10200	1219	11820	480	1640	2220	---	3930	

* See Figure 45 for gage locations.

Up	Bottom	Remarks
80	100	
140	140	
200	170	Flange cracked 18.2^k
420	560	
680	690	
840	990	
080	1140	
280	1380	
480	1700	
3080	2160	
--	--	
4320	2790	
--	--	Ultimate 57.9^k

Table D.11. Steel and Concrete Strains - Beam III T - 4*

Load (kips)	No. 6 Bar (MII) at Support	Stirrups (MII) (a)	(b)	(c)	(d)	Compression Zone 3-1/2" From Support 3" Up	2" Up	1" Up	1/2" Up	Bottom	Remarks
5	24	13	10	13	10	0	40	40	80	100	
10	43	13	7	10	9	60	100	60	140	140	
15	77	20	11	15	14	100	160	140	200	170	Flange cracked 18.2^k
20	982	7	22	15	14	100	280	340	420	560	
25	1264	1	452	22	13	100	340	480	680	690	
30	1569	20	906	208	18	0	380	520	840	990	
35	1817	48	1036	575	15	120	540	820	1080	1140	
40	2100	101	1228	838	31	100	580	980	1280	1380	
45	2482	173	1350	1113	193	- 80	640	1140	1480	1700	
50	8663	318	1382	1344	538	20	680	--	3080	2160	
53	12234	1034	1444	1365	854	1460	740	--	--	--	
56	14920	1132	--	1438	1058	--	--	--	4320	2790	
57.9	--	--	--	--	--	--	--	--	--	--	Ultimate 57.9^k

* See Figure 46 for gage locations.

Table D.12. Steel and Concrete Strains - Beam IV T - 1.*

Load kips	No. 6 Bar (MII) at Support	Compression Zone 3-1/2" From Support					Remarks
		3" Up	2" Up	1" Up	1/2" Up	Bottom	
5	18	20	100	100	120	140	
10	33	80	120	0	180	110	
15	53	140	140	60	280	160	
20	75	180	200	140	300	220	
25	1071	280	420	580	680	530	
30	1438	260	460	680	800	710	
33	1711	260	520	760	920	800	
36	1954	- 80	440	720	1060	980	
39	2084	- 40	460	800	1100	1030	
42	2225	60	480	940	1180	1150	
45	2374	160	520	1020	1200	1260	Ultimate 48 k.
48	----	---	---	----	----	---	

*See Figure 54 for gage locations.

Table D.13. Steel and Concrete Strains - Beam IV T - 2.*

Load kips	No. 6 Bar (MII) at Support	Stirrup (MII) (a)	Compression Zone 3-1/2" From Support					Remarks
			3" Up	2" Up	1" Up	1/2" Up	Bottom	
5	18	11	60	0	40	80	10	
10	35	15	60	0	80	120	40	
15	65	21	100	0	140	160	100	
20	133	29	120	60	200	240	170	
								Flange cracked at 22.8k.
25	1270	20	160	160	460	480	490	
30	1585	32	160	280	600	680	670	
35	1792	35	- 20	280	660	880	920	
39	1970	37	- 20	380	860	1100	1070	
42	2144	183	- 40	380	940	1160	1220	
45	2314	308	- 40	360	1020	1300	1400	
48	2595	382	- 20	560	1200	1540	1470	
51	3006	420	20	620	1300	1660	1610	
54	4451	442	40	740	1500	1940	1780	
57	----	469	100	860	1760	2540	2080	
60	----	559	380	880	1880	2800	2330	
61.3	----	---	---	---	----	----	----	Ultimate 61.3k.

*See Figure 55 for gage locations.

Bottom	Remarks
50	
140	
170	Flange cracked
200	
520	
750	
870	
1010	
1090	
1250	
1430	
1550	
1810	
2240	
--	Ultimate 59.2^{k}

Table D.14. Steel and Concrete Strains - Beam IV T - 3*

Load (kips)	No. 6 Bar (MII) at Support	Stirrups (MII) (a)	(b)	(c)	Compression Zone 3-1/2" From Support 3" Up	2" Up	1" Up	1/2" Up	Bottom	Remarks
5	16	5	0	0	0	20	80	20	50	
10	38	17	6	6	60	60	120	40	140	
15	55	23	6	6	120	120	160	100	170	Flange cracked
20	891	30	6	8	140	140	200	140	200	
25	1203	29	10	8	140	260	420	420	520	
30	1516	68	13	8	160	300	520	640	750	
35	1777	214	56	8	-200	340	600	--	870	
39	2016	606	368	20	- 60	320	660	800	1010	
42	2196	728	580	58	20	280	660	840	1090	
45	2397	746	842	108	- 20	380	780	960	1250	
48	2633	749	886	210	20	380	880	1080	1430	
51	3244	752	858	335	20	400	920	1140	1550	
54	4742	747	863	486	0	400	980	1360	1810	
57	--	800	974	706	40	380	1180	1580	2240	
59.2	--	--	--	--	--	--	--	--	--	Ultimate 59.2[k]

See Figure 56 for gage locations.